PROCEEDINGS OF

The 6th Workshop on Innovative Engineering for Fluid Power - WIEFP 2022

22 - 23 November 2022

ABIMAQ, São Paulo, SP, Brazil

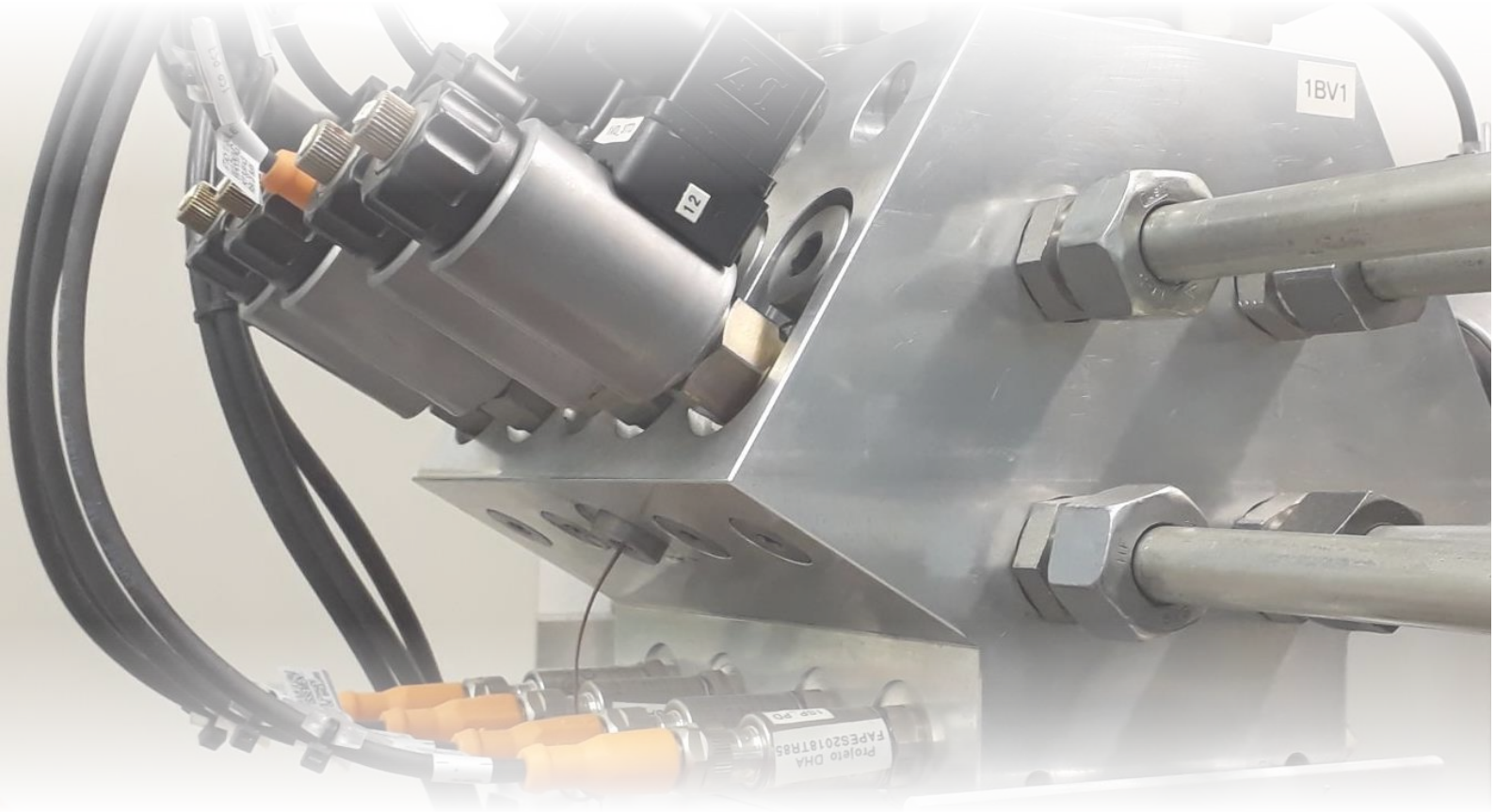

Organized by the Federal University Santa Catarina (UFSC), Linköping University (LiU), Federal University of ABC (UFABC), Swedish-Brazilian Research and Innovation Centre (CISB), and Hydraulic, Pneumatic, and Industrial Automation Equipment Sectorial Chamber (CSHPA/ABIMAQ).

lashipp.ufsc.br/site/wiefp2022/

Proceedings of the 6th Workshop on Innovative Engineering for Fluid Power - WIEFP 2022

ABIMAQ, São Paulo, SP, Brazil

22 - 23 November 2018

Editors

Victor Juliano De Negri, Petter Krus, Luciana Pereira, Edmilton Stein, Vinícius Vigolo

Published by:

Linköping University Electronic Press

Series info: Linköping Electronic Conference Proceedings Nr. 196

ISSN: 1650-3686

eISSN: 1650-3740

ISBN: 978-91-8075-190-2 (PDF)

DOI: https://doi.org/10.3384/ecp196

Organized by:

Federal University Santa Catarina (UFSC)

Linköping University (LiU)

Federal University of ABC (UFABC)

Swedish-Brazilian Research and Innovation Centre (CISB)

Hydraulic, Pneumatic, and Industrial Automation Equipment Sectorial Chamber (CSHPA/ABIMAQ).

Supporting agency:

Coordination for the Improvement of Higher Education Personnel (CAPES - Brazil)

Cover photo:

Laboratory of Hydraulic and Pneumatic Systems

General Co-chairs

Victor De Negri, UFSC, Brazil
Petter Krus, Linköping University, Sweden
Luciana Pereira, UFABC, Brazil

Chair CISB

Alessandra Holmo, CISB, Brazil

Chair CSHPA/ABIMAQ

Maurício Garcia

Conference Administrators

Vinícius Vigolo, UFSC, Brazil
Edmilton Stein, UFSC, Brazil

Scientific committee

Liselott Ericson, Linköping University, Sweden
Alessandra Cristina Santos Akkari, IFSul, Brazil
Emilia Villani, ITA, Brazil
Luiz Carlos Sandoval Góes, ITA, Brazil
Antonio Carlos Valdiero, UFSC, Brazil
Thiago Boaventura, USP/São Carlos, Brazil
Henrique Raduenz, Volvo CE, Sweden
Thomas Heeger, Linköping University, Sweden
Samuel Kärnell, Linköping University, Sweden
Rafael Rivelino da Silva Bravo, IFSC, Brazil
Marcos Paulo Nostrani, UFSC, Brazil
Vinícius Vigolo, UFSC, Brazil
Dimitri Oliveira e Silva, UNIFESSPA, Brazil

The WIEFP is a Swedish-Brazilian initiative started in 2012 whose focus is to promote collaboration in the development of technologies, education, innovation management, and methods and tools for hydraulic and pneumatic system development and design, aiming to bring together industry and academia interested in this evolving multidisciplinary field of fluid power, driver, actuation, and control systems present in almost all industrial sectors.

In the 2022 edition, besides the panel discussions with panelists from industry and academia, the workshop had selected presentations from industry engineers and papers submitted by master's and doctoral students, which were peer-reviewed by the scientific committee. Furthermore, the workshop had short courses offered by experts from industry and academia.

The topics of the workshop are focused, but not limited to:

- Electrification and digital transformation
- Applied artificial intelligence
- Energy efficiency solutions
- Fluid power applications and design
- Modeling and simulation
- Innovation and management
- Sustainability
- Components and systems

PAPERS

A NOVEL MULTI-PUMP SYSTEM FOR HYDRAULIC ACTUATION IN ELECTRIC MOBILE MACHINERY

Artur Tozzi de Cantuaria Gama
Linköping University
artur.tozzi@liu.se
Linköping, Östergötland, Sweden

Kim Heybroek
Volvo CE
kim.heybroek@volvo.se
Eskilstuna, Södermanland, Sweden

Liselott Ericson
Linköping University
liselott.ericson@liu.se
Linköping, Östergötland, Sweden

ABSTRACT

An observable trend nowadays is the change in the prime movers of mobile heavy machinery to electric alternatives to achieve more eco-friendly equipment. These solutions often require large and heavy batteries with limited capacity, making the research of more efficient components and the development of different system architectures an important topic of study. Hydraulic actuation is still a relevant application for these vehicles because of its reliability, controllability, and high power density. The electrification and digitalization of mobile machinery allow for innovative designs and control strategies to be implemented that take advantage of electro-hydraulic systems and their characteristics. Similar research has shown that a higher number of degrees of freedom allow for the system to operate with higher total efficiency. This paper introduces a novel actuation architecture that combines multiple fixed displacement hydraulic pumps and on/off directional valves to control the position and force of two hydraulic actuators for the working functions of a mobile machine. Each pump is powered by a variable speed electric drive so that each one can be operated independently, and together with the set of directional valves, allows the selection of different combinations of pumps and flow sharing between the actuators' chambers to achieve the desired flow and pressure on each cylinder. The multi-pump system favours the use of smaller pumps, and the possibility of combining their flows reduces the need to operate the components at lower efficiency points such as partial displacement. At the same time, controlling the pumps' flow through the variable-speed electric motors means that throttling valves are not needed. The development of this architecture will allow for its use in mathematical models to analyse its behaviour and efficiency and to obtain insights regarding points of improvement in the system architecture.
[DOI: https://doi.org/10.3384/ecp196001]

Keywords: *Electrification, digitalization, multi-pump system, control optimization*

INTRODUCTION

A traditional solution for the operation of loads in heavy machinery, such as excavators and wheel loaders, is hydraulic actuators because of their high power density, controllability, and reliability. Load-sensing systems have been traditionally used to control the system pressure so that multiple loads can be operated with the same pump [1]. This commonly involves one or more pumps connected to the internal combustion engine that adjust their displacement continuously to reach the required pressure [2]. To guarantee that the loads can achieve the desired speed, it is possible to combine pumps so that higher flows can be achieved. On the other hand, two or more actuators can be used at the same time, meaning that the flow of a pump might be distributed between them, resulting in what is called flow sharing. Although this process allows the operator to use different functions continuously to increase productivity, the loads often require different pressure levels, meaning that proportional valves are needed to limit the flow to each cylinder or motor, which often results in losses through pressure drop [3].

The load sensing system is well established in the industry for being a reliable solution that has seen constant improvement and is capable of adapting the system to different working conditions as needed by the operator, but the high losses encourage the search for different alternatives [4]. One option is the development of new pumps and motors, such as the Digital Displacement Pump® (DDP) [5]. Another research topic is reducing the system losses by modifying the conventional system [2, 4] or by exploring new architectures that aim at reducing the losses in hydraulic systems by changing the throttling valves to a series of on/off valves to operate the actuators [6, 7] and that take advantage of the higher control capabilities of a combined electric-hydraulic system by controlling the pump speed, and thus the flow [8].

 Proceedings of the 6th Workshop on Innovative Engineering for Fluid Power – WIEFP 2022, 22-23 November 2022. ABIMAQ, São Paulo, SP, Brazil.

The electrification and digitalization trend of heavy machinery supports the development of both these alternatives. The use of electric batteries with limited capacity requires more frequent and longer recharge times [9] or a complete battery exchange [10]. In this regard, having a hydraulic system with higher efficiency is advantageous, as the machine can operate for longer periods, but also reduce the overall energy cost even for newer or conventional fossil fuel equipment or hybrid solutions, thus also reducing emissions.

With a focus on the system architecture, this paper presents a novel solution for the hydraulic system in excavators. A multi-pump system is considered, where a series of fixed displacement pumps are used to provide the required flow. With a fully electric vehicle, it is possible to separate the pumps from the main engine and have each being operated by a different electric motor, thus granting operation independency to these components. Finally, a manifold block with on/off valves allows for the system to connect any number of pumps to any of the actuators as needed, as well as connect different chambers to regenerate energy.

The challenge in the development of such a system is finding a way to estimate its performance and possible benefits since the control strategy to be used is not clear because of the high number of control variables. This paper finishes with a discussion about dynamic programming, which has been used before to evaluate another highly complex system with a DDP [11]. This method aims at finding the optimal control strategy for a given operating cycle, thus offering insights on how to improve the system and develop an adequate controller.

ELECTRIFICATION AND DIGITALIZATION

Valve-controlled systems

A traditional valve-controlled system with actuators operating at different pressures always includes the loss of part of the total power [2, 12]. Figure 1.a) presents a simplified model of a load-sensing system with two cylinders, where the pressures in the actuators are compared and the higher one is used as a reference to control the displacement of the pump so that both pump flow and, consequently, pressure are adjusted as needed.

In Figure 1.b) the power consumption of the system is shown. One actuator consumes a total power of P_1 based on its flow and pressure while the second actuator needs flow at a lower pressure, thus consuming P_2. But since they share the same pump, the system must keep the pressure on a higher level, thus a large pressure drop is required on the proportional valve of the lower pressure cylinder, resulting in the previously mentioned power loss. The dashed line represents the extra power loss derived from internal losses in the system such as friction and leakage.

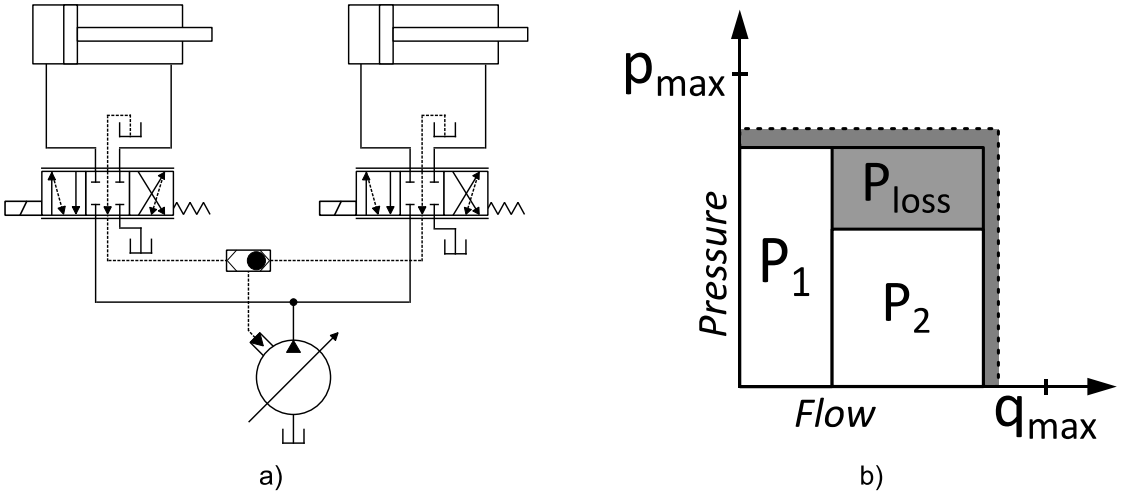

Figure 1 - Load-sensing system. a) Simplified hydraulic circuit for two actuators. b) Loads power consumption and losses

Although this system has been a successful change when compared to an open-centre valve circuit or a pressure-controlled system concerning system efficiency [1] and improvements have been proposed by combining, for example, load-sensing with open-centre solutions and controlling both the pressure and flow

of the pump [3], the energy loss is still present through the load interference since a pump is always shared between actuators.

Current research on electrified systems

Different countries are instituting regulations with a focus on reducing the consumption of fossil fuels and emissions from vehicles. For companies that require heavy machinery, such as mining and civil construction, new laws and requirements should be followed, and OEMs are now searching for different ways to power the vehicles, such as battery, fuel cell and hydrogen combustion [13].

New challenges arise when sizing these vehicles regarding operation time, energy management and cost, but it also opens new possibilities for the design of the different systems in the machine. If a fully electric vehicle is considered, then having the hydraulic pumps connected directly to the prime mover is not a necessity anymore, since smaller electric motors and pumps can be installed on different spots of the machine and powered through electric cables. The hydraulic connections could also be done with shorter hoses, for example, since the pumps could be installed closer to the machine's actuators.

One topic nowadays is pump-controlled systems. When considering the flexibility provided by electric systems, one example is [14], which analyses a pump-controlled solution to operate differential cylinders. A single electric motor is used to power two fixed displacement pumps/motors and a control strategy is discussed. There are no throttling losses through valves and the flow is only provided to each of the chambers when needed. [15, 16] discuss different electro-hydraulic solutions regarding the number of pumps and utilization of hydraulic transformers or accumulators, while also comparing different architectures, benefits, and controllability challenges.

[11] discusses the application of the Digital Displacement Pump® in an electric scooptram. In this case, the electric motor speed is based on the operating cycle and the operator actions and two DDPs are used to provide flow to three actuators. Based on the design of the DDP, each one is modelled as a set of four small pumps with independent variable displacement connected to the same mechanical shaft, thus simulating an eight-pump system. The main advantages derive from the higher efficiency of the machines in a larger range of operating points and the fact that the valves can be used only to change the direction of the flow without acting as throttling components.

Another alternative for electric-powered hydraulic systems is presented in [17]. Here the discussion revolves around controlling two cylinders with multiple fixed pumps connected to different chambers of the actuators and powered by variable-speed electric motors, a system denominated as an electro-hydraulic variable-speed drive network. Different architectures are compared, considering how pumps can interconnect different chambers and how to size them, while completely removing the need for throttling valves.

A MULTI-PUMP ARCHITECTURE FOR MODULAR EXPANSION

The previous research shows the potential for electrification and digitalization and how those systems can improve overall efficiency by eliminating throttling losses. To expand on these ideas, a new architecture for two cylinders is proposed in Figure 2. The basic components considered are two actuators that should be operated by four fixed displacement pumps/motors plus four variable speed drives (VSD) for electric motors and thirty on/off valves. In the figure, A_n are the actuators, P_n are the pumps, P_{nm} are the pump ports connected to the valves and S_n refer to the service lines that connect the valves to each actuator chamber.

Another goal of this study is to evaluate how the system could benefit from using smaller fixed-displacement pumps. Smaller machines can normally operate at higher speeds to reach the same flow as a larger pump, which could reduce the overall weight and space required for installation. Scooptrams and excavators also commonly work under operating cycles that do not always require the maximum power at the actuators, thus having multiple pumps would allow the system to operate only the number of components needed at the adequate speed to reach maximum overall efficiency.

The considerations and ideas behind the proposed architecture can be summarized in the following points:

- The proposal considers identical-size pumps and valves, which can reduce the overall cost of production and allow for modularity,
- The system should operate by transferring fluid between the actuators directly through the valves, allowing for energy recuperation or through a pump if a higher pressure is needed,
- An auxiliary pump connected to the tank is available for use when extra flow is required or when excess flow should be returned to the reservoir. This extra pump allows the system to adjust the low-pressure level during operation,
- The variable speed drives also allow for energy recuperation by charging the vehicle batteries with the hydraulic machines operating as motors.

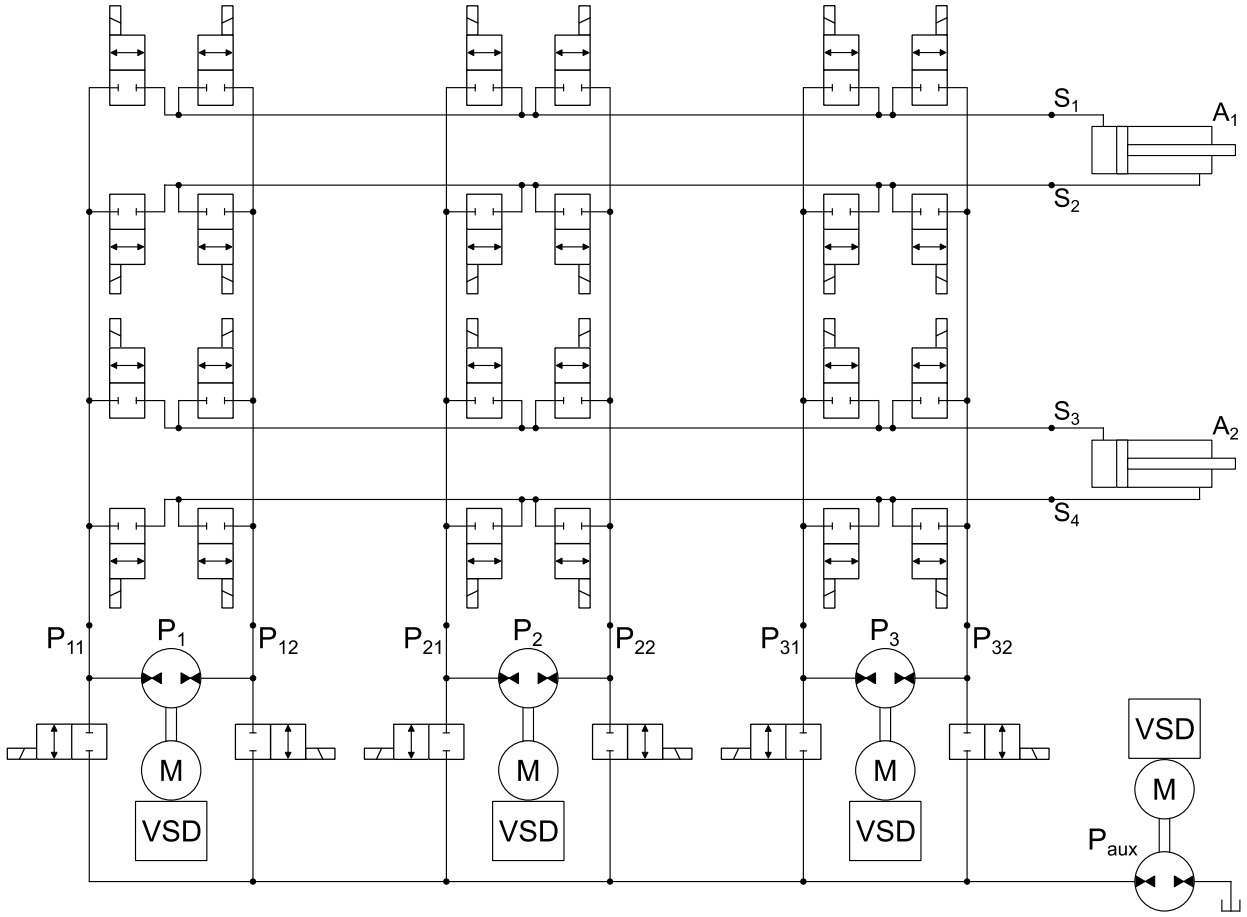

Figure 2 - System diagram for two actuators

The architecture shown allows for all possible interconnections between components. This means that each chamber from each actuator can be connected to any one of the pumps' inlets or outlets or the auxiliary pump. A single pump can be used if the required flow is low or multiple pumps can be activated simultaneously if a function requires a higher flow.

As an example, one could consider actuators A_1 returning and A_2 advancing. One possible operation could be connecting S_1 to S_4 through the valves on the pump P_3 column for direct energy recuperation, and if there is excess flow, it can be directed to the auxiliary line. At the same time, S_3 could be connected to P_{22} so that P_2 can set the pressure for P_{21} which would be connected to S_2. If extra flow is needed, then the system could add flow from the auxiliary line or send it back to the tank through the auxiliary pump if there is an excess flow.

The number of valves needed can be calculated based on the number of pumps that are connected to the actuators' services lines (connection points S_n) times the number of valves needed for each pump setup, which are two valves connected to the auxiliary line plus four valves for each actuator, thus

$$n_v = (n_p - 1)(2 + 4n_a), \tag{1}$$

where n_v is the total number of valves, n_p is the total number of pumps and n_a is the number of actuators. Increasing the number of actuators means adding an extra line of valves while adding an extra pump adds a column of valves connecting to the actuators and two extra valves to the auxiliary line.

This proposal also allows for some level of modularity. Figure 3 below represents how the system can be expanded to include any number of actuators and pumps for application on different machines. In this regard, having a standardized valve block solution would allow for the basic system to be adapted to an excavator, for example, that includes an arm, boom, bucket, and swing, totalling four actuators, while the number of pumps could be increased to achieve the maximum required flow instead of increasing the size of the components.

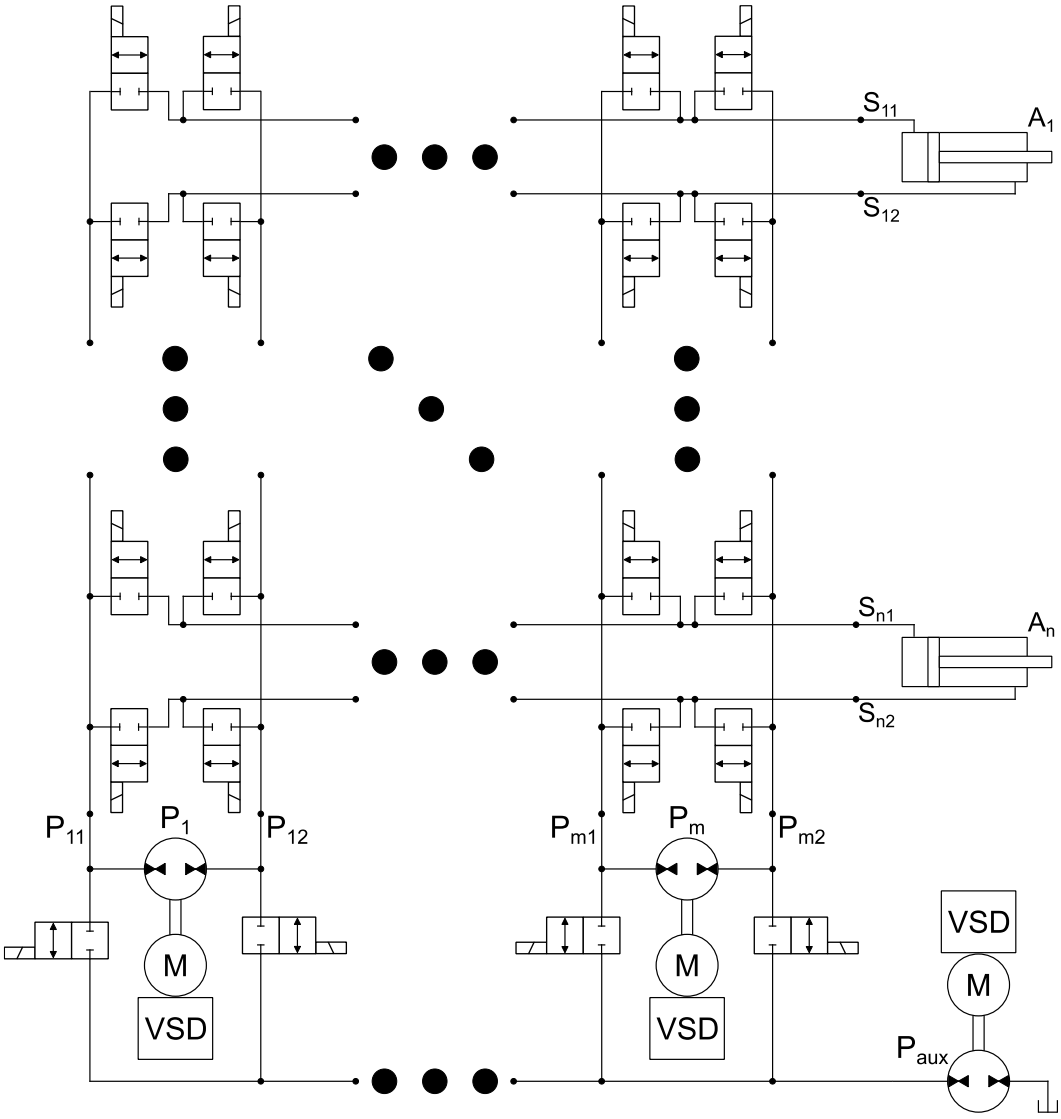

Figure 3 - General modular diagram for the multi-pump architecture

Evaluation proposal for the multi-pump system

The first step in evaluating this system will consist in analysing the possible gains of using multiple pumps. When the maximum flow is not needed, then a single pump operating at high speed could provide all the flow or multiple pumps could be active at the same time at a lower speed. The ideal solution could depend on the drive cycle considered and on the efficiency of the machines at the operating conditions. A sizing study and static evaluation with one or two actuators will provide insight into the system's behaviour and operating limitations.

The multi-pump system includes a high number of components that need to be operated. It also shows how to achieve a high degree of freedom, meaning that each pump can be connected to each actuator chamber at any moment. A system with four actuators and eight pumps (seven work pumps and one auxiliary pump) would require a total of 126 valves. A fair assumption is that the actual system would not need all these components to work adequately, but identifying what parts are redundant is a hard task to be done through an empirical analysis.

To tackle this problem, dynamic programming can be used to find the optimal solution. The system can be modelled as a discrete-time optimization problem where a target function, for example, minimizing the total energy consumption, is the main objective [18]. By setting the vehicle to work on a drive cycle, it is possible to estimate what would be the optimal selection of valves and pumps and when to activate them at each time step.

This method was applied before in [11] to find the optimal control strategy for the scooptram with DDPs and estimate the system's efficiency. For the current application, besides giving more information regarding the multi-pump solution capabilities and how it would operate, the results should also indicate which

parts of the circuit are redundant. It would be possible, for example, to identify certain valves (or valves combination) that are never used because a more efficient alternative exists, which can be used as a basis for adapting the system architecture to a simpler alternative.

Finally, the results of the dynamic programming and the simplified architecture can then be analysed from the dynamic perspective to develop an adequate control strategy. Rule-based controllers tend to increase drastically in complexity as the number of control variables increases, in this case, pump speeds and valves, so alternative methods should be studied. Machine learning is one alternative that should be considered, where the system is trained with different drive cycles to define the ideal combination of valves and pumps that should be active based on, for example, pressure levels and operator commands.

CONCLUSIONS

This paper focuses on the broad research area of electrification and digitalization, more specifically on the integration of hydraulic systems into fully electric machines and how to make the hydraulic system more efficient. A discussion about the different subtopics is presented and which methods and approaches have been considered by different research groups, including component development, digital hydraulics, electro-hydraulic solutions, and multi-pump systems.

A novel multi-pump architecture is presented that combines a series of fixed displacement pumps with variable speed electric motors and a set of on/off valves that can be used to control different actuators. The system is presented at its most generic state with a high degree of freedom for controllability and a discussion about its modularity and how it can be adapted to different machines is presented.

Dynamic programming is then discussed as a mathematical algorithm that can be used to identify the optimal solution for a given drive cycle. The results would serve not only to estimate the capabilities of the system but also to identify redundant components that could be excluded from the system architecture since, for example, a more efficient combination of valves and pumps should be used. Another analysis could revolve around determining which parts of the system are unfrequently used, thus a compromise between the number of degrees of freedom and the overall cost of the system could be studied.

ACKNOWLEDGMENTS

This research was funded by the Swedish Energy Agency (Energimyndigheten, Grant Number 50181-1).

REFERENCES

[1] P. Krus, “On Load Sensing Fluid Power Systems with Special Reference to Dynamic Properties and Control Aspects,” Linköping University, 1988. [Online]. Available: https://www.researchgate.net/publication/230688224_On_Load_Sensing_Fluid_Power_Systems

[2] M. Axin, “Mobile Working Hydraulic System Dynamics,” Linköping University, 2015. doi: 10.3384/diss.diva-121070.

[3] M. Axin, B. Eriksson, and P. Krus, “A flexible working hydraulic system for mobile machines,” *Int. J. Fluid Power*, vol. 17, no. 2, pp. 79–89, 2016, doi: 10.1080/14399776.2016.1141635.

[4] B. Eriksson, “Mobile Fluid Power Systems Design,” Linköping University, 2010. [Online]. Available: http://liu.diva-portal.org/smash/record.jsf?pid=diva2%3A370276&dswid=6380

[5] J. J. Budden and C. Williamson, “Danfoss Digital Displacemente Excavator: Test Results and Analysis,” in *Symposium on Fluid Power and Motion Control - FPMC2019*, 2019, p. 10. [Online]. Available: https://asmedigitalcollection.asme.org/FPST/proceedings/FPMC2019/59339/V001T01A032/1071794

[6] H. C. Belan, P. Krus, B. Lantto, and V. J. De Negri, “Digital Hydraulic Actuator DHA Concept for Aircraft Actuation Systems,” in *Recent Advances in Aerospace Actuation Systems and Components*, 2016, pp. 216–220.

[7] M. P. Nostrani, “Development of a Digital Electro Hydrostatic Actuator for Application in Aircraft Flight Control Surfaces,” Federal University of Santa Catarina, 2021. [Online]. Available: http://lashiip.ufsc.br/site/en/2021-development-of-a-digital-electro-hydrostatic-actuator-for-application-in-aircraft-flight-control-surfaces/

[8] D. Oliveira e Silva, L. A. Barros de Carvalho, V. J. De Negri, and G. Waltrich, “Digital Hydraulic Pump: an energy efficiency study,” 2021. doi: 10.26678/abcm.cobem2021.cob2021-1613.

[9] D. Fassbender, V. Zakharov, and T. Minav, “Utilization of electric prime movers in hydraulic heavy-duty-mobile-machine implement systems,” *Automation in Construction*, vol. 132. Elsevier, p. 103964, Dec. 01, 2021. doi: 10.1016/j.autcon.2021.103964.

[10] Ł. Bołoz, “Global Trends in the Development of Battery-Powered Underground Mining Machines,” *Multidiscip. Asp. Prod. Eng.*, vol. 4, no. 1, p. 178, 2021.

[11] L. V. Larsson, R. Lejonberg, and L. Ericson, “Optimisation of a Pump-Controlled Hydraulic System using Digital Displacement Pumps,” *Int. J. Fluid Power*, vol. 23, no. 1, pp. 53–78, Nov. 2021, doi: 10.13052/ijfp1439-9776.2313.

[12] S. Kärnell, “On Electrified Fluid Power Systems in Mobile Machinery,” Linköping University Electronic Press, Linköping, 2022. doi: 10.3384/9789179294410.

[13] M. Reyes-Valenzuela, A. Sánchez-Squella, R. Barraza, M. Osses, and P. Valdivia-Lefort, “Economic evaluation of fuel cell-powered OFF-ROAD machinery using stochastic analysis,” *Int. J. Hydrogen Energy*, vol. 47, no. 5, pp. 2771–2782, Jan. 2022, doi: 10.1016/j.ijhydene.2021.10.247.

[14] V. Zakharov and T. Minav, “Influence of Hydraulics on Electric Drive Operational Characteristics in Pump-Controlled Actuators,” *Actuators*, vol. 10, no. 12, p. 17, Dec. 2021, doi: 10.3390/ACT10120321.

[15] D. Fassbender, V. Zakharov, and T. Minav, “Utilization of electric prime movers in hydraulic heavy-duty-mobile-machine implement systems,” *Autom. Constr.*, vol. 132, p. 26, Dec. 2021, doi: 10.1016/J.AUTCON.2021.103964.

[16] S. Ketelsen, D. Padovani, T. O. Andersen, M. K. Ebbesen, and L. Schmidt, “Classification and review of pump-controlled differential cylinder drives,” *Energies*, vol. 12, no. 7, p. 27, Apr. 2019, doi: 10.3390/en12071293.

[17] L. Schmidt and K. V. Hansen, “Electro-Hydraulic Variable-Speed Drive Networks—Idea, Perspectives, and Energy Saving Potentials,” *Energies*, vol. 15, no. 3, p. 1228, Feb. 2022, doi: 10.3390/en15031228.

[18] O. Sundstrom and L. Guzzella, “A generic dynamic programming Matlab function,” in *2009 IEEE Control Applications, (CCA) & Intelligent Control, (ISIC)*, 2009, pp. 1625–1630. doi: 10.1109/CCA.2009.5281131.

DIGITAL HYDRAULIC ACTUATORS: A RESEARCH OVERVIEW FOR AIRCRAFT CONTROL SURFACES

Dimitri Oliveira e Silva
Federal University of Santa Catarina
dimitri.oliveira@unifesspa.edu.br
Florianópolis, Santa Catarina, Brazil

Marcos Paulo Nostrani
Federal University of Santa Catarina
marcos.nostrani@gmail.com
Florianópolis, Santa Catarina, Brazil

Rodrigo Simões Lopes Junior
Federal University of Santa Catarina
rodrigo_lopesjr@hotmail.com
Florianópolis, Santa Catarina, Brazil

Victor Juliano De Negri
Federal University of Santa Catarina
victor.de.negri@ufsc.br
Florianópolis, Santa Catarina, Brazil

ABSTRACT

In the last decades, digital hydraulics has emerged as a new alternative for the development of more efficient hydraulic systems, where the effects of throttling losses and internal leakages are minimized through the use of conventional hydraulic components associated in parallel or through switching hydraulics. In the aviation industry, hydraulic systems are commonly applied to control highly relevant systems, such as landing gear and flight control surfaces. In this context, digital hydraulics can be used as an alternative solution to improve the energy efficiency of aircraft hydraulic systems. Based on that, this paper aims to present three new hydraulic actuators for application on aircraft flight control surfaces using digital hydraulics. The actuators are being studied by the Laboratory of Hydraulic and Pneumatic Systems - LASHIP of the Federal University of Santa Catarina - UFSC and are called Digital Hydraulic Actuator - DHA, Digital Electro Hydrostatic Actuator - DEHA and Variable Speed Digital Electro Hydrostatic Actuator - VSDEHA. The simulation results show that the actuators developed can be 23 times more efficient than conventional servo-hydraulic actuators, with equivalent dynamic characteristics, demonstrating the potential for application of these new actuators in aeronautical systems.
[DOI: https://doi.org/10.3384/ecp196002]

Keywords: *Digital hydraulics, Digital hydraulic pump, Efficiency, Variable speed, Dynamic simulation.*

INTRODUCTION

Hydraulic systems are mainly applied when it is necessary to develop a large amount of power combined with a compact volume. This characteristic makes hydraulic systems be applied in several areas, such as in construction machinery, hydroelectric plants, and the aeronautical industry. In the aviation industry, hydraulic systems are used in aircraft flight control surfaces, cargo doors, steering, landing gears. [1]. Additionally, hydraulic systems are known for their high reliability and fast dynamic response, making these systems suitable for aircraft application. However, one of the disadvantages of using hydraulic systems is the low energy efficiency, which is caused by the use of valves that throttle the flow and by the internal leakage of the hydraulic components. In order to develop a more efficient actuator solution, studies using digital hydraulics began to be carried out aiming at aircraft applications [2 – 6]. In this technology, components such as the servo or proportional valves are replaced by a set of on/off valves connected in parallel or by a fast switching on/off valve, which is capable of delivering discrete outputs, avoiding the throttling control and minimizing the internal leakage. On/off valves can also be applied to control the pump output, in cases of parallel connection two or more fixed displacement pumps can be connected through the same shaft to provide different flow levels in place of variable displacement pumps. Therefore, using the digital hydraulics approach, throttle losses and internal leaks can be reduced and the system is controlled by the interaction of simple on/off hydraulic components.

In this paper, an overview of researches provided by the Laboratory of Hydraulic and Pneumatic Systems - LASHIP of the Federal University of Santa Catarina – UFSC in the development of digital hydraulic actuators for aeronautical applications will be presented.

 Proceedings of the 6th Workshop on Innovative Engineering for Fluid Power – WIEFP 2022, 22-23 November 2022. ABIMAQ, São Paulo, SP, Brazil.

STUDIES ON DIGITAL HYDRAULICS TOPOLOGIES

The Laboratory of Hydraulic and Pneumatic Systems at the Federal University of Santa Catarina is one of the main centers in Latin America in the development of hydraulic and pneumatic systems. Currently, the laboratory has a research line focused on the study of different topologies for aircraft actuators applying digital hydraulics to flight control surfaces. In this context, three digital hydraulic topologies are being studied, which are called Digital Hydraulic Actuator – DHA, Digital Electro Hydrostatic Actuator – DEHA, and Variable Speed Digital Hydrostatic Actuator – VSDEHA. These solutions will be presented according to the chronological development in the laboratory.

Digital Hydraulic Actuator (DHA)

In this topology, a multi-chamber cylinder with different areas is supplied by different pressure lines (Figure 1). The on/off valves are used to direct the flow rate from the supply lines to the cylinder chamber, where each cylinder chamber can be connected to each supply line independently [2]. The secondary control system of this solution is based on the combination of the pressure lines with the areas of the cylinder chambers to produce the necessary force to move the cylinder, according to the load condition estimated by the system [4]. In this solution, a centralized hydraulic power unit is used to supply the pressure lines.

In [4], the authors proposed a way to define the areas of the multi-chamber cylinder and the pressure values of the supply lines, with a focus on the use for aircraft control surface applications. In the experimental study developed by [2], a four-chamber cylinder connected to three pressure lines through twelve on/off valves was used. Using the combinations of areas and pressures, it was possible to obtain 81 discrete output forces values.

The study carried out by [2], the authors presented an evaluation of the energy saving potential of the solution, where it was possible to reach levels between 80% and 96% of reduction in energy dissipation using the DHA solution when compared to a Servo Hydraulic Actuator under the same simulation conditions. In [6], the simulations performed by the author showed a reduction in energy dissipation of 15.7 times.

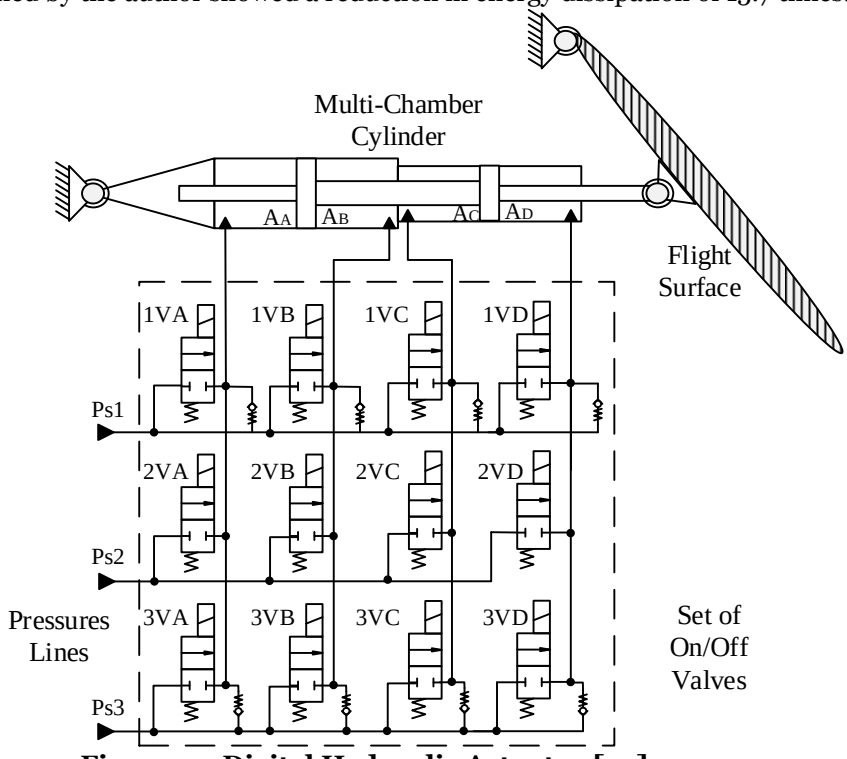

Figure 1 – Digital Hydraulic Actuator [10].

Digital Electro Hydrostatic Actuator (DEHA)

In this topology, a digital hydraulic pump (DHP) is used to provide different flow rate levels, which combined with different areas of the cylinder chamber, produce different cylinder velocities, for the cylinder control [3] (Figure 2). The on/off valves are used to control the output combination of the digital hydraulic pump and direct the flow rate to the cylinder chambers. In [3], the author proposed a DEHA using a digital

hydraulic pump with three pump units and a four-chamber cylinder, using a block valve with 8 valves to connect the DHP and the cylinder chambers.

With the use of three pump units, seven different flow rates are obtained, which combined with the four-chamber cylinder areas, it is possible to obtain 28 cylinder velocities. However, as in the DHA solution, in the DEHA is possible to connect each cylinder chamber to each supply line. In [7], the same configuration is used and the authors propose the use of the DEHA in regenerative mode, increasing the number of different cylinder velocities to 43.

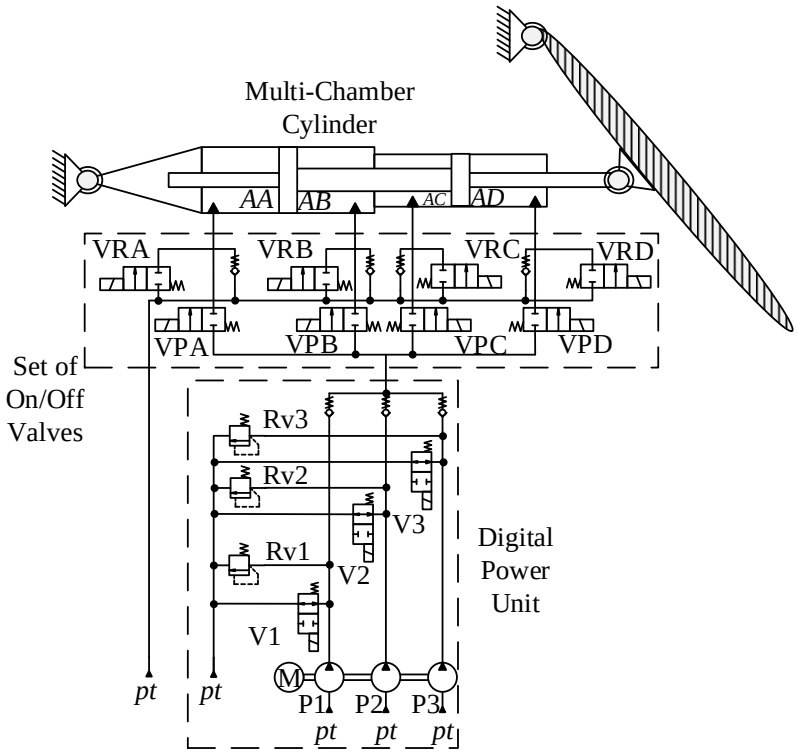

Figure 2 – Digital Electro Hydrostatic Actuator [10].

Variable Speed Digital Electro Hydrostatic Actuator (VSDEHA)

This topology is an evolution of the two topologies presented previously, where a variable-speed digital hydraulic pump is used to supply a cylinder (Figure 3). Unlike the DEHA topology, the flow rate can be changed continuously, where it is not mandatory to have a combination of chamber area and flow rate to increase or decrease the cylinder speed. Speed control is performed by the combination of the angular speed source and pump unit. According to [8], the use of the variable speed increases the number of different flow rates of the DHP, which becomes a continuous flow rate source and allows using the power-on-demand concept to adjust the angular speed for each pump unit combination. This strategy aims to achieve the best operating point for each work condition.

The use of a variable speed digital hydraulic pump is justified by the possibility of changing the pump unit combination to supply a certain operation point or flow rate range without sacrificing efficiency [8]. For example, under low demand conditions, the smaller pump unit can be used more efficiently to supply the low flow rate demand, and under high demand conditions, the higher pump unit combination can be used to achieve this point. Whereas, in a variable displacement pump, the volumetric efficiency generally decreases drastically with the reduction of the volumetric displacement [8; 9].

In this topology, during cylinder movement, there is no cylinder chamber switching to change cylinder speed. This is an advantage from a valve-commutation number perspective, as valve-commutation is only used to change the direction of the cylinder, reducing the number of valve cycles per operating time. However, when the external load is acting in the same direction as the cylinder movement, there is a risk of cylinder overspeed, which may impair the controllability of the system. To overcome this risk, during this condition a second set of on/off valves (V_{bA}, V_{bB}, V_{bC}, and V_{bD}) is used to limit the maximum cylinder velocity by dissipating the extra energy supplied by the external load.

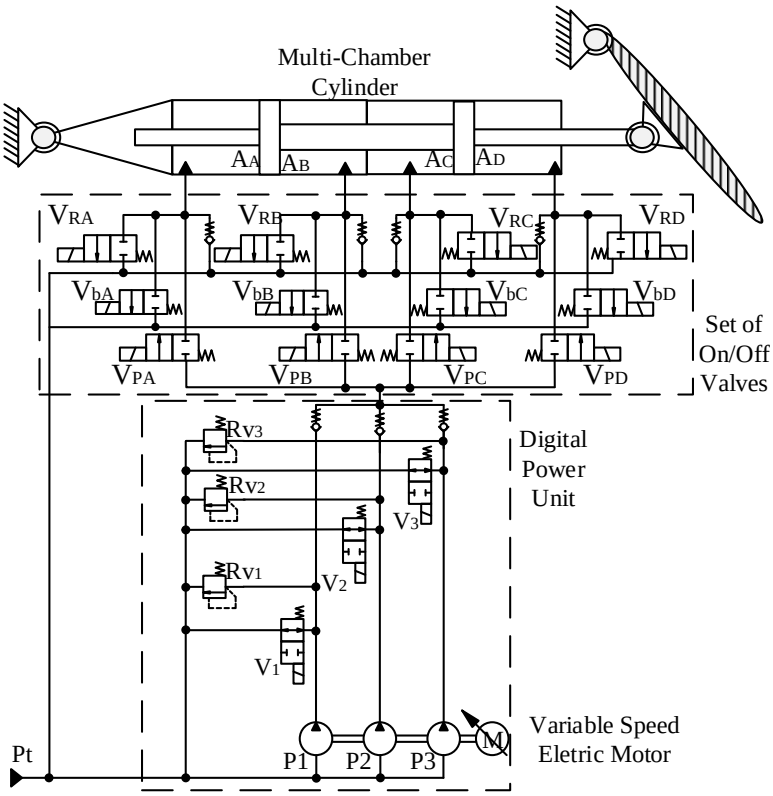

Figure 3 – Variable Speed Digital Electro Hydrostatic Actuator [10].

TOPOLOGY COMPARISON

With the development of new solutions, it is natural to perform some comparisons between their characteristics and research evolutions. Table 1 presents a comparison of the main characteristics of the digital solutions presented in this paper.

Table 1 – Characteristics of the digital hydraulic actuators studied.

Characteristic	DHA	DEHA	VSDEHA
Controlled hydraulic variable	Pressure	Flow rate	Flow rate
Controlled mechanical variable	Force	Velocity	Velocity
Hydraulic supply unit	Not considered	Digital Hydraulic Pump	Digital Hydraulic Pump
MEA concept	Not considered	Considered	Considered
Electric motor control	Not considered	Fixed angular speed	Variable angular speed
Cylinder valve commutation	To change force and direction	To change velocity and direction	To change direction
Pump valve commutation	Not considered	To change the pump unit combination	To change the pump unit combination
Number of forces or velocities	Limited by the number of pressure lines and cylinder chamber combinations	Limited by the number of discrete flow rate and cylinder chamber combinations	Limited by the angular speed range available for each pump unit combination

Dynamic and energy saving potential

In [10], the authors present a comparison between DHA, DEHA, and VSDEHA topologies, which were designed for the aircraft primary control surfaces. The three topologies were implemented in a generic aircraft

model called Aero-Data Model in a Research Environment (ADMIRE) [11]. The ADMIRE implemented in MatLab/Simulink ® was used to perform simulations of the actuators in a virtual aircraft environment to simulate flight commands, behavior, and load conditions. Different flight maneuver missions were used to verify the behavior of the digital hydraulic solutions and perform dynamic and energetic analyses of the systems. The control surfaces analyzed were the left inner elevon (LIE) and left outer elevon (LOE) [10].

Table 2 presents a summary of the dynamic evaluation results highlighted by [10] in relation to the reference, where the overshoot and response time presented are in the maximum condition for the evaluated maneuver, which in this case was the roll-turn flight maneuver. Due to the non-linearities of the system, the dynamic behavior is not the same for different input signals [10].

Table 2 – Dynamic characteristics of digital hydraulic actuators. Adapted from [10].

	ADMIRE	DHA	DEHA	VSDEHA
Overshoot (%)	-	13.8%	4.8%	10.9%
Time response (s)	0.168	0.241	0.351	0.241

Table 3 presents the energy efficiency of the systems during three different maneuvers, landing, roll-turn, and longitudinal, for each digital actuator. The servo hydraulic actuator is a conventional hydraulic system used in aircraft control surfaces, which are known for their low energy efficiency caused by the throttling control and internal leakage of the system components. In [10], a servo hydraulic actuator model was used as a baseline and presented an energy efficiency lower than 2% for the maneuvers. This demonstrates the high energy-saving potential of the digital hydraulic solutions, where energy efficiency values above 30% have been achieved during some maneuvers.

Table 3 – Energy efficiency of digital hydraulic actuators. Adapted from [10].

	DHA		DEHA		VSDEHA	
Control surface	LIE	LOE	LIE	LOE	LIE	LOE
Landing	1.93 %	1.86 %	8.49 %	8.04 %	5.85 %	6.06 %
Roll-turn	6.2 %	6.23 %	14.41 %	14.86 %	35.05 %	34.95 %
Longitudinal	11.3 %	6.47 %	34.87 %	41.63 %	39.9 %	27.9 %

CONCLUSIONS

This paper presented an overview of three digital hydraulic topologies developed at the Laboratory of Hydraulic and Pneumatic Systems of the Federal University of Santa Catarina, designed to be applied to primary control surfaces of aircraft. The use of digital hydraulic solutions is focused on reducing the use of dissipative control strategies and improving system efficiency by using simpler components, reducing costs, and improving reliability.

One of the main features of digital hydraulics is the use of intelligent control to control the output of the system. In this aspect, it is possible to notice that the three topologies presented have almost the same physical structure. However, due to the different control strategies adopted for each one, the results obtained were quite different for each simulated condition.

From an aircraft design point of view, more experimental studies using prototypes should be developed to validate the dynamics and energy savings presented by the proposed systems. In addition, with the use of prototypes, other characteristics such as occupied volume and weight can be evaluated.

ACKNOWLEDGMENTS

The authors are grateful for all the support offered by the entities CISB, CNPq, Saab AB and Linköping University for the sandwich doctorate scholarship CNPq 201325/2020-9, the Federal University of South and Southeast of Pará and the Federal University of Santa Catarina. The research is supported also by the CNPq Grant 315239/2018-2.

REFERENCES

[1] Ward, S. Digital Hydraulics in Aircraft Control Surface Actuation. Fluid and Mechatronic Systems Master Thesis. Linköping University. 2017.

[2] Belan, H. C. “Sistemas de atuação hidráulicos digitais para aviões com foco em eficiência energética,” Doctoral thesis, Federal University of Santa Catarina, Florianópolis, Brazil, 2018.

[3] Nostrani, M. P. Development of a digital electro hydrostatic actuator for application in aircraft flight control surfaces. 2021. 1–192 f. Federal University of Santa Catarina, 2021.

[4] Belan, H. C.; Locateli, C. C.; Lantto, B.; Krus, P.; De Negri, V. J. Digital Secondary Control Architecture for Aircraft Application. The Seventh Workshop on Digital Fluid Power. p. 21–39, 2015.

[5] Lopes, R. S. "Avaliação do desempenho dinâmico de um atuador hidráulico digital para aplicações aeronáuticas em condição de falha". Master thesis, Federal University of Santa Catarina, Florianópolis, Brazil, 2021.

[6] Lopes, R. S.; Nostrani, M. P.; Carvalho, L. A. B.; Dell'Amico, A.; Krus, P. and De Negri, V. J., "Modeling and Analysis of a Digital Hydraulic Actuator for Flight Control Surfaces," Symposium on Fluid Power and Motion Control FPMC2021. online, October, 2021, doi: 10.1115/FPMC2021-68923

[7] Nostrani, M. P.; Raduenz, H.; Dell'amico, A.; De Negri; V. J.; Krus, P. Multi-Chamber Actuator Using Digital Pump for Position and Velocity Control Applied in Aircraft. Global Fluid Power Society - GFPS 2020 PhD Symposium., 2020.

[8] Silva, D. O.; Carvalho, L. A. B.; De Negri, V. J.; Waltrich, G. Digital Hydraulic Pump: an energy efficiency study. 2021. Proceedings of the 26th International Congress of Mechanical Engineering: ABCM, 2021. https://doi.org/10.26678/ABCM.COBEM2021.COB2021-1613.

[9] Maré, J.C. Aerospace Actuators 1: Needs, Reliability and Hydraulic Power Solutions. Hoboken, NJ, USA: John Wiley & Sons, Inc., 2016.

[10] Lopes, R. S; Silva, D. O.; Nostrani, M. P.; Dell'amico, A.; KRUS, P.; De Negri, V. J. A comparative analysis of innovative digital hydraulic actuators for primary flight control. 2022. 33RD Congress of the International Council of the Aeronautical Sciences. Stockholm, 2022. p. 18.

[11] Forssell, L. and Nilsson, U. "ADMIRE The Aero-Data Model. In a Research Environment Version 4.0, Model Description," FOI Report No. FOI-R-1624-SE, December, 2005.

ENERGY EFFICIENCY ANALYSIS AND EXPERIMENTAL TEST OF A CLOSED-CIRCUIT PNEUMATIC SYSTEM

Fedor Nazarov
Technische Universität Dresden,
Institute of Mechatronic Engineering
Chair of Fluid-Mechatronic Systems
fedor.nazarov@tu-dresden.de (c/o)
Dresden, Saxony, Germany

Jürgen Weber
Technische Universität Dresden,
Institute of Mechatronic Engineering
Chair of Fluid-Mechatronic Systems
fluidtronik@mailbox.tu-dresden.de
Dresden, Saxony, Germany

ABSTRACT

In a closed-circuit pneumatic system the air from the pneumatic cylinder is not exhausted directly in the atmosphere, as done in traditional open-circuit systems, but is captured and fed to the compressor inlet. This provides an opportunity to increase the compressor inlet pressure above the atmospheric and consequently enables both higher compression efficiency and volumetric flow rate. Until the present, the advantages of the closed-circuit pneumatics were assessed only within theoretical studies without being verified experimentally due to uncertainties in performance of a real compressor under oscillating pressure and flow rate, as well as due to a risk of mutual cylinder interference caused by differences in load and required pressure profiles. Hence, this study focuses on experimental investigation of energy efficiency and practicability issues of the closed-circuit pneumatics. It is shown that simultaneous operation of two pneumatic cylinders of different size (Ø32×200 and Ø50×200) performing different tasks (high-dynamic mass handling and extension against the constant force) does not have any negative effect neither on the cylinder dynamics nor on the compressor performance. Inlet pressure increase up to 1.5 bar_{rel} leads to by factor 2.5 higher volumetric flow rate and total efficiency gain of 72 % (increase from 10.7 % to 18.4 %). The experimentally obtained results show a great potential of the closed-loop pneumatics and indicate the need in further research into design and control methods of such systems to enable technology deployment to the industry. Industrial applications can profit from the reduced energy consumption especially in case of pneumatic systems with decentralized air supply.
[DOI: https://doi.org/10.3384/ecp196003]

Keywords: *closed-circuit pneumatics, compressor, efficiency, thermodynamics, pressure ratio*

INTRODUCTION

Pneumatics is commonly used in modern automation, robotic and nutrition sectors. It offers such advantages as low investment costs, high robustness, ease of use, and lightweight components. Alongside the Industry 4.0 transition, improving the energy efficiency of pneumatic systems has been one of the most challenging and important research fields in the pneumatics within the last decades, essential to keep this technology environmentally friendly and competitive on the global market.

The total efficiency of a pneumatic drive depends on the energy losses brought about by: i) energy conversion (prime mover, compressor, pneumatic actuator), ii) transportation (pressure drops throughout the air cooler, dryer, filter, pipeline system), and iii) power management (pressure and flow rate control, usually by throttling). An efficient design of a pneumatic system implies that all the components needed for energy conversion, transportation, and power management are selected and tuned for an operation with minimal energy losses. The contribution of energy saving measures feasible within each of the group i-iii) was evaluated and assessed within several studies such as [1] and [2]. However, a simultaneous implementation of all these energy saving measures in practice can appear as tedious and costly when retrofitting an already existing pneumatic system. Besides, pneumatic drives are often not the only consumers of compressed air delivered by the compressor plant. Therefore, an exact quantification of energy losses and total efficiency of one particular drive, counting from the plug of the compressor power unit up to the mechanical coupling on the cylinder shaft, is very challenging. The consequence is a common splitting of calculation of energy consumption into two parts: firstly, estimation of how efficiently the air is compressed, prepared, and transported, and secondly, how efficiently is it consumed. The first part provides information about the energy needed to compress a unit quantity of air to nominal pressure, to cool, to dry, and to transport it (usually referred as “specific energy consumption” or “compressed air index”, measured in

 Proceedings of the 6th Workshop on Innovative Engineering for Fluid Power – WIEFP 2022, 22-23 November 2022. ABIMAQ, São Paulo, SP, Brazil.

kWh×Nm^{-3}) [2]. The second part tells how much air is consumed by a pneumatic drive or a group of drives (measured in Nm³ per time unit or per cycle) [3].

Once knowing the specific energy consumption, this approach provides an easy and transparent assessment of energy consumption by pneumatic drives without having to take into consideration other air consumers and having an exact knowledge about efficiency of each process involved in the air compression and preparation. On the other side, this reduction of complexity displaces the focus of the research in pneumatics to the question "how efficient is the air consumed", whilst often leaving out the question "how efficient the air is compressed and prepared". This can hinder a generation and investigation of new high-efficient methods and system structures, where the compressed air production and consumption are coherent and both questions are equally important. An example of such a system, considered within this paper, is a closed-circuit pneumatic system, where the exhausted air is fed back to the compressor inlet port and hence circulates in the circuit without leaving it.

THEORETICAL ADVANTAGES OF A CLOSED-CIRCUIT AIR COMPRESSION

Theoretical advantages of a closed-circuit pneumatic system rely on a simple observation that theoretical work W_{compr} needed for an adiabatic compression of air with mass $m = \rho_1 \times V_1$ from inlet pressure p_1 to outlet pressure p_2 depends on the relation of these pressures $\varepsilon = p_2 / p_1$, whereas the work W_{displ} performed by the displacement machine, such as a pneumatic cylinder acting against the constant force F_{load}, depends on the pressure difference in the cylinder chambers. Assuming a lossless air transportation from the compressor to the frictionless cylinder with an infinitely large stroke, this pressure difference equals to $\Delta p = p_2 - p_1$. For the sake of simplicity no losses are considered in this section.

$$W_{compr} = V_1 \times \rho_1 \times R \times T_1 \times \frac{\kappa}{\kappa - 1} \times \left[\left(\frac{p_2}{p_1} \right)^{\left(\frac{\kappa-1}{\kappa}\right)} - 1 \right] \quad (1)$$

$$W_{displ} = V_2 \times (p_2 - p_1) = \frac{m \times R \times T_1}{p_2} \times (p_2 - p_1) \quad (2)$$

From Equations (1) and (2) can be obtained that an increase in p_1 at constant pressure difference Δp increases the relation of the theoretical cylinder displacement work (Equations (2)) to theoretical compression work (Equations (1)). This relation can be used as a measure of total efficiency $\eta = W_{displ} / W_{compr}$ of the system. Hence the idea of the closed-circuit pneumatics is to increase the η by raising the inlet compressor pressure over the atmospheric pressure while keeping constant the pressure difference Δp, relevant for the application.

Figure 1 illustrates these relations by comparison of p-V diagrams of a compression cycle from 1 bar_{abs} to 5 bar_{abs} with compression cycle of the same air mass from 3 bar_{abs} to 7 bar_{abs}. Both scenarios provide the same differential pressure $\Delta p = 4$ bar allowing the cylinder to overcome the force F_{load}. The orange-colored area on the diagrams a) and b) corresponds to the work of adiabatic compression cycle composed of the compression work, displacement work and suction work (first, second and third terms in Equation (3) respectively), and is equal to the result of Equation (1).

$$W_{compr}^{ad} = \frac{p_1 \times V_1}{\kappa - 1} \times \left[\left(\frac{p_2}{p_1} \right)^{\left(\frac{\kappa-1}{\kappa}\right)} - 1 \right] + p_2 \times V_2 - p_1 \times V_1 \quad (3)$$

Adiabatic compression is taken here as a simplification of a real compression process that can proceed as a polytropic (with partial heat flow from compressed gas to environment, calculated with polytropic exponent $n < \kappa$) or superadiabatic process (with heat flow from environment, calculated with polytropic exponent $n > \kappa$) [4]. From diagrams a) and b) in Figure 1 can be obtained that compression with $\varepsilon = 7/3$ (closed circuit) takes less than the half of the energy needed to compress the same air quantity with $\varepsilon = 5/1$ (open circuit).

After being compressed, the air needs to be cooled down to the ambient temperature and the absorbed heat is extracted from the system. The air volume shrinks from $V_{2.ad}$ to $V_{2.is}$ and takes the state equivalent to the result of an isothermal compression (Figure 1, c) and d)):

$$W_{compr}^{is} = m \times R \times T_1 \times \ln\left(\frac{p_2}{p_1} \right) \quad (4)$$

From the diagrams c) and d), Figure 1, is visible that the heat losses also decrease with the reduction of compression ratio. In the given case the heat loss in closed circuit is almost four times lower than that after compression from the atmospheric pressure.

Because the air volume V_2 at pressure p_2 = 7 bar_{abs} is smaller than at p_2 = 5 bar_{abs}, it can perform lower displacement work, as can be seen from Figure 1, e) and f). Nevertheless, when considering the relation $\eta = W_{displ}/W^{ad}_{compr}$ the closed-circuit system is about 50 % more efficient then the open one.

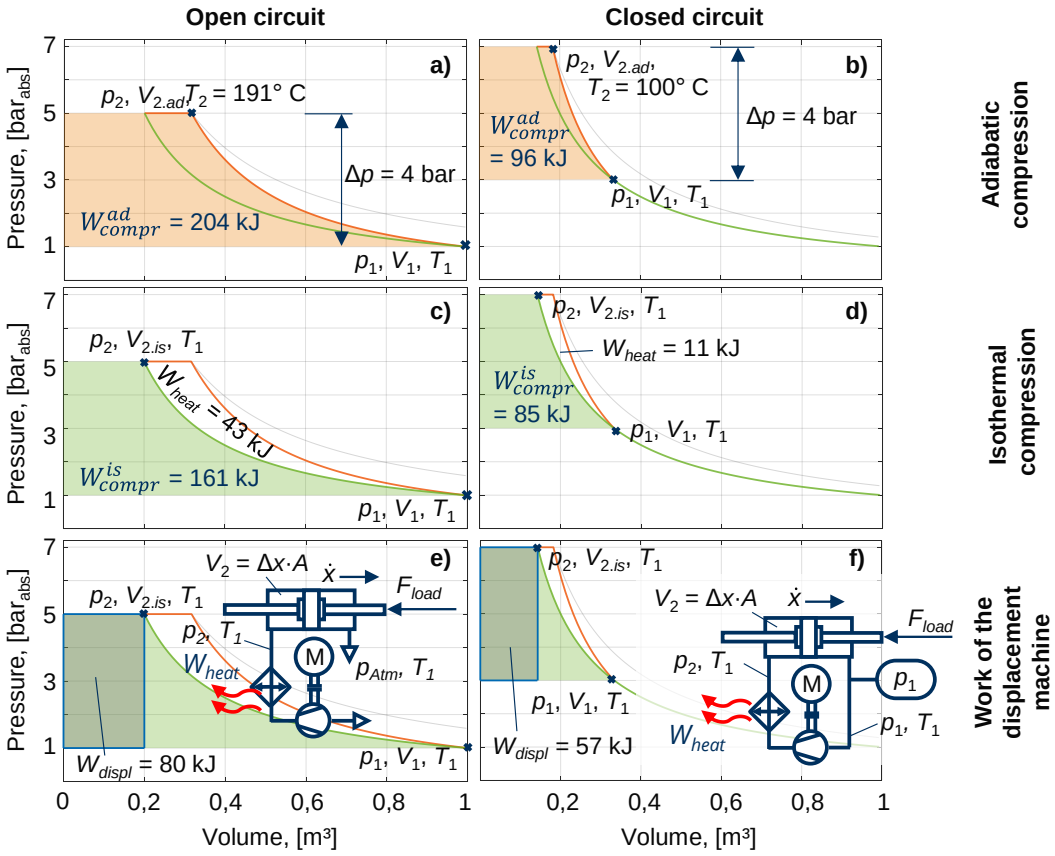

Figure 1 – p-V-diagrams for compression from atmospheric inlet pressure (open circuit, left column) and from inlet pressure of p_1 = 3 bar_{abs} (closed circuit, right column)

Furthermore, the increase in inlet pressure results in higher compressor delivery rate. In case of a real compressor, the geometrical suction volume V_1 is always constant. When referring to the example on diagrams b) and d) in Figure 1, the starting point of compression would always have an abscisse of V_1 = 1 m³ regardless of the inlet pressure. Hence, higher air mass is inhausted within the suction stroke at increased inlet pressure because of higher inlet air density. This amplifies delivered mass flow rate $\dot{m}$ and volumetric flow rate $\dot{V}_2$ at the outlet port, giving an opportunity to supply more pneumatic cylinders with the same compressor.

$$\dot{m} = \frac{V_1 \times \rho_1}{\Delta t} = \frac{V_1 \times p_1}{\Delta t \times R \times T_1} \tag{5}$$

$$\dot{V}_2 = \frac{\dot{m}}{\rho_2} = \frac{V_1 \times \rho_1}{\Delta t \times \rho_2} = \frac{V_1 \times \rho_1}{\Delta t \times \rho_2} \tag{6}$$

Although an increase in inlet air density gains the energy consumption according to Equation (1), the relation $\eta = W_{displ}/W^{ad}_{compr}$ remains in favor of the closed circuit. The advantage is that the compressor (but not the prime mover) needed to supply a given number of pneumatic drives can be downsized when operating in a closed-circuit system. A further notable effect is a decrease in discharge temperature brought about by reduction of the compression ratio:

$$T_2 = T_1 \times \varepsilon^{\left(\frac{\kappa-1}{\kappa}\right)} \tag{7}$$

Low discharge temperature contributes to lower thermal strain in the piston block and valve plates, reduces the wear of the sealing rings and carbonizing in oiled compressors. Hypothetically, bringing ε down to ε ≈ 1.8 enables discharge temperatures of about T_2 ≈ 50...60 °C. These temperatures are safe in case of a skin contact (with regards to the safety regulations ISO 13732-1) as well as tolerable by almost all pneumatic

components. This allows to operate the compressor without a cooler and hence almost without any heat losses. However, very high inlet pressure, needed to reach the compression ratios of $\varepsilon < 1.8$, narrows the usable pressure difference to $\Delta p < 5$ bar, because the maximum operational pressure of most pneumatic cylinders and valves is usually limited to ~10 bar_{rel}.

STATE OF THE ART AND THE AIM OF THE STUDY

The observations noted and illustrated in the previous section are well-known in the literature. The most relevant for pneumatics theoretical study is carried out by Weiß [6]. He analyses the thermodynamic relations, considered above, and assesses the benefits of the closed-circuit compressed air systems. He shows that to achieve a typical for pneumatics differential pressure of 6 bar compression from 4 to 10 bar_{rel} brings significant benefits compared to the conventional compression from 0 to 6 bar_{rel}. In detail, the delivered flow rate, normalized to the normal conditions according to ISO 1217, increases by factor of five, whilst compression power is only doubled. This results in a significant reduction of specific energy consumption: 1.31 instead of 3.24 $kW \times m^{-3} \times min^{-1}$. A practical implementation of a closed-circuit system is expected to be challenging due to the effect of pressure oscillations caused by the non-continuity of air demand from the cylinders on efficiency of the continuously operated compressor. The components need to be optimized for one specific pressure ratio. To ensure an efficient air transportation (i. e. low pressure drop in the pipeline) piping tubes must be upsized because of higher volumetric flow rate and air density. Moreover, extra low-pressure piping line is needed to collect the exhausted air from the cylinders and convey it to the inlet port of the compressor, being an extra source of leakage and pressure loss. The closed-circuit system can only be applied, if no exhaust in the atmosphere is needed by the application, that is no vacuum ejectors or air-blasting are used. Finally, a technical solution for compensation of some inevitable air leakage from the closed system is needed.

A positive effect of the closed-circuit system is observed by authors of [7]. Here a closed system was implemented to supply the pneumatic tools typically used in the car repair shops. The toolkit proposed in [7] is suitable for modification of any compressor for an operation at inlet pressure up to 2 bar_{abs}. The influence of the inlet pressure increase on torque of the prime mover is not discussed. According to the authors the closed-circuit system enables energy costs savings of up to 40 %.

The impact of the back-pressure on the cylinder with a servo control as well as evaluation of energy savings are discussed in [8]. Apart from efficiency increase, a lower noise level due to absence of exhaust is noted by the authors as a further benefit. Another closely related approach for boosting the inlet pressure without closing the pneumatic circuit completely is proposed and successfully implemented by [9]. A special unit is designed to forward the exhausted air from the cylinder chamber through an ejector nozzle forcing the atmospheric air to pass to a low-pressure tank (~1.5 bar_{abs}) at the inlet port of compressor. On this way the energy intake by compressor can be reduced up to 15 %. The project is focused primary on the efficient ejector nozzle design capable of operating at different pressures.

Summing up, the evidence of thermodynamic advantages of pneumatic closed-circuit systems is shadowed by their possible drawbacks noted in the above-mentioned studies. These drawbacks put a question, whether a closed-circuit system can operate reliably and is economically sound. Up to the present moment no successful implementation of the closed-circuit pneumatics could be found in the published sources. In this context, the aim of this research is to study experimentally the performance of a compressor with increased inlet pressure as well as to implement and to test a pneumatic system operating in the closed circuit. Basing on the practical experience, the conclusions about applicability, prospects, and need in further research of such systems are drawn.

EXPERIMENTAL STUDY ON COMPRESOR PERFORMACE

Basically, any positive displacement compressor can operate with inlet pressure above the atmospheric, provided the suction line is mechanically strong enough to resist it. However, a compressor in closed circuit is more likely to operate at variable compression ratio ε because of temporary discrepancies between the volumetric flow rate delivery and demand. In this case, piston compressors, though being in general less efficient than rotary-screw compressors, are a better option, for their compression ratio is defined by the outlet pressure. That means, air is compressed in the piston chamber until the pressure level of discharge piping is reached, and a discharge valve opens. In case of rotary-screw or gear machine, the pressure ratio is defined by the inner geometry and is constant. If pressure in discharge line is higher or lower than pressure reached by the internal compression, the pressurized air volume shrinks or expands respectively, causing vibrations and energy losses. For this reason, a piston compressor was chosen for this experimental study. The aim of the experiment was to obtain the information about compressor performance at various inlet pressures and pressure differences, and to compare the open and the closed circuits. The pneumatic plan of the test rig is shown in Figure 2. Pressures and temperatures at inlet port, discharge port and after the cooler were measured along with normal flow rate $\dot{V}_0$ and real power $\dot{W}$ of the asynchronous motor. The rotational speed n

was estimated from the Fourier analysis of the pressure oscillations. The inlet pressure was set by a pressure regulator to $p_1 \in \{0, 0.5, 1, 1.5, 2\}$ bar_{rel} and kept constant during each measurement. The pressure difference was adjusted by a throttle until outlet pressure of $p_2 \approx 8$ bar_{rel} was reached or the motor was overloaded.

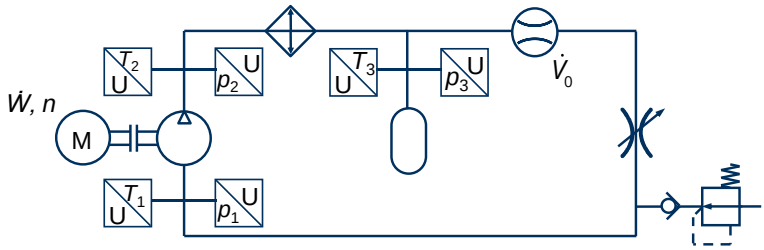

Figure 2 – Test circuit for experimental investigation of the 500-W-compressor performance

The data were obtained within at least 2 minutes of a steady compressor operation, i. e. after pressures and flow rate have settled down to a constant value. The results calculated from the mean values measured over this time are plotted in Figure 3.

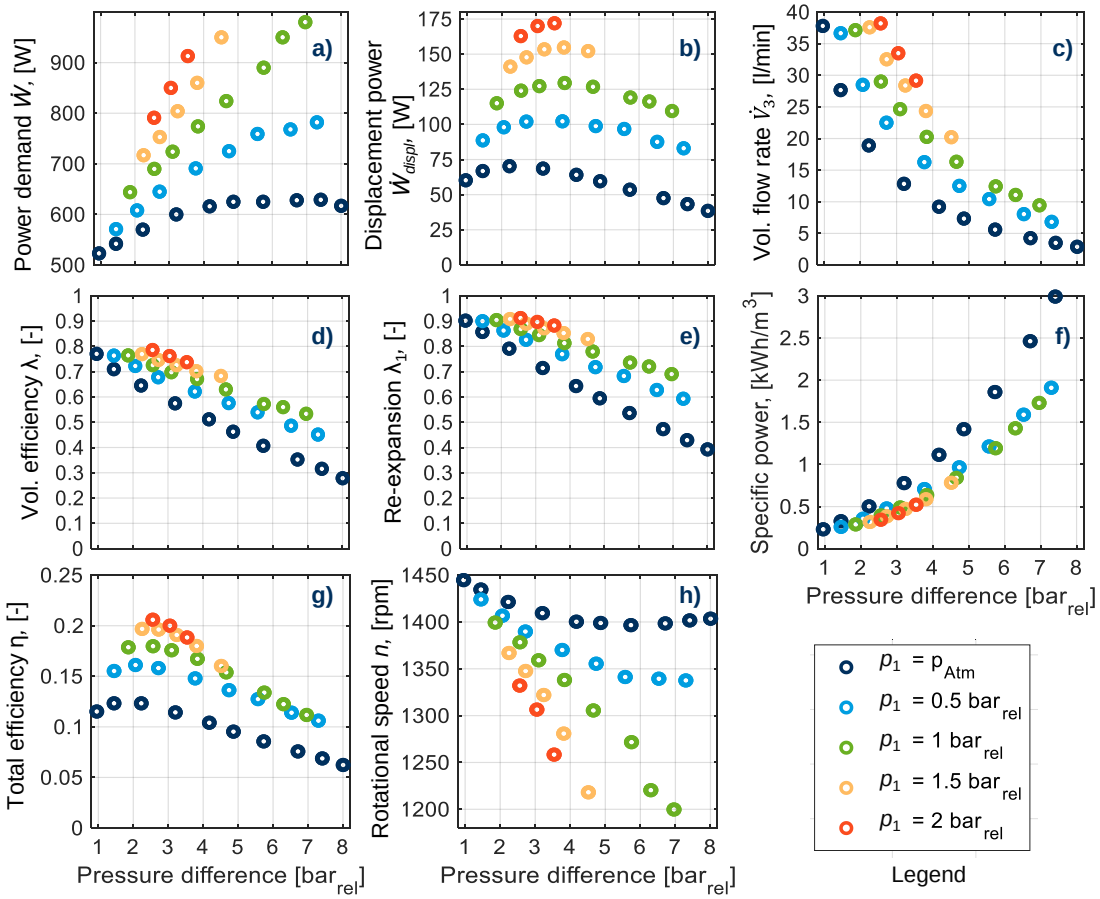

Figure 3 – Experimentally obtained performance characterization of the 500-W-compressor at various inlet pressures p_1 and pressure differences $\Delta p = p_2 - p_1$

Due to compressors under 1 kW designed for operation at inlet pressure above the atmospheric (usually called "booster compressors") are difficult to acquire, the experiments were carried out on a small one-stage, double-piston compressor designed for air intake from the atmosphere only. Despite on sufficient mechanical strength of the inlet port, this matter limited the maximum level of inlet pressure because of an overload of the asynchronous motor at $p_1 \geq 2$ bar_{rel} and $\dot{W} > 900$ W (Figure 3, a)). The motor overload can be also observed by a drastic sagging of rotational speed at high inlet pressures (s. Figure 3, h)).

The theoretical power $\dot{W}_{displ}$ (Figure 3, b) that can be obtained with a displacement machine, such as pneumatic cylinder, driven by the delivered compressed air is calculated from Equation (2). Volumetric flow rate $\dot{V}_3$ (Figure 3, c) is estimated from the measured normal flow rate $\dot{V}_0$, pressure p_3 and temperature T_3 basing on Equation (6). As expected from the theoretical analysis, power demand $\dot{W}$, displacement power $\dot{W}_{displ}$ of a

pneumatic cylinder and volumetric flow rate $\dot{V}_3$ increase with inlet pressure. Volumetric flow rate drops with rising discharge pressure due to the compressibility of air and the pressure-dependence of volumetric efficiency λ. Similar relations of volumetric flow rate and power demand to the pressure difference were also observed within tests of a scroll compressor for natural gas, carried out at different inlet pressures [10]. For displacement power $\dot{W}_{displ}$ being a product of pressure difference Δp and flow rate $\dot{V}_3$, the maximum peak is present. It is noticeable that the point of maximum power shifts towards the higher pressure differences with an increase in inlet pressure. This shift is caused by a lower gradient of the Δp-dependent volumetric efficiency λ at higher inlet pressures additionally contributing to increase in flow rate $\dot{V}_3$.

Volumetric efficiency λ is estimated from the displacement volume V_{displ} = 33.2 cm³ per piston, and rotational speed n applying Equation (8). According to [5], volumetric efficiency is a product of factors, representing re-expansion of the clearance volume λ_1, inlet air density reduction due to throttling in the inlet valve λ_2 and heat absorption while passing the inlet channels λ_3, as well as the leakage factor λ_4 (Equation (9)). While measuring λ_2, λ_3, and λ_4, requires sophisticated equipment, λ_1 can be estimated from the pressure values and the clearance volume of V_{clear} = 5.3 cm³ using Equation (10):

$$\lambda = \frac{\dot{V}_{measured}}{\dot{V}_{theor.}} = \frac{\dot{V}_1}{V_{displ} \times n} \tag{8}$$

$$\lambda = \lambda_1 \times \lambda_2 \times \lambda_3 \times \lambda_4 \tag{9}$$

$$\lambda_1 = 1 - \frac{V_{clear}}{V_{displ}} \times \left[\varepsilon^{\frac{1}{\kappa}} - 1\right] \tag{10}$$

It is remarkable that the volumetric efficiency that mostly depends on the re-expansion term λ_1, rises significantly with increase in inlet pressure. For this reason, the volumetric flow rate is gained even stronger than predicted alone with Equation (6). For example, at Δp = 4 bar and p_1 = 1.5 bar_{rel} compressor delivers more than 2.5 times the flow rate delivered at $p_1 = p_{Atm}$ and the same Δp. This observation dispels the doubts about the poor compressor efficiency at increased inlet pressure. However, it can be expected that at very high inlet pressures p_1 > 5 bar_{rel} the volumetric efficiency will be influenced by inlet air density decrease due to pressure losses in the inlet valve (λ_2). That may be especially relevant for the simple feather valves as in case of the studied compressor.

This discussion leads to analysis of relation of displacement cylinder power $\dot{W}_{displ}$ to power demand $\dot{W}$, noted here as total efficiency η. As in case of $\dot{W}_{displ}$, this relation has a clear optimal point, that moves towards the higher values of Δp with rising p_1. Since inlet pressure reaches p_1 = 1.5…2 bar_{rel}, the efficiency does not increase significantly anymore. However, this phenomenon can be explained with a poor motor performance in the overloaded region above $\dot{W}$ > 800 W. It is expected, that driving the compressor with a more powerful asynchronous motor would enable a further performance increase and operation at higher inlet pressures over p_1 > 2 bar_{rel}.

Nevertheless, the present study shows that the performance improvement of a closed-circuit compressor is measurable and distinguishes itself by both increasing efficiency and compressor delivery. In the given case, volumetric flow rate was more than doubled, and efficiency was increased by about 50…60 %. Another measure of compressor efficiency, specific energy consumption (Figure 3, f) or relation of power demand to the volumetric flow rate, also illustrates a lower energy consumption in the closed system. In contrary to the standard definition of specific energy consumption, the relation of volumetric flow rate to the normal conditions can be misleading in the closed-circuit systems. Therefore, the volumetric flow rate $\dot{V}_3$ related to the conditions after compression and cooling is used here. Facing the fact that large high-performance rotary-screw compressors have a specific energy consumption of ~0.7…0.9 kWh·m³×h⁻¹ at Δp = 7 bar and the tested compressor needs double this specific energy, must be noticed that the smaller the compressor is the lower is its efficiency. Implementation of a closed-circuit system with a well-sized prime mover and a small compressor of industrial quality with a power range of 1…5 kW makes feasible the decrease in specific energy consumption up to the values currently typical only for the large high-performance rotary-screw compressors. This offers a great market opportunity for small compressors to be used for decentralized air supply in the closed-circuit architecture.

EXPERIMENTAL IMPLEMENTATION OF CLOSED-CIRCUIT PNEUMATIC SYSTEM

In the previous section the compressor performance under the constant load, that is constant pressure difference caused by continuous air consumption, was analyzed. To address the uncertainty and anticipations of a negative effect of oscillating pressure and volumetric flow rate consumption by real consumers with discontinuous behavior two pneumatic cylinders were added to the studied compressor. For the sake of demonstrativeness, the cylinders of different size performing different tasks were chosen, as specified in the

Table 1: high-dynamic horizontal handling of a mass within the specified time and extension against the constant force (lifting and descending of a large mass).

Table 1 – Operational cases for two cylinders at pressure Δp = 4 bar_{rel}

Load specification for extension and retraction	Horizontal cylinder H, Ø32×200	Vertical cylinder V, Ø50×200
Handled mass m, [kg]	10	65
Force, F_{ext} // F_{restr}, [N]	0 // 0	640 // -640
Travel time, t_{ext} // t_{retr}, [s]	0.34±0.02 // 0.44±0.03	<3 // <3

The cases were parameterized in the way that both cylinders are properly loaded and not oversized for their tasks. The horizontal cylinder was sized using the Pneumatic Frequency Ratio (PFR) approach proposed by [11]. According to that, both PFR Ω_{retr} = 1.37 and Ω_{ext} = 1.77 correspond to a properly sized cylinder that can operate safely with a standard pneumatic end cushioning. The constant force of the vertical cylinder is calculated to be about 80 % of its theoretical pneumatic force, hence leaving some space for acceleration and overcoming the friction force, not included into the load forces in Table 1. The test circuit is shown in Figure 4.

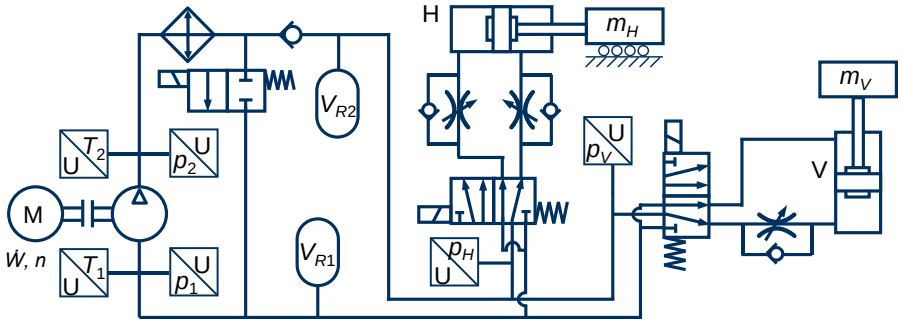

Figure 4 – Test circuit with compressor and two cylinders operating in a closed circuit. Tank volumes on the discharge and suction site are V_{R1} = 9 l and V_{R2} = 2 l respectively.

Before starting the measurements, the system was filled with dry compressed air. The filling pressure depends on the volumes of low-pressure and high-pressure sides (mostly composed of tanks V_{R1} = 9 l and V_{R2} = 2 l), desired steady-state inlet pressure p_1, differential pressure Δp_{cyl} needed for operation of cylinders and their flow rate demand. To estimate Δp_{cyl}, pressure was measured at supply and exhaust ports of the cylinder valve. Differential pressure on compressor Δp is greater than the differential pressure on the cylinder Δp_{cyl} by the value of pressure losses in the piping tubes. Due to no simple method for calculation of the filling pressure is currently present, this pressure was estimated empirically within the tests and amounted p_{fill} = 2…2.65 bar_{rel} for the studied cases. After being filled, the system was disconnected from the pressure source and operated completely autonomous.

Volumetric flow rate, delivered from the compressor, is consumed by the both cylinders, switched every $t_{H.takt}/2$ and $t_{V.takt}/2$ seconds (s. Table 2) in such a way, that cumulative air consumption of the horizontal cylinder is about two times that of the vertical cylinder. The total volumetric flow rate can be determined from the already known compressor performance data shown in Figure 3, c) depending on the inlet pressure and pressure difference. With regards to the different volumes of the cylinders, the horizontal cylinder represents a nearly constant load, and the vertical cylinder brings low-frequent (with frequency of $2/t_{V.takt}$), high-amplitude peak load. In Figure 5 two forms of pressure oscillations caused by overlapping of these different consumption profiles can be easily distinguished.

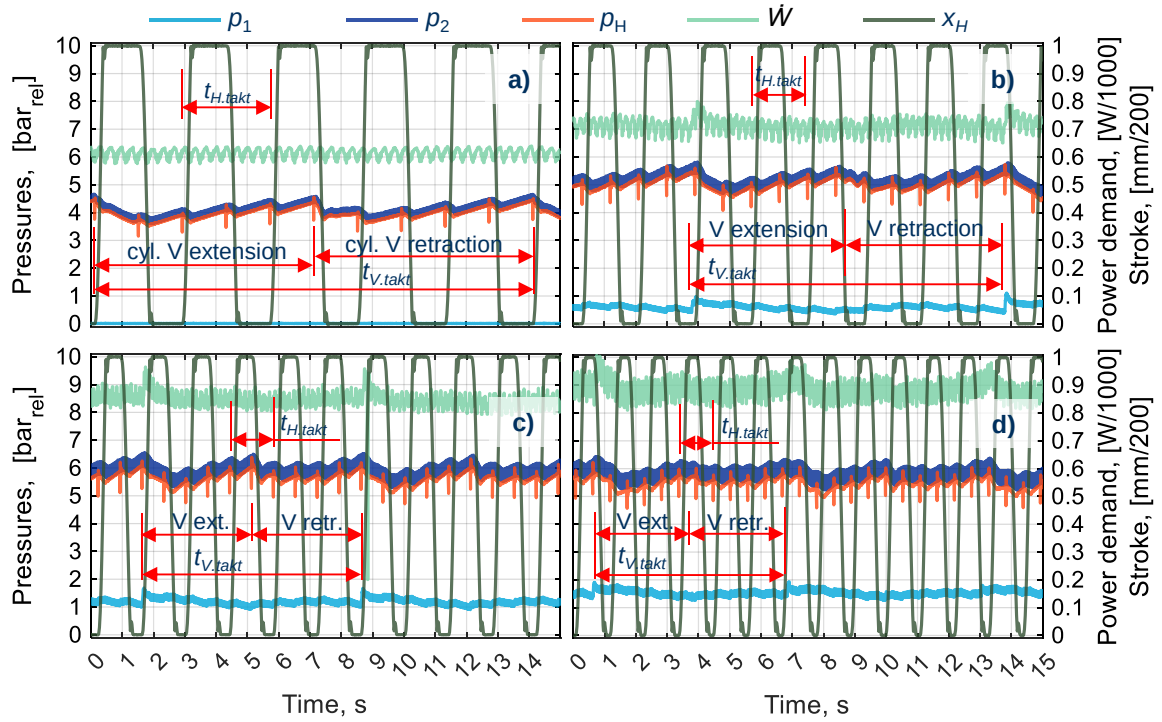

Figure 5 – Fragments of the measured inlet pressure p_1, discharge pressure p_2, supply pressure of horizontal cylinder p_H, power demand $\dot{W}$, and horizontal cylinder stroke x_H at a) p_1 = 0 bar_{rel} (open circuit), b) $p_{1.mean}$ = 0.59 bar_{rel}, c) $p_{1.mean}$ = 1.17 bar_{rel}, d) $p_{1.mean}$ = 1.5 bar_{rel}.

To evaluate the quality of the cylinder operation at different inlet pressures, travel times of both cylinders were captured during the operation for extension and retraction strokes ($t_{H.ext}$ and $t_{H.retr}$ for horizontal and $t_{V.ext}$ and $t_{V.retr}$ for the vertical cylinder in Table 2). Due to the mean differential pressure was slightly above the desired value of Δp_{cyl} = 4 bar_{rel} in cases b) and c), travel times of the vertical cylinder appears to be slightly lower in these cases. The dispersion of travel times within one measurement session is similar for all experiments with the closed circuit and does not exceed that for the open-circuit operation. Hence, the expectations of disruptive and non-representative dynamic behaviour of cylinders in the closed system could not be confirmed. The closed-circuit pneumatics seems to operate as reliable as the classical open system even with the non-constant load. Remarkable is an amplitude decrease of the high-frequent and low-frequent pressure oscillations with increasing inlet pressure.

Table 2 – Cylinder operation in the closed-circuit pneumatic system at $\Delta p \approx 4$ bar_{rel}

$p_{1.mean}$, [bar_{rel}]	Δp, [bar_{rel}]	Δp_{cyl}, [bar_{rel}]	$t_{H.takt}$, [s]	$t_{V.takt}$, [s]	$t_{H.ext}$, [s]	$t_{H.retr}$, [s]	$t_{V.ext}$, [s]	$t_{V.retr}$, [s]	$\dot{W}_{mean}$, [W]	$\dot{V}_3$, [l/min]	η_{cyl}, [-]
0	4.07	3.93	2.8	14	0.36... ...0.37	0.43... ...0.46	2.3... ...2.65	2.64... ...2.65	620	10.1	0.107
0.59	4.62	4.42	1.8	10	0.33... ...0.34	0.41... ...0.43	1.64... ...1.67	2.74... ...2.77	720	15.2	0.155
1.17	4.82	4.52	1.4	7	0.33... ...0.34	0.42... ...0.45	1.61... ...1.69	2.84... ...2.85	851	20.2	0.181
1.5	4.41	4.04	1.1	6.2	0.33... ...0.35	0.43... ...0.46	1.95... ...1.96	2.76... ...2.8	906	24.8	0.184

Considering the efficiency as relation of the mean displacement power of both cylinders to the mean power demand of compressor $\eta_{cyl} = \Delta p_{cyl} \times \dot{V}_3 / \dot{W}_{mean}$, an efficiency increase of 72 % (from 10.7 % to 18.4 %) can be observed when comparing the open circuit and the closed circuit at p_1 = 1.5 bar_{rel}. These values match good with the measurements carried out on compressor with constant pressure and constant flow rate in the previous section (Figure 3, g)).

CONCLUSION

The aim of this study was firstly, to prove experimentally the earlier analytically outlined theory about the increase in efficiency and delivery of a compressor operating at the boosted inlet pressure, and secondly,

to perform the test of a real pneumatic system that is supplied from this compressor and feeds the exhausted air back to its inlet at various pressures within a range from 0 (open circuit) to 1.5 bar_{rel}. The test rig included a small one-stage double-piston compressor with a displacement volume of ca. 33 cm^3 per piston and two pneumatic cylinders of 32 and 50 mm in diameter. The experiments have shown a real increase in efficiency of up to 72 % and the volumetric flow rate gain by factor 2.5. The compressor performance is very similar in both standalone test with continuous volumetric flow demand and in the experiments with discontinuous air consumption. In the latter case, a smaller cylinder has imitated a constant load and the larger cylinder a peak load. No disturbances were observed in the cylinder operation. Both types of operational cases, i. e. high-dynamic motion and extension against the constant force, were performed with the repeatability of the classical open-circuit system. Besides, following points should be noted:

- Volumetric efficiency of compressor rises significantly with increasing inlet pressure.
- The prime mover must be properly sized for an optimal operation with a closed-circuit compressor because of higher torque at higher inlet air density.
- An additional benefit is a considerably lower noise level observed during experiments because the air is neither taken from nor exhausted in the atmosphere.
- Increase in pressure level in both low-pressure and high-pressure sides is favourable for high-dynamic tasks because it increases the stiffness of the air springs in the cylinder.
- Increase in pressure losses caused by higher flow rate and air density is measurable (compare the differences between Δp and Δp_{cyl} for various inlet pressures in Table 2), but not crucial and easily avoidable by a proper sizing of the piping system.
- Due to the relatively short test phases in this study (several minutes only), no major issues with the air leakage from the closed system were observed. However, this will be the case in real applications and a system for leakage compensation must be designed.

An economic benefit of the closed-circuit pneumatic system relies on a higher energy efficiency and hence lower energy costs as well as the possibility to downsize the compressor and hence to decrease investment costs. On the other hand, additional piping lines are needed to convey the exhausted air from the valves to the compressor as well as components for compensation of the leakages. Therefore, especially pneumatic systems with closely located drives can profit from the closed-circuit architecture with a local and decentralized air supply. In this case, the further corners can be cut on the absent piping infrastructure and non-present pressure losses throughout the central pipeline. Besides, in a smaller decentralized closed system with a constant air mass, the leakages are easier to detect, access and eliminate, saving further energy costs.

OUTLOOK

The further research is needed to design and validate the methods and algorithms for calculation of large and complex pneumatic closed-circuit systems. Cost-effective strategies for the volumetric flow management for different types of the air consumption profiles are of a highest interest. As already noted, an automated leakage compensation must be designed in order to make the closed-circuit system appliable for real industrial conditions.

NOMENCLATURE

ε	Compression ratio [-]
η	Efficiency [-]
κ	Isentropic exponent [-]
λ	Volumetric efficiency [-]
ρ	Density [$kg \times m^{-3}$]
Ω	Pneumatic frequency ratio [-]
F	Force [N]
m	Mass [kg]
$\dot{m}$	Mass flow rate [$kg \times s^{-1}$]
n	Rotational speed [s^{-1}]
p	Pressure [bar]
R	Specific gas constant [$J \times kg^{-1} \times K^{-1}$]
t	Time [s]
T	Temperature [°C]
V	Volume [m^3]

$\dot{V}$ Volumetric flow rate [$m^3 \times s^{-1}$]
W Work [J]
$\dot{W}$ Power [W]
x Stroke [m]

REFERENCES

[1] Radermacher, T. et al. “Potenzialstudie Energie- / Kosteneinsparung in der Fluidtechnik. Abschlussbericht”. Climate Change 19/2021, Verlag Umweltbundesamt, 2021, 140 p.

[2] EnEffAH Project Consortium, “EnEffAH – Energy efficiency in production in the drive and handling technology field“, 2012.

[3] Stoll, K. “Pneumatische Steuerungen - Einführung und Grundlagen”. Vogel Business Media, 1999, 288 p.

[4] Gauchel, W. et al. “Using thermodynamic changes of condition for describing system behaviour of air compressor stations”. In: 9th International Conference on Fluid Power, Aachen, 2014, p. 45-55.

[5] Groth, K. „Grundzüge des Kolbenmaschinenbaus. Buch 2: Kompressoren,“ Braunschweig: Vieweg, 1995, 256 p.

[6] Weiß, A. P. „Höhere Energieeffizienz. Theoretische Überlegungen zu einem idealen Druckluftsystem mit geschlossenem Luftkreislauf,“ O+P, Number 5, 2009, pp. 201-205.

[7] E.A.R.S. North America. “Benefits of “Closed Loop” Air Compressor and Air Tool Technology,” I-CAR annual meeting, Technical Presentation, Championsgate, Florida, 2007.

[8] Siminiati, D. “Energy Saving with Close Circuit Pneumatic System”. In: Eng. Rev. 30-2, 2010, pp. 111-116.

[9] von Grabe, C., Murrenhoff, H. “Efficiency Improvement by Air Recuperation through the Use of Ejectors,” In: 8th International Conference on Fluid Power, Dresden, 2012.

[10] Wen, J., Liu, C., Peng, X. “Experimental Investigation of a Horizontal Hermetic Scroll Compressor with Novel Oil Circuit Design,” In: Proceedings of International Compressor Engineering Conference, 2018.

[11] Doll, M., Neumann, R., Sawodny, O. “Dimensioning of pneumatic cylinders for motion tasks”. In: International Journal of Fluid Power, 2015 Vol. 16, No. 1, pp. 11–24.

AN ESTIMATOR FOR AIRCRAFT ACTUATOR CHARACTERISTICS USING SINGULAR VALUE DECOMPOSITION

Felix Larsson
Saab Aeronautics/Linköping University
Felix.larsson@liu.se
Linköping, Östergötland, Sweden

Ludvig Knöös Franzén
Linköping University
Ludvig.knoos.franzen@liu.se
Linköping, Östergötland, Sweden

Christopher Reichenwallner
Saab Aeronautics
Christopher.reichenwallner@saabgroup.com
Linköping, Östergötland, Sweden

Alessandro Dell'Amico
Saab Aeronautics/ Linköping University
Alessandro.dellamico@saabgroup.com
Linköping, Östergötland, Sweden

ABSTRACT

This paper illustrates how Singular Value Decomposition (SVD) and regression analyses can be used to create estimation models for aircraft actuator components by use of industrial data. The estimation models are at the end used to show how an electromechanical actuator´s weight and size will evolve with respect to output force. An essential step in the early design of aircraft is to be able to predict the weight and size of a resulting concept. This weight and size typically include contributions of main components such as wing and fuselage. Weight and size estimations at this stage can also range down to components at a sub-system level, for example, the aircraft actuators. The weight and size of an actuator depends on many parameters, and it is desirable to understand any underlying relationship to make qualified estimations of an actuator's characteristics. However, the knowledge about a design is often limited at an early design stage and the required information is not always available. Consequently, estimations must be made from limited information and desired properties of the actuator. One way to approach this problem is to use SVD. An SVD analysis determines the most influential parameters in a data set and uses these to create an estimation model that only requires a few inputs for estimating the remaining parameters in the data set. An SVD can thereby be used for both identifying the driving parameters in a statistical dataset of existing solutions and to estimate the characteristics of new designs to be developed.
[DOI: https://doi.org/10.3384/ecp196004]

Keywords: *Aircraft Actuation System, Singular Value Decomposition, Statistical Analysis, Estimation Model, Principal Component Analysis*

INTRODUCTION

The aircraft actuation system is one of the most critical systems in an aircraft. The most common actuator technology with high maturity and safety is the servo-hydraulic actuator. Today, electrification of the actuation system is emerging and has been shown promising, where the electromechanical- and the electro-hydrostatic actuators are the most common solutions. Benefits in energy consumption, maintenance and in some cases system weight has been reported. [1] [2] [3]

System weight and size are directly related to cost, performance and fuel burn of an aircraft, especially for fighter aircraft. The size and weight of an aircraft actuator is typically dependent on many different parameters, such as required maximum force, speed, acceleration, redundancy level and thermal time constant. Also, the chosen technology will highly influence the size and weight, where the relationship to the previously mentioned parameters may be different. This can make the selection of technology, with regards to size and weight, dependent on, for example, the required maximum force.

Both size and weight are essential parameters when it comes to the early design of an aircraft and are directly tied to the overall results of the sizing procedure for a new aircraft to be developed. It is consequently important to be able to estimate the weight of the actuation system of an aircraft as early as possible in the design process. However, information about a new design is typically scarce at such a stage and this creates a desire of being able to estimate the characteristics of the actuators with limited information. At a conceptual design stage of a new aircraft platform, the desired aircraft performance and wing geometry to fulfil the given operational requirements should at least be known. From this, it should be possible to derive the maximum hinge moments and roll rates of the aircraft, which in turn can be derived to required force and speed of the actuators. Thereby, a desired model to estimate size and weight of the actuators is presented in Figure 1.

 Proceedings of the 6th Workshop on Innovative Engineering for Fluid Power – WIEFP 2022, 22-23 November 2022. ABIMAQ, São Paulo, SP, Brazil.

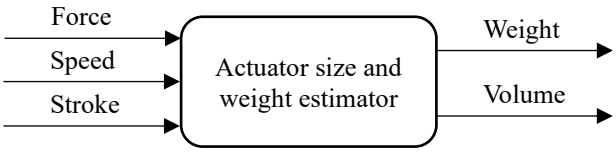

Figure 1: Outline of the desired estimation model.

The main power converters in most electromechanical actuators (EMAs) designed for flight applications are a power electronics control unit (PECU), an electric motor, a ball screw and in some cases a gearbox in between the ball screw and electric motor. There are also many other components and elements needed, such as extra bearings, anti-rotation devices and in some cases brakes. These components include many different parameters which in some sense will affect the final weight and size. The main drivers for size and weight are however the main power converters, i.e., the electric motor, ball screw and gearbox. Previous research provides thorough frameworks for estimation of actuator size and weight, but often much information about the final product is required, and the frameworks often aims at optimizing designs rather than providing simple frameworks for first estimations of size and weight based on limited information. [4] [5] [6] [7]

Objectives

This work aims to provide estimation models for an electromechanical actuator which can be used at an early aircraft conceptual design phase for technology comparisons and selections. The purpose is to use the estimation models for high level comparison of actuators based on the few inputs seen in Figure 1, and to analyse how electromechanical actuators will change in size and weight with respect to the requirements.

Since there is little information publicly available for flight actuators, industrial data will be used to find the relationships between size and weight, and the set inputs shown in Figure 1, for the different components within an EMA. The estimation models will then be used to compile an architecture of an electromechanical actuator where the inputs, which primarily is the maximum output force, will be varied to show how the total weight and size change.

Overall, the long-term objective of this work is to understand whether it may be feasible or not to use electric actuators for a certain platform with respect to size and weight. Today, there is insufficient data present within literature to answer this. This, combined with the lack of high-level estimation methods emphasizes the objectives of this paper.

Additionally, this paper aims to illustrate how a Singular Value Decomposition (SVD) analysis can aid in the identification of principal actuator parameters from statistics of existing solutions and how these can be used to create estimation models that only require a few input parameters. The theoretical fundamental section of this paper describes the underlying theory of an SVD analysis, and some information about the actuator components, while the results and analysis section illustrate the applicability on a data set of existing solutions. The discussion section highlights some alternative approaches and expands on possible opportunities for future work and next steps for this analysis.

THEORETICAL FUNDAMENTALS

This section mentions and elaborates on the approaches and methods that make up the theoretical fundament of this presented work.

Singular Value Decomposition

A Singular Value Decomposition (SVD) utilizes statistical data in order to create estimation models and to improve the understanding of relationships between involved parameters [8]. This is similar to, for example, statistical analyses based on linear regressions. However, a key feature with an SVD is that only a few input parameters are required. This means that all parameters in a data set can be estimated with reasonable accuracy with only a limited number of known or desired parameters. The reason for this is that an SVD builds upon a Principal Component Analysis (PCA) and the dominating parameters in a used data set are thereby identified [9]. An SVD analysis can consequently be used to provide quick estimates of new designs from limited information and to show the dominating relationships between involved parameters. Designs suggested by the SVD model can thereafter be investigated in detail and then possibly be added to the original data set that the SVD once was based on. Similarly, an SVD can also act as a meta model, in for example, optimizations to reduce the computational effort.

Actuator fundamentals

As mentioned in the introduction, an EMA generally consists of at least a PECU, an electric motor and a ball screw. This is illustrated in Figure 2. The weight- and volume studies will be based on this architecture, where a trendline with respect to the inputs mentioned in the introduction is of interest. However, in this work, the PECU will not be included. The focus will thereby be on finding estimation models for the electric motor and the ball screw.

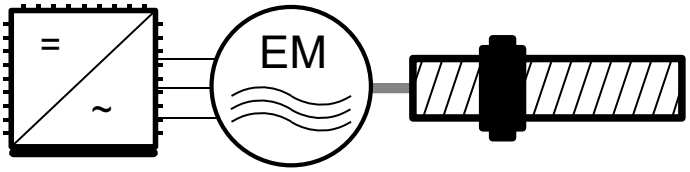

Figure 2: The studied actuator architecture.

The final EMA estimation models for size and weight will be structured as equation (1) and (2).

$$V_{EMA} = \mathrm{V_{BS}(F,S)} + \mathrm{V_{em}(T)} \tag{1}$$

$$m_{EMA} = m_{\mathrm{BS}}(\mathrm{F,S}) + m_{\mathrm{em}}(\mathrm{T}) \tag{2}$$

Where V is the volume, F is the force, S is the stroke, T represents torque and m is the mass. The notation BS stands for ball screw and em stands for electric motor.

Ball screw fundamentals

A ball screw is used for transformation of rotational- into linear-mechanic power. A schematic view of a ball screw is presented in Figure 3. The ball screw estimation models for size and weight will be structured as equation (3) and (4).

$$V_{BS} = A_s(F) * (l_{stroke} + l_{nut}(F)) + V_n, V_n = l_n(F)\frac{\pi(d_n^2(F) - d_S^2(F))}{4} \tag{3}$$

$$m_{BS} = m_{sm}(F) * (l_{stroke} + l_{nut}(F)) + m_n(F) \tag{4}$$

Where A_s is the cut-through shaft area, l is length, V_n is the nut volume, $d_{n,S}$ is the nut and shaft outer diameters, m_{sm} is the shaft mass per meter and m_n is the nut mass.

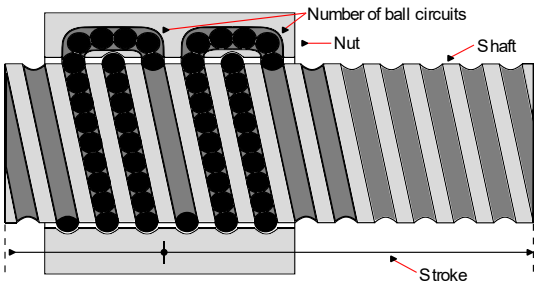

Figure 3: A schematic view of a ball screw.

Electric motor

Previous research has shown that the size and weight of an electric motor can be estimated from motor torque [5]. The torque that the electric motor needs to fulfil can be calculated with equation (5). [10]

$$T = F\frac{L}{2\pi\eta} \tag{5}$$

Where L is the screw lead, η is the screw efficiency, and F is the load force acting on the nut. The torque can thereby be minimized through minimizing the lead, which in turn should minimize the size of the electric motor. The electric motor estimation models for size and weight will be estimated with torque as input which can be calculated from the force requirement with equation (5).

METHODOLOGY

The used methodology in this work is presented in Figure 4. First, the necessary data was gathered from well-known component manufactures. When sufficient data had been found, regression analyses were used to find the relationship between inputs, size and weight for the electric motors. For the ball screw size and weight estimation, SVD analyses were used since many different parameters had to be estimated from very few inputs.

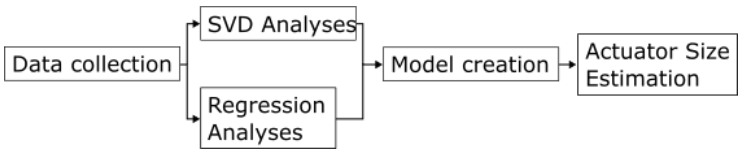

Figure 4: The used methodology and workflow to arrive at an estimator model for actuator sizes.

Subsequently, the component estimation models were connected to create an actuator architecture according to Figure 2. This was thereafter used to study how weight and size evolved with the inputs according to industrial data.

RESULTS AND ANALYSIS

To perform the SVD- and regression analyses, statistics of existing electric motors and ball screws had to be gathered and compiled. The ball screw data was collected from THK, where their caged ball and precision ball screws were selected (SBN, BNFN). [11] The gathered parameters from these specifications were:

- Shaft diameter, lead and mass per length
- Number of closed ball circuits in nut
- Static load rating of ball screw
- Nut volume and mass

With this data, an SVD analysis was performed in Microsoft Excel using an implemented macro. The obtained statistical values were converted into log scale before the SVD analysis. The reason for this was to obtain a better structure of the model due to the size difference of the entries in the collected data set.
The results of the analysis and resulting SVD model can be seen in Figure 5. The four leftmost columns in Figure 5 shows that the "*SBN 1604-5*" reference ball screw from the data set is estimated with zero percent relative error for every variable in the SVD model. The reason for this is that all SVD variables are used and that the ball screw is included in the used data set. However, as mentioned before, one of the benefits with an SVD model is that only a few input parameters are required, and many of the SVD variables in the right-hand side column marked in yellow can consequently be set to zero. The "*w-diagonal*" column on the right side in Figure 5 indicates the significance of the different variables, and it can be seen that the most significant variables for the estimation model are the once corresponding to outer shaft diameter, screw lead and the number of recirculating circuits of balls. Consequently, all SVD variables except the ones in the first three rows are set to zero to create an estimation model that only require three inputs. This reduced SVD model can be seen in Figure 6. The maximum relative error of the estimation has now increased to 20% as seen in the second leftmost column. The largest difference comes from the dynamic load rating while all other parameters are estimated with little difference. Only three parameters are thereby used to estimate the remaining 10 from the data set within 20% relative error.

	Rel error	SBN 1604-5	Estimate	Adjusted	Result	Average														SVD variables	w-diagonal	residual
Outer diameter shaft	0,00	16,00	16,00	1,20	-0,48	1,68	0,177	-0,027	0,002	-0,019	0,011	-0,002	0,005	-0,002	0,007	-0,003	-0,001	0,005	0,002	-2,72	9,11	75,14
Lead	0,00	4,00	4,00	0,60	-0,44	1,04	0,143	0,041	-0,112	0,002	-0,021	-0,020	0,008	0,015	0,001	-0,003	0,000	0,000	-0,001	-0,53	2,86	0,42
Number of circuits	0,00	1,00	1,00	0,00	-0,17	0,17	0,057	0,122	0,136	0,004	-0,021	-0,012	0,004	0,001	0,010	-0,001	0,000	-0,001	-0,001	0,13	1,65	0,21
Dynamic load rating	0,00	5,30	5,30	0,72	-0,98	1,70	0,302	0,132	-0,028	0,038	0,024	-0,014	0,010	-0,002	0,002	0,006	0,000	0,000	0,001	-0,66	0,79	0,20
Static load rating	0,00	8,00	8,00	0,90	-1,22	2,12	0,403	0,143	0,035	0,010	0,023	0,000	-0,008	0,001	-0,011	-0,005	0,000	0,000	-0,001	-1,56	0,53	0,15
Nut outer diameter	0,00	36,00	36,00	1,56	-0,41	1,97	0,149	-0,011	-0,017	-0,010	0,006	0,005	0,010	-0,006	0,003	-0,002	0,002	0,003	-0,002	0,74	0,39	0,15
Nut flange diameter	0,00	59,00	59,00	1,77	-0,36	2,13	0,134	-0,003	-0,024	-0,010	0,006	0,002	0,003	-0,009	0,007	-0,004	0,000	-0,004	0,004	-1,90	0,32	0,17
Nut lange width	0,00	11,00	11,00	1,04	-0,23	1,27	0,107	0,012	-0,048	-0,002	-0,002	-0,015	-0,031	-0,009	0,007	0,001	0,000	0,001	-0,001	-1,05	0,26	0,06
Nut length	0,00	53,00	53,00	1,72	-0,50	2,23	0,184	0,119	0,004	-0,008	-0,027	0,015	-0,009	0,009	-0,003	0,002	0,001	0,002	0,004	1,58	0,19	0,06
Shaft inertia per length	0,00	0,00	0,00	-7,30	-1,88	-5,42	0,731	-0,205	0,032	0,039	-0,014	0,001	-0,001	0,001	-0,001	0,000	0,000	0,000	0,000	1,53	0,09	0,02
Nut mass	0,00	0,42	0,42	-0,38	-1,20	0,82	0,442	0,097	-0,052	-0,024	-0,015	0,021	0,006	-0,010	0,002	0,002	-0,001	-0,001	-0,002	0,07	0,02	0,01
Shaft mass/meter	0,00	1,35	1,35	0,13	-0,95	1,08	0,364	-0,054	0,033	-0,070	0,017	-0,012	-0,001	0,010	-0,001	0,003	0,000	-0,001	0,000	-0,75	0,06	0,01
Turns	0,00	2,50	2,50	0,40	-0,01	0,40	-0,005	0,002	-0,010	0,016	0,024	0,024	-0,007	0,017	0,011	0,000	0,000	-0,001	-0,001	-1,01	0,06	0,01
	0,00																					

Figure 5: The Singular Value Decomposition (SVD) model of the ball screw.

	Rel error	SBN 1604-5	Estimate	Adjusted	Result	Average														SVD variables	w-diagonal	residual
Outer diameter shaft	0,03	16,00	16,44	1,22	-0,47	1,68	0,177	-0,027	0,002	-0,019	0,011	-0,002	0,005	-0,002	0,007	-0,003	-0,001	0,005	0,002	-2,72	9,11	75,14
Lead	0,04	4,00	4,14	0,62	-0,43	1,04	0,143	0,041	-0,112	0,002	-0,021	-0,020	0,008	0,015	0,001	-0,003	0,000	0,000	-0,001	-0,53	2,86	0,42
Number of circuits	0,07	1,00	0,93	-0,03	-0,20	0,17	0,057	0,122	0,136	0,004	-0,021	-0,012	0,004	0,001	0,010	-0,001	0,000	-0,001	-0,001	0,13	1,65	0,21
Dynamic load rating	0,20	5,30	6,37	0,80	-0,90	1,70	0,302	0,132	-0,028	0,038	0,024	-0,014	0,010	-0,002	0,002	0,006	0,000	0,000	0,001	0,00	0,79	0,20
Static load rating	0,13	8,00	9,00	0,95	-1,17	2,12	0,403	0,143	0,035	0,010	0,023	0,000	-0,008	0,001	-0,011	-0,005	0,000	0,000	-0,001	0,00	0,53	0,15
Nut outer diameter	0,02	36,00	36,83	1,57	-0,40	1,97	0,149	-0,011	-0,017	-0,010	0,006	0,005	0,010	-0,006	0,003	-0,002	0,002	0,003	-0,002	0,00	0,39	0,15
Nut flange diameter	0,02	59,00	58,05	1,76	-0,37	2,13	0,134	-0,003	-0,024	-0,010	0,006	0,002	0,003	-0,009	0,007	-0,004	0,000	-0,004	0,004	0,00	0,32	0,17
Nut lange width	0,16	11,00	9,29	0,97	-0,30	1,27	0,107	0,012	-0,048	-0,002	-0,002	-0,015	-0,031	-0,009	0,007	0,001	0,000	0,001	-0,001	0,00	0,26	0,06
Nut length	0,13	53,00	46,10	1,66	-0,56	2,23	0,184	0,119	0,004	-0,008	-0,027	0,015	-0,009	0,009	-0,003	0,002	0,001	0,002	0,004	0,00	0,19	0,06
Shaft inertia per length	0,01	0,00	0,00	-7,29	-1,88	-5,42	0,731	-0,205	0,032	0,039	-0,014	0,001	-0,001	0,001	-0,001	0,000	0,000	0,000	0,000	0,00	0,09	0,02
Nut mass	0,14	0,42	0,36	-0,44	-1,26	0,82	0,442	0,097	-0,052	-0,024	-0,015	0,021	0,006	-0,010	0,002	0,002	-0,001	-0,001	-0,002	0,00	0,02	0,01
Shaft mass/meter	0,02	1,35	1,33	0,12	-0,96	1,08	0,364	-0,054	0,033	-0,070	0,017	-0,012	-0,001	0,010	-0,001	0,003	0,000	-0,001	0,000	0,00	0,06	0,01
Turns	0,04	2,50	2,59	0,41	0,01	0,40	-0,005	0,002	-0,010	0,016	0,024	0,024	-0,007	0,017	0,011	0,000	0,000	-0,001	-0,001	0,00	0,06	0,01
	0,20																					

Figure 6: The reduced SVD model.

As a small validation test, an analysis was made on a ball screw not included in the original data set that the SVD was based on. This was done to see how well the ball screw could be estimated with the obtained model. Here, the three SVD variables were varied in order to minimize the overall difference between the reference and the estimate of the ball screw. The results of this can be seen in Figure 7.

	Rel error	BNFN 10020A-7.5	Estimate	Adjusted	Result	Average														SVD variables	w-diagonal	residual
Outer diameter shaft	0,04	100,00	104,05	2,02	0,34	1,68	0,177	-0,027	0,002	-0,019	0,011	-0,002	0,005	-0,002	0,007	-0,003	-0,001	0,005	0,002	2,00	9,11	75,14
Lead	0,01	20,00	19,88	1,30	0,26	1,04	0,143	0,041	-0,112	0,002	-0,021	-0,020	0,008	0,015	0,001	-0,003	0,000	0,000	-0,001	0,72	2,86	0,42
Number of circuits	0,06	3,00	2,81	0,45	0,28	0,17	0,057	0,122	0,136	0,004	-0,021	-0,012	0,004	0,001	0,010	-0,001	0,000	-0,001	-0,001	0,54	1,65	0,21
Dynamic load rating	0,05	253,80	242,25	2,38	0,68	1,70	0,302	0,132	-0,028	0,038	0,024	-0,014	0,010	-0,002	0,002	0,006	0,000	0,000	0,001	0,00	0,79	0,20
Static load rating	0,02	1105,40	1125,52	3,05	0,93	2,12	0,403	0,143	0,035	0,010	0,023	0,000	-0,008	0,001	-0,011	-0,005	0,000	0,000	-0,001	0,00	0,53	0,15
Nut outer diameter	0,04	170,00	177,58	2,25	0,28	1,97	0,149	-0,011	-0,017	-0,010	0,006	0,005	0,010	-0,006	0,003	-0,002	0,002	0,003	-0,002	0,00	0,39	0,15
Nut flange diameter	0,01	243,00	241,33	2,38	0,25	2,13	0,134	-0,003	-0,024	-0,010	0,006	0,002	0,003	-0,009	0,007	-0,004	0,000	-0,004	0,004	0,00	0,32	0,17
Nut flange width	0,08	32,00	29,43	1,47	0,20	1,27	0,107	0,012	-0,048	-0,002	-0,002	-0,015	-0,031	-0,009	0,007	0,001	0,000	0,001	-0,001	0,00	0,26	0,06
Nut length	0,03	471,00	482,98	2,68	0,46	2,23	0,184	0,119	0,004	-0,008	-0,027	0,015	-0,009	0,009	-0,003	0,002	0,001	0,002	0,004	0,00	0,19	0,06
Shaft inertia per length	0,07	0,00	0,00	-4,08	1,33	-5,42	0,731	-0,205	0,032	0,039	-0,014	0,001	-0,001	0,001	-0,001	0,000	0,000	0,000	0,000	0,00	0,09	0,02
Nut mass	0,08	51,84	56,01	1,75	0,93	0,82	0,442	0,097	-0,052	-0,024	-0,015	0,021	0,006	-0,010	0,002	0,002	-0,001	-0,001	-0,002	0,00	0,02	0,01
Shaft mass/meter	0,08	57,13	61,72	1,79	0,71	1,08	0,364	-0,054	0,033	-0,070	0,017	-0,012	-0,001	0,010	-0,001	0,003	0,000	-0,001	0,000	0,00	0,06	0,01
Turns	0,02	2,50	2,46	0,39	-0,01	0,40	-0,005	0,002	-0,010	0,016	0,024	0,024	-0,007	0,017	0,011	0,000	0,000	-0,001	-0,001	0,00	0,06	0,01
	0,08																					

Figure 7: The validation test and estimation of a reference ball screw.

As seen in Figure 7, the characteristics for the reference ball screw of type *BNFN 10020A-7.5* has been inserted in the third column from the left. The maximum relative error found is consequently around 8% after adjusting the three SVD variables. In this case, the largest difference is found in the *nut flange width* and the *shaft mass/meter* parameters.

It can be assumed that the lead should be as low as possible to reduce the required torque by the electric motor, which should keep the motor as small as possible. Thereby, it is interesting to find the relationships between the ball screw rated load, and all the other parameters, when the lead is kept as low as possible. These

relationships can be found by utilizing the SVD estimation model from Figure 7 with the built-in solver in Excel. Characteristics of "yet-to-be-designed" ball screws can thereby be estimated with the three remaining SVD variables. This is done by optimizing their values so that the given requirements are fulfilled as best as possible. The built-in solver in Excel was consequently used for this purpose. The solver's objective function was specified as a minimization of the lead requirement with the three SVD variables as design parameters. The SVD variables were constrained to only vary between -2 and 2 to allow light extrapolation from the original data set (values between -1 and 1 corresponds to an interpolation in an SVD analysis). Additional constraints were subsequently added to account for different requirements on static-load rating and number of circuits. The solver was then used on the SVD model to give estimates for all characteristics under varying requirements and constraints. More specifically, the requirement on static-load rating was varied between 0 and 300kN for each number of circuits requirement, which was specified as either 1, 2 or 3. Consequently, this analysis resulted in 37 different estimated ball screw designs. Figures 8, 9 and 10 shows some of the resulting characteristics for the estimated ball screw designs.

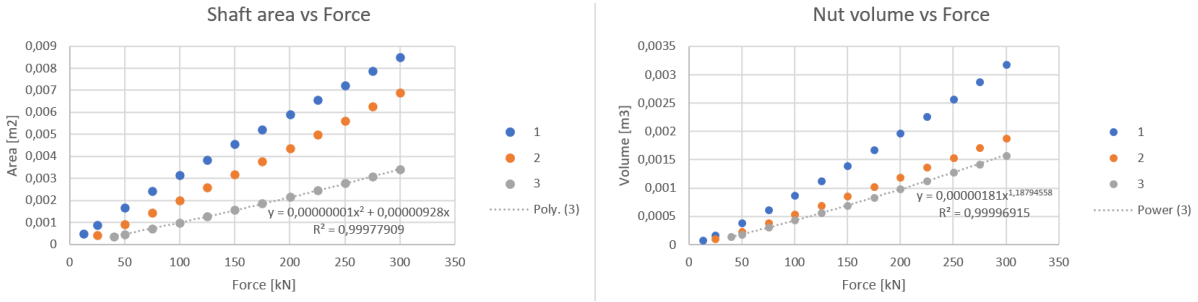

Figure 8: The left graph shows the relationship between force and shaft area and the relationship between force and nut volume is shown to the right.

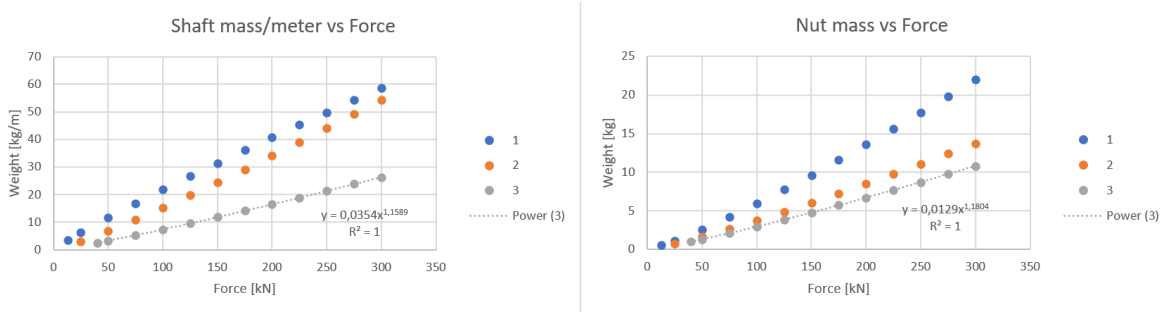

Figure 9: The left graph shows the relationship between force and shaft mass per meter while the relationship between force and nut mass is shown in the right graph.

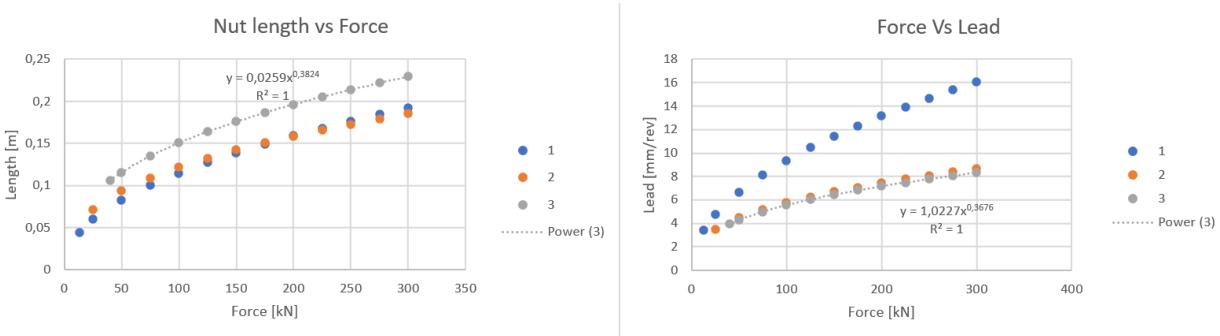

Figure 10: The left graph shows the relationship between force and nut length while the relationship between force and lead is shown in the right graph.

The results from Figures 8, 9 and 10 were thereafter used to create the final estimation model for the ball screws. This was done by fitting exponential trendlines to the presented graphs. However, as seen in Figure 9, the ball screws with 3 rows of balls are generally the lighter options in terms of weight. Consequently, these are

of most interest and their corresponding relationships from the trendline fitting are presented below in equations (6-11).

$$m_{sm} = 0{,}0354 * F^{1{,}16}\ [kg/m] \tag{6}$$

$$A_s = 1 * 10^{-8} * F^2 + 9{,}28 * 10^{-6} * F\ [m^2] \tag{7}$$

$$m_n = 0{,}0129 * F^{1{,}18}\ [kg] \tag{8}$$

$$l_n = 0{,}0259 * F^{0{,}38}\ [m] \tag{9}$$

$$V_n = 1{,}8 * 10^{-6} * F^{1{,}19}\ [m^3] \tag{10}$$

$$L = 1{,}023 * \mathrm{F}^{0{,}37}\ [mm/rev] \tag{11}$$

Here, F represents the static load rating in kN.

The electric motor data was collected from Bosch Rexroth, where the selected motor type was a permanent magnet synchronous motor (PMSM) [12]. This motor type is used in aircraft EMAs due to its high-power density, high efficiency and high response.

For the estimation of electric motor size and weight, regression analyses were made to find how weight and volume varies with output torque. For every electric motor size and weight, four output torque levels were specified in the data. These were the *maximum torque* that the motor can produce, and the *continuous torque* which can be held at standstill with a maximum temperature increase of 60 K in the stator when it is cooled by *natural convection, forced convection* or *liquid cooling*. The results of this can be seen in Figure 11 and 12.

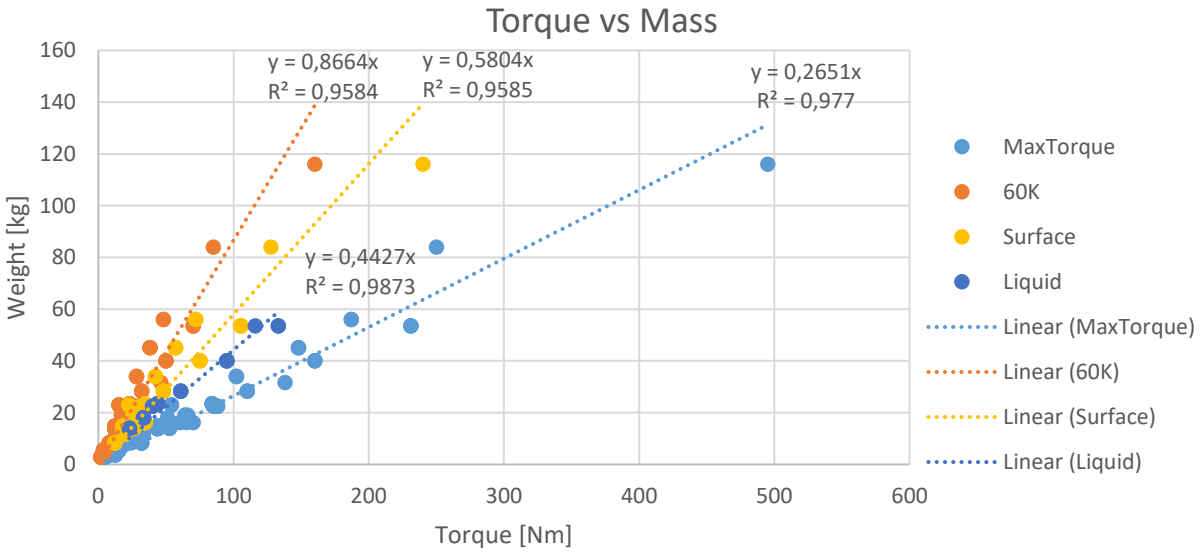

Figure 11: Torque and weight regression analysis of the PMSM data.

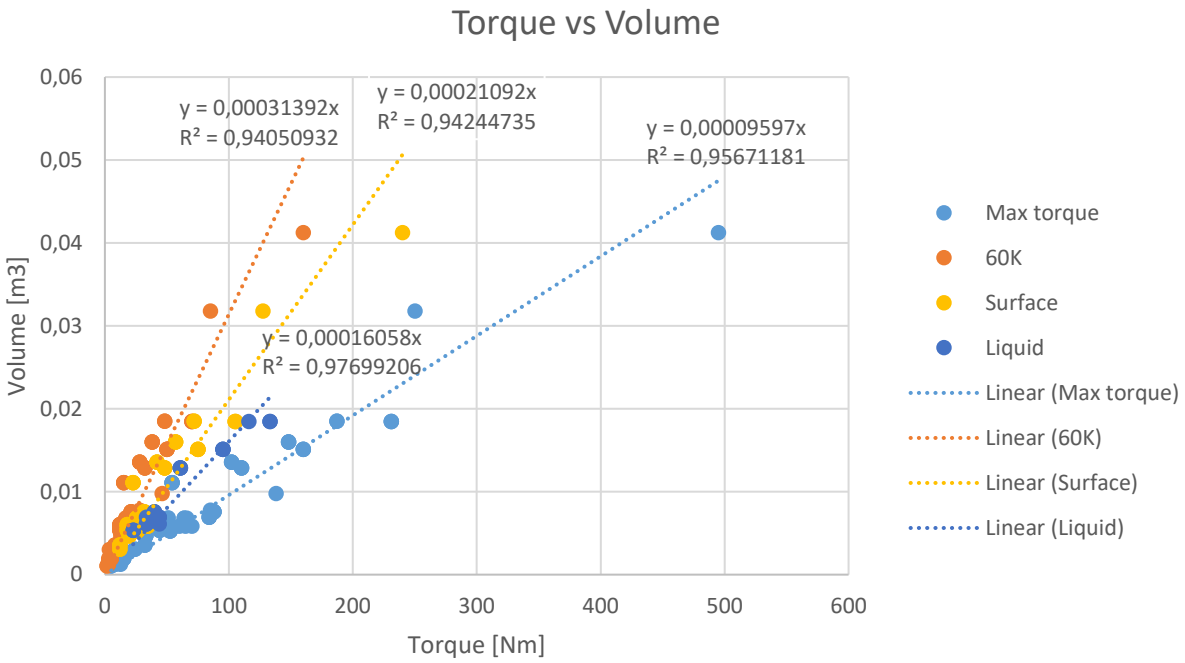

Figure 12: Torque and volume regression analyses of the PMSM data.

The weight and volume estimation models for the PMSM based on the regression analyses are presented in equations (12-19).

$$m_{MaxTorque} = 0{,}265 * T_{Max} \tag{12}$$

$$m_{LiquidCooled} = 0{,}443 * T_{Max} \tag{13}$$

$$m_{FanCooled} = 0{,}580 * T_{Max} \tag{14}$$

$$m_{NaturalConvection} = 0{,}866 * T_{Max} \tag{15}$$

$$V_{MaxTorque} = 9{,}597 * 10^{-5} * T_{Max} \tag{16}$$

$$V_{LiquidCooled} = 1{,}606 * 10^{-4} * T_{Max} \tag{17}$$

$$V_{FanCooled} = 2{,}109 * 10^{-4} * T_{Max} \tag{18}$$

$$V_{NaturalConvection} = 3{,}139 * 10^{-4} * T_{Max} \tag{19}$$

With the estimation models created for the ball screw and electric motor, the total mass and volume of an EMA with a single ball screw and PMSM was estimated with equations (1-5). The results of these models with varying force requirement can be found in Figures 13 and 14.

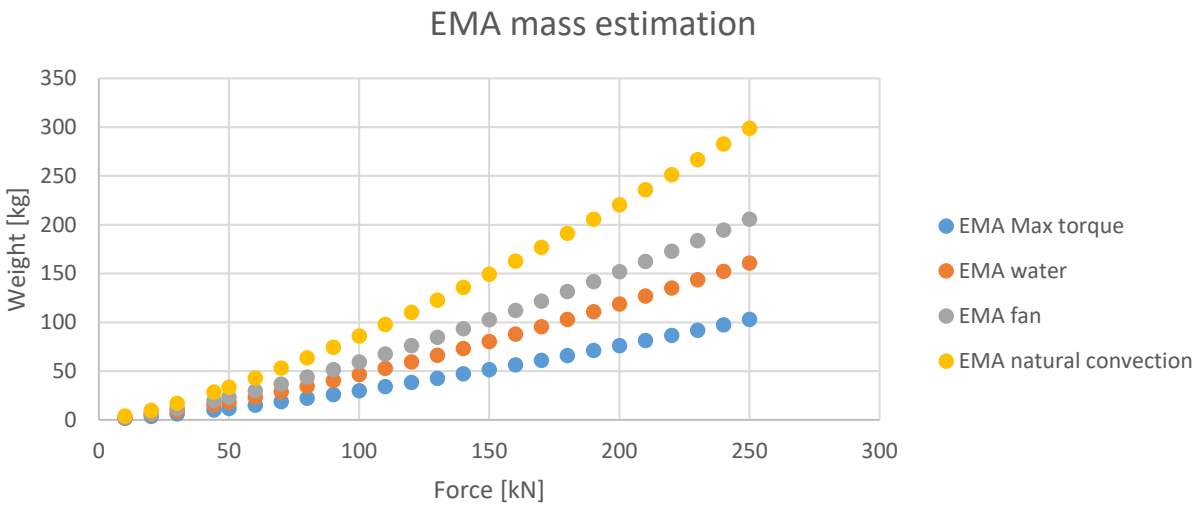

Figure 13: The result of the EMA weight estimation model with varied force input.

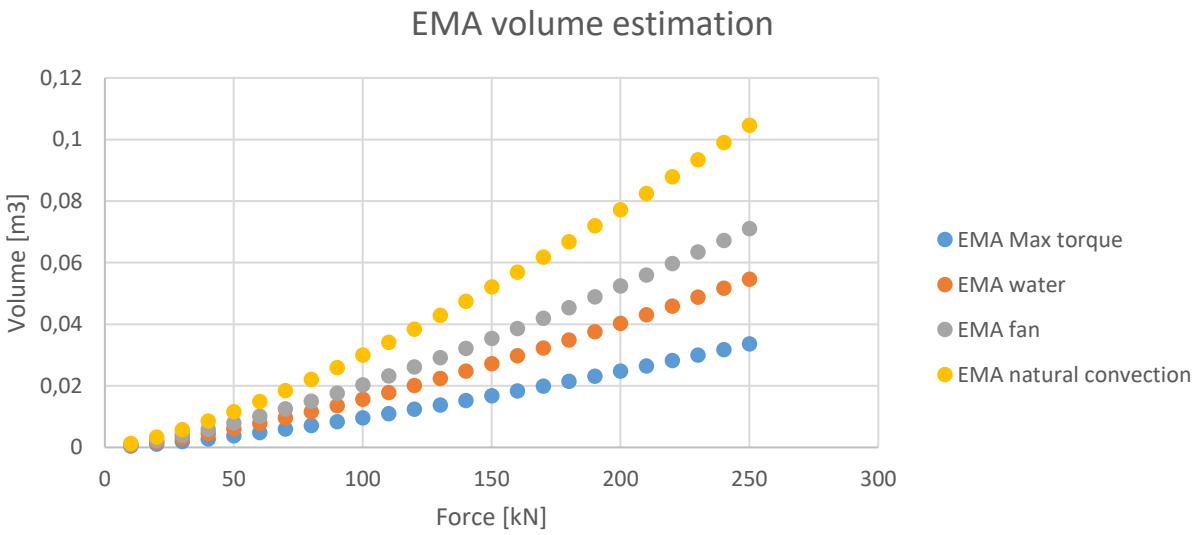

Figure 14: The result of the EMA volume estimation model with varied force input.

DISCUSSION

The results in the previous section have shown how statistics of existing solutions can be used to create estimation models for the design of new actuators. A combination of regression and SVD analyses were used in this study, although, there are many other ways for creating estimation models, such as machine learning techniques. However, such techniques typically offer less transparency compared to, for example, regular regressions between variables and SVD analyses. The SVD analyses were only performed on the ball screw statistics. Regular regression models could have worked in this case as well, however, the relationships between parameters would in that case have to be determined manually. This would have added to the complexity of the method and uncertainty about the estimations.

The validation of the SVD analysis showed good agreement with the reference ball screw's characteristics with the three SVD variables. However, a future validation of the SVD estimation model could involve approximating the characteristics for several ball screws that have been excluded from the used data set and SVD analysis. This could thereby give a better indication of the model's validity over a wider range of ball screw designs. Another possibility is to also create an SVD analysis of the electric motor data. This could possibly

ease the design process and an optimization could be used to obtain a complete actuator design automatically, rather than doing it manually.

One of many possible topics for future work is to expand the used datasets to include even more parameters. This could include parameters that are required to set up simulation models for analysis of, for example, performance and power consumption. With such estimation models, actuators could be compared with respect to many attributes at an early stage of aircraft conceptual design, and thereby provide a better decision basis with respect to actuator technologies. An SVD could consequently be used to estimate an even higher number of unknown parameters for a new actuator system than shown in this paper, thus increasing the overall fidelity. The SVD estimations with the solver currently involve some manual labour. Consequently, future improvements of this presented work involve automizing the estimation process. This could, for example, be done with user-implemented macros in Excel together with a design of experiments (DOE) that specifies the different cases that are to be run. A higher degree of automation would also allow for easier continues updates in the underlying data set that the estimations originally are based on. This would therefore ensure that the estimates are up to date if additional information is introduced to the used data set. Consequently, this is a prominent area for future work for the presented study.

Overall, this work is part of a larger scope, where the intention is to compare different actuator technologies, such as electro-hydrostatic-, electromechanical- and servo-hydraulic actuators, with respect to size and weight. The next step within the scope of this work is to use the obtained estimation models to predict the size and weight of an actuator architecture which has been used in an aircraft, and were weight and size is known. Then, it would be possible to compare the estimation with real data and in that way adjust the estimation model to be more accurate.

CONCLUSIONS

This paper has shown how an estimator for aircraft actuator characteristics can be created with statistics and various regression analyses. A Singular Value Decomposition (SVD) was used as a convenient way for identifying the principal components of a used data set and to estimate characteristics from limited information. The results from the performed SVD and regression analyses showed that simple estimation models could be obtained. The results also show that the methodology used in this work can be used to create estimation models of electromechanical actuators with respect to industrial data where growth trends with based on output force and stroke can be found. The estimation models were found to be accurate with respect to the relative errors in the SVD model and the R^2-values in excel. This means that it is possible to estimate size and weight of the actuator components based on limited information, and from this, a good indication of the total size and weight of an aircraft actuator can be found. However, to predict the weight and size of aircraft actuators, the data must be compared and, if found necessary, adjusted with realistic data of physical actuators.

REFERENCES

[1] S. C. Jensen, G. D. Jenney, B. Raymond and D. Dawson, "Flight test experience with an electromechanical actuator on the f-18 systems research aircraft," in The 19th Digital Avionics Systems Conference, 2000.

[2] J. Li, Z. Yu, Y. Huang and Z. Li, "A review of electromechanical actuation system for more electric aircraft," in IEEE/CSAA International Conference on Aircraft Utility Systems (AUS), Beijing, 2016.

[3] G. Qiao, G. Liu, Z. Shi, Y. Wang, S. Ma and T. C. Lim, "A review of electromechanical actuators for more/all electric aircraft systems," Journal of Mechanical Engineering Science, Vols. 232, Part C, 2018.

[4] M. Budinger, A. Reysset, T. El Halabi, C. Vasiliu and J.-C. Maré, "Optimal preliminary design of electromechanical actuators," Journal of Aerospace Engineering, pp. 1-19, 2013.

[5] M. Budinger, O. Stephane and J.-C. Maré, "Automated preliminary sizing of electromechanical actuator architectures," 2008.

[6] Chakraborty, D. N. Marvis, M. Emeneth and A. Schneegans, "A Methodology for Vehicle and Mission Level Comparison of More Electric Aircraft Subsystem Solutions - Application to the Flight Control Actuation System," Journal of Aerospace Engineering, 2014.

[7] Linderstam, "Analytical tool for electromechanical actuators for primary and secondary flight control.," Master´s thesis, Karlstad University, 2019.

[8] P. Krus, "Models Based on Singular Value Decomposition for Aircraft Design," in In proceedings of the Aerospace Technology Congress, Stockholm, 2016.

[9] Z. Jaadi, "A Step-by-Step Explanation of Principal Component Analysis (PCA)," Built In, 26 September 2022. [Online]. Available: https://builtin.com/data-science/step-step-explanation-principal-component-analysis. [Accessed 26 October 2022].

[10] Mathworks, "Leadscrew," Mathworks, [Online]. Available: https://se.mathworks.com/help/sdl/ref/leadscrew.html. [Accessed 28 10 2022].

[11] THK, "Product information - Ball Screw," THK, [Online]. Available: https://tech.thk.com/en/products/thkdlinks.php?id=359. [Accessed 10 09 2022].

[12] Bosch Rexroth, "Synchronous servo motors - MSK," Bosch Rexroth, 07 07 2021. [Online]. Available: https://www.boschrexroth.com/en/xc/products/product-groups/electric-drives-and-controls/motors-and-gearboxes/synchronous-servo-motors/msk/self-cooled. [Accessed 10 09 2022].

THERMOHYDRAULIC MODELING OF AN ELECTRO-HYDRAULIC SERVO ACTUATOR ON DAMPED MODE

Marina Brasil Pintarelli
ITA, Embraer
mabrapin@gmail.com
São José dos Campos, SP, Brazil

Emília Villani
ITA
evillani@ita.br
São José dos Campos, SP, Brazil

Ronaldo Horácio Cumplido Neto
Embraer
ronaldo.neto@embraer.com.br
São José dos Campos, SP, Brazil

ABSTRACT

Hydraulically powered flight control systems are widely used in aviation, especially for commercial aircraft, which require significant forces from system actuators to control the applicable surfaces as demanded. These systems are being studied and are evolving to become smaller, lighter, and more efficient. These improvements bring several advantages, such as payload increase and drag reduction. However, as these systems are optimized, and their dimensions are reduced, the thermal effects of fluid flow become more relevant. Especially when the working fluid passes through small orifices, excessive heat can eventually compromise the equipment's performance and damage its internal subcomponents. When we analyze the damped mode operation of actuation systems presented on some commercial aircraft, these restrictions become even more relevant – knowing that the damping orifice diameter can be significantly reduced to provide the desired performance for the operation. Therefore, the main goal of this study is to analyze and evaluate the thermal impact on an Electro-Hydraulic Servo Actuator (EHSA) while in damped mode operation, contributing to the industry and the literature in this kind of assessment. Through the research presented, it's possible to estimate the temperature of the system's components and, consequently, avoid malfunctions caused by overheating. Furthermore, developing a model allows the simulation of various environmental conditions, reducing rig costs or in-flight tests. The modeling approach was conducted on the MATLAB/Simulink platform. It was based on two main points that improved model comprehension during its development and minimized errors: the building blocks philosophy of segregating each component's influence and model, and the continuous validation of the model through a comparison with a physics-integrated software (AMESim).
[DOI: https://doi.org/10.3384/ecp196005]

Keywords: *flight control system, thermohydraulic modeling, damped operation, electro-hydraulic servo actuator (EHSA)*

INTRODUCTION

Hydraulically powered flight control systems are widely used in aviation, mainly for primary and secondary flight control surfaces. The primary surfaces are essential for aircraft control and must meet safety requirements, leading to complex architectures. One requirement is to have redundancies to guarantee a low failure probability [1]. Usually, the redundancy required in a flight control system can be met with two actuators for each primary surface with independent power sources [2]. Depending on the aircraft design, the operating flight control system mode is called active-active (both actuators apply force at the surface) or active-standby (one actuator activated and one on standby). The redundancy configuration is chosen during aircraft development due to weight, performance, and load requirements.

For both configurations (active-active and active-standby), if there is a failure in one actuator, the faulty actuator goes into the damped or bypass mode, and the remaining actuator needs to be engaged. However, during this operation, the interaction between actuators' dynamic damping and/or stiffness with the aeroelastic characteristics of the aircraft wing is impacted. Thereby, the vibratory behavior of the system is affected. If vibrations at specific frequencies occur, they can increase in case there is no energy dissipation from the system, resulting in a catastrophic aircraft failure. Thus, during the design of flight control system components, mainly primary actuators, a damped valve, which embeds a calibrated orifice, can provide damping forces to change the vibratory behavior of the system precluding a flutter.

 Proceedings of the 6th Workshop on Innovative Engineering for Fluid Power – WIEFP 2022, 22-23 November 2022. ABIMAQ, São Paulo, SP, Brazil.

The damper effect is due to the passage of hydraulic fluid between the actuator chambers through a mode select valve. From the system design point of view, active-active has two operating modes: normal operation (when both actuators are suitable for operation) and operation with failure (when one of the actuators has a fault) [3]. Figure 1 shows the main components of the flight control hydraulic system. In this case, its mode select valve determines whether the mode is active, bypassed, or damped. Figure 1 represents the Solenoid Valve (SOV) not energized, consequently the Mode Select Valve (MSV) is not actuated and remains in the damped position for the analyzed system.

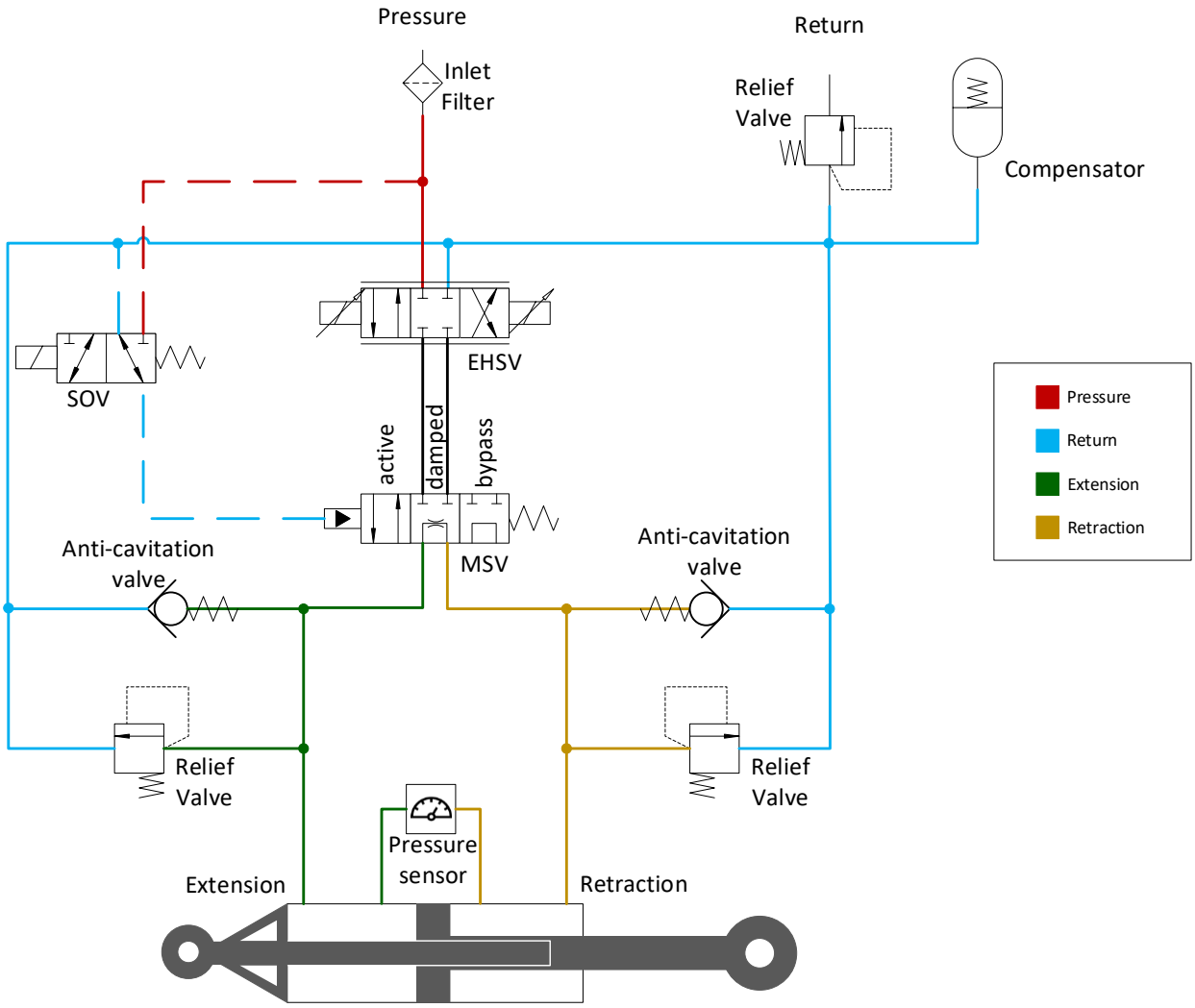

Figure 1 – Actuation architecture comprising active, bypass, and damped modes of an electro-hydraulic servo actuator.

Fluid passing through small orifices can impact the temperatures of the hydraulic system and consequently compromise the equipment's performance and damage its internal subcomponents. Previous studies discussed the influence of temperature variation on the system time and frequency response and aeroelastic requirements [2][4] or the temperature behavior of the hydraulic system during normal operation [5][6][7][8][9].

This study focuses on modeling the thermal behavior of the main components of a flight control system in the damped operation of a certified civil aircraft. The analysis was selected since the damped orifice can have restricted dimensions and may cause fluid heating inside the system. Also, the behavior can be amplified as the fluid is restricted to the manifold lines and cycled in this operation. The configuration investigated has a complete fly-by-wire control system, and its actuators are electro-hydraulic (actuation is hydraulically powered, and control is electro-electronically). The actuation surface is a primary surface type and features redundancy with two actuators in operation to carry out the flight demands. The hydraulic fluid is a fire-resistant phosphate ester hydraulic fluid type IV detailed at the standard SAE AS1241 [10].

THERMAL HYDRAULIC MODEL

The modeling was developed considering the main components of the hydraulic system in damped mode operation, and some simplifications were performed. Figure 2 represents the components modeled to evaluate the thermal behavior: the damping orifice of the mode select valve, two anti-cavitation valves, two relief valves, one balanced actuator with two chambers, and the return line. The compensator and the relief valve linked to the return line were not modeled; thus, the temperature of the return was considered the average value of the return temperature and the chambers mean temperature.

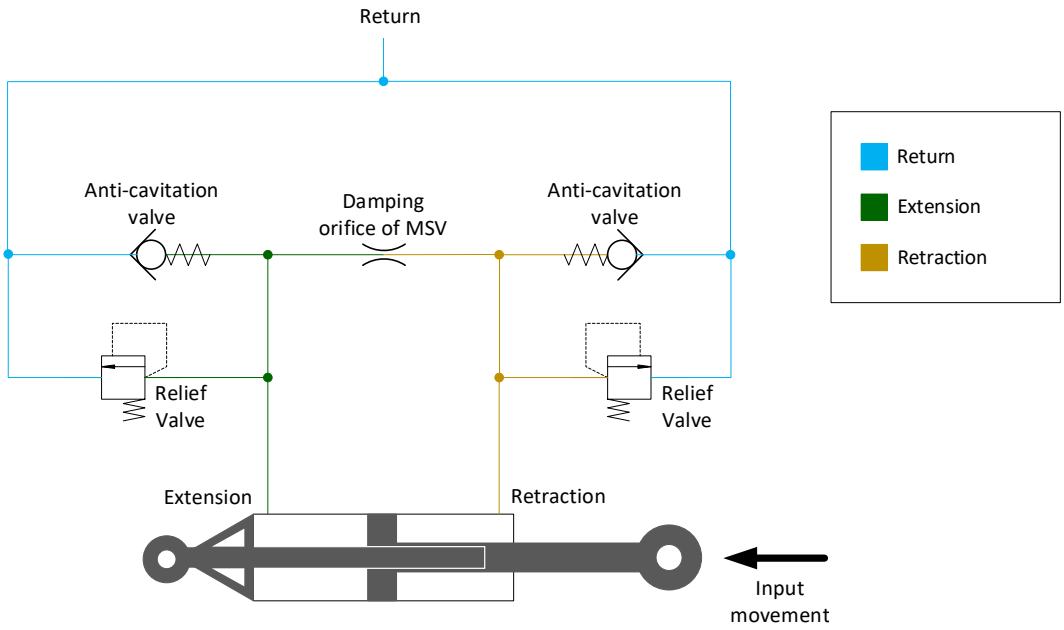

Figure 2 – Simplified damped hydraulic system.

Also, the input of the model is the position of the actuator stroke, as a position sensor often measures it. The model converted this input into stroke speed and consequently into the volumetric rate of the actuator chambers. The volume change generated a pressure difference between the chambers and a mass flow rate.

Two fundamental elements describe the physical behavior of thermohydraulic systems: capacitive and resistive blocks [6]. The following subsections detail the mathematical modeling of both.

Resistive Elements

Two equations govern the thermohydraulic behavior of resistive elements (e.g., restrictions). The first calculates the mass flow in the region – Equation (1) –, and the second the temperature increase – Equation (3). Because of viscous friction, a coefficient is introduced for the mass flow to address the power loss effects [11]. The discharge coefficient (c_q) is a dimensionless number, function of the characteristics of the flow, and geometric aspects of the orifice. The mass flow rate equation is indicated by Equation (1) [12].

$$\dot{m} = \rho \cdot c_q \cdot A \cdot \sqrt{\frac{2}{\rho}(p_1 - p_2)} \tag{1}$$

The enthalpy equation for thermohydraulic fluids can be written as Equation (2), a function of the temperature derivative (dT/dt) and the pressure derivative (dp/dt) [6].

$$\frac{dh}{dt} = c_p \frac{dT}{dt} + \frac{(1 - \alpha T)}{\rho} \frac{dp}{dt} \tag{2}$$

Considering that the heat generated by the restriction is transferred to the fluid, the transformation can be classified as isenthalpic. Thereby, it is possible to estimate the temperature variation in the fluid using Equation (2) and considering that the derivative of the enthalpy (dh/dt) is zero as shown in Equation (3).

$$T_{out} = T_{in} + \frac{(1 - \alpha T_{in}) \cdot |\Delta p|}{\rho \cdot c_p} \tag{3}$$

Capacitive Element

The fundamental capacitive element is considered a control volume with variable volume (e.g., each actuator chamber). Two equations govern the thermohydraulic behavior of capacitive elements: The first relates the pressure variation to the temperature and density variation using two experimental parameters (the bulk modulus and the expansion coefficient) – Equation (10) –, and the second estimates the temperature rise – Equation (15).

The mass variation inside a control volume (dm/dt) is the difference between the mass flow rate entering and the mass flow rate leaving the volume. The mass of a control volume (m) is given by its density (ρ) multiplied by its volume (V). Equation (4) evaluates the derivative of the equation, a relation between the derivatives of mass (dm/dt), volume (dV/dt), and density ($d\rho/dt$) [12].

$$\frac{dm}{dt} = \rho \frac{dV}{dt} + V \frac{d\rho}{dt} \tag{4}$$

In addition to density, properties such as kinematic viscosity, specific heat, volumetric expansion coefficient, and bulk modulus are a function of the pressure and temperature of the fluid. The density (ρ) is a function of pressure (p) and temperature (T). With partial derivatives, the relation of Equation (5) is obtained [12].

$$d\rho = \left(\frac{\partial \rho}{\partial p}\right)_T dp + \left(\frac{\partial \rho}{\partial T}\right)_p dT \tag{5}$$

To address the density variation, two empirical quantities of fluids - the bulk modulus (β) and the thermal expansion coefficient (α) - relate pressure, temperature, and density variations. Equation (5) was manipulated to highlight these parameters.

$$dp = \frac{\rho}{\left(\frac{\partial \rho}{\partial p}\right)_T} \cdot \left[\frac{d\rho}{\rho} - \frac{1}{\rho}\left(\frac{\partial \rho}{\partial T}\right)_p \cdot \mathrm{dT}\right] \tag{6}$$

The thermal expansion coefficient (α) is a volumetric expansion coefficient that describes a fluid's contraction or expansion with a specific temperature change. It is calculated as a function of density (ρ) and temperature (T) [11].

$$\alpha(\mathrm{p}, \mathrm{T}) = -\frac{1}{\rho} \cdot \frac{\partial \rho}{\partial \mathrm{T}} \tag{7}$$

One of the most relevant properties of flight control system is the bulk modulus. The bulk modulus is a term used to denote fluid resistance to uniform compression [13]. The selection of the proper bulk modulus is based on the function performed. AIR 1362 (2008) suggests that dynamic systems with small pressure excursions, *e.g.*, oscillating servo actuators, shall be modeled using the adiabatic tangent module (β_t) showed in Equation (8).

$$\beta_t = -\mathrm{V} \cdot \frac{\partial \mathrm{p}}{\partial \mathrm{V}} = \rho \frac{\partial \mathrm{p}}{\partial \rho} \tag{8}$$

The tangent bulk modulus (β_t) is calculated using the derivative of pressure (p) and volume (V) or as a function of the density (ρ) and the pressure (p). Returning to Equation (6) and applying Equations (7) and (8), Equation (9) is obtained:

$$\frac{dp}{dt} = \beta_t \left(\frac{1}{\rho}\frac{d\rho}{dt} + \alpha \frac{dT}{dt}\right) \tag{9}$$

This equation relates the pressure variation (dp/dt) with two empirical parameters – the bulk modulus (β) and the volumetric expansion coefficient (α) – and with the density ($d\rho/dt$) and temperature variation (dT/dt).

Combining expressions (4) and (9), Equation (10) is obtained. The relation for the derivative of the pressure is a function of the bulk modulus (β), the mass flow rate balance ($\Sigma(\dot{m})$), the density (ρ), the volume derivative (dV/dt), the volume (V), the thermal expansion coefficient (α) and the temperature derivative (dT/dt).

$$\frac{dp}{dt} = \beta\left(\frac{\Sigma(\dot{m}) - \rho\frac{dV}{dt}}{\rho V} + \alpha\frac{dT}{dt}\right) \tag{10}$$

For temperature evaluation, the first law of thermodynamics is used. The system's energy variation (ΔE) is a function of the heat transferred to the system (Q) and the work applied or done by the system (W). When applied to control volumes, the equation of the first law can be written as Equation (11) [14]:

$$\frac{dE}{dt} = \dot{Q} - p\frac{dV}{dt} + \sum\dot{m}h \tag{11}$$

Also, the mass enthalpy (mh) is the sum of the internal energy (U) and the product of the pressure and volume (PV) of a thermodynamic system [15]:

$$mh = U + pV \tag{12}$$

The energy (E) inside the control volume is the sum of the internal energy (U), the kinetic energy, and the potential energy [6]. Thus, if the kinetic and potential energies are neglected, based on Equations (12), the time rate of change of the system's energy can be expressed as Equation (13).

$$\frac{dE}{dt} = \frac{dU}{dt} = \frac{d(mh - pV)}{dt} \tag{13}$$

Combining Equations (11) and (13), Equation (14) is obtained.

$$\frac{dh}{dt} = \frac{1}{\rho V}\left(\dot{Q} + \sum\dot{m}h - h\sum\dot{m}\right) + \frac{1}{\rho}\frac{dp}{dt} \tag{14}$$

Finally, combining Equations (2) and (14), the following relation is obtained:

$$\frac{dT}{dt} = \frac{\dot{Q} + \Sigma(\dot{m}\mathrm{h_i}) - h\cdot\Sigma(\dot{m})}{\rho\cdot c_p\cdot V} + \frac{\alpha\cdot T}{\rho\cdot c_p}\frac{dp}{dt} \tag{15}$$

Thermal exchanges

In addition to the thermohydraulic components, the manifold's heat exchanges, and thermal capacitances need to be addressed mathematically. For the modeling developed, the temperature on the surface of the chambers is calculated. The manifold is being evaluated with a simplified approach. The thermal capacitance between the fluid inside the chambers and the manifold surface is modeled as a single mass. Also, the resistive coefficients are modeled with an equivalent thermal coefficient.

With complex systems, it is possible to simplify the model and work with an overall heat transfer coefficient (U_t) [16]. This approach is used when intermediate temperatures are not an objective of the study. The transferred heat ($\dot{Q}$) is also dependent on the heat exchange area (A) and the temperature difference (ΔT).

In addition, an analogy exists between heat transfer and electrical systems. Electrical resistance is associated with the conduction of electricity; likewise, thermal resistance may be related to heat conduction. Therefore, the thermal resistance is defined as the ratio of a driving potential, the temperature difference (ΔT), to the corresponding transfer rate ($\dot{Q}$). The following equation summarizes the total thermal resistance (R_{tot}) as the sum of the resistances ($\sum R$) that are part of the heat transfer system. Also, the overall heat transfer coefficient (U_t) is related to the total thermal resistance and the heat exchange area (A).

$$R_{tot} = \sum R = \frac{\Delta T}{\dot{Q}} = \frac{1}{U_t A} \tag{16}$$

The equivalent capacitance (C_t) of a volume can be expressed as the material's specific heat multiplied by its mass.

$$\frac{dT}{dt} = \frac{\sum \dot{Q}}{mc_p} = \frac{\sum \dot{Q}}{C_t} \tag{17}$$

Modeling Platforms

Software such as MATLAB/Simulink or AMESim is often used to perform the simulations of dynamic models. MATLAB and Simulink combine textual and graphical programming to design in their simulation environment. AMESim is widely used for one-dimensional multi-domain system simulation by assembling and linking pre-defined components of a set of libraries. This research was mainly conducted in MATLAB/Simulink. However, AMESim was used to assess the results. This was possible since the AMESim libraries were developed and validated in cooperation with industrial partners, and the libraries are constantly being verified by the software users. In addition, the mathematical formulation of the blocks is available to users assess if the boundary conditions and hypotheses made during its development complies with the system to be modeled [17]. The comparison between software was very important in the development of the model because it was possible to identify modeling errors at the beginning of the development.

This modeling aims to be versatile for future developments; therefore, it was constructed by building each component separately. The Simulink model was developed based on two main blocks: the resistive (with equations (1) and (3)) and the capacitive (with equations (10) and (15). The blocks were linked by additional blocks representing the relations between the components of the system. Figure 3 shows the schematic of the Simulink model.

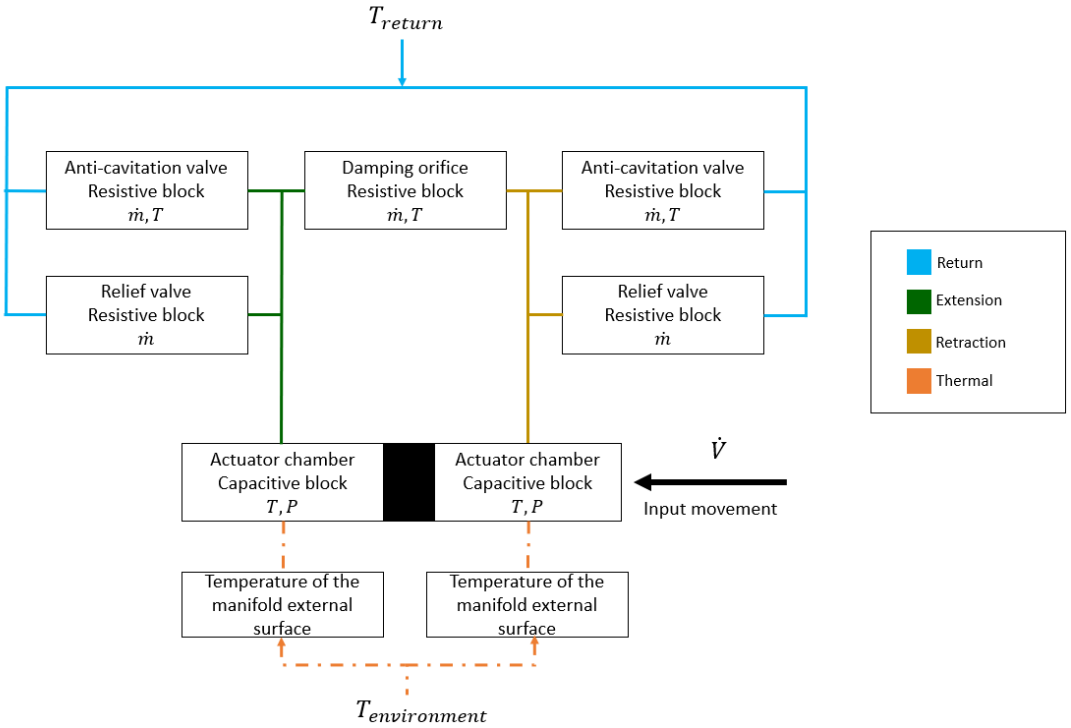

Figure 3 – Modeling schematic of Simulink with the blocks developed, classification (resistive or capacitive), and properties calculated.

The AMESim model was created using the thermal hydraulic library (damping orifice, anti-cavitation valves, and relief valves), the thermal hydraulic component design (actuator), and the thermal library (thermal capacitances and resistances). The complete model is represented in Figure 4.

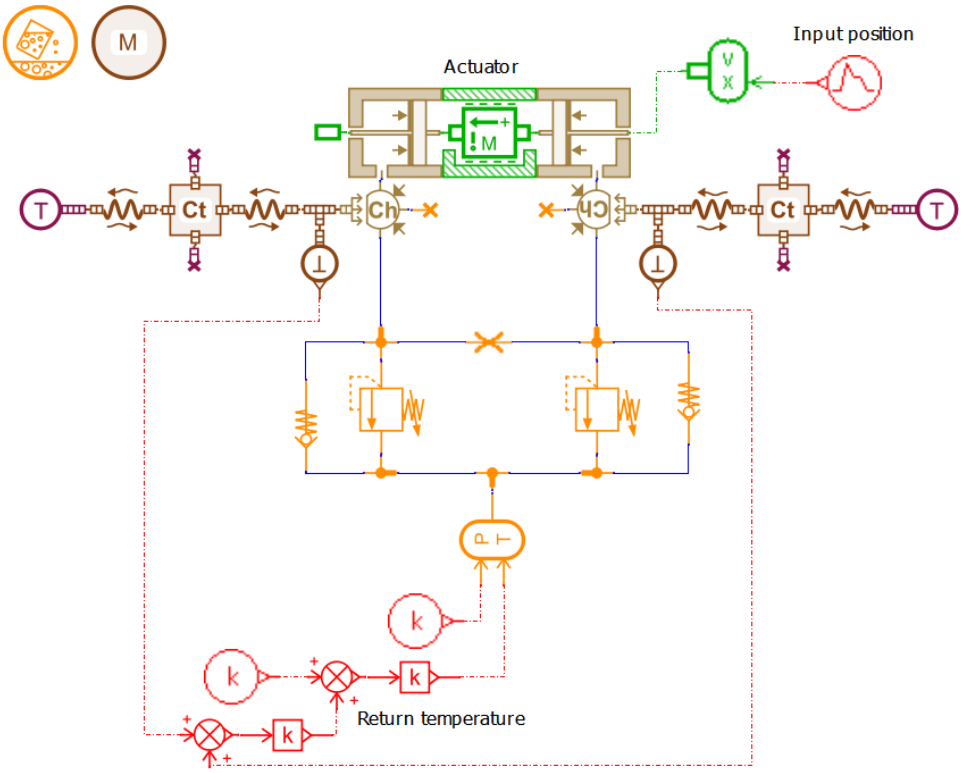

Figure 4 – AMESim complete model.

The main difference between both models is the fire-resistant phosphate ester hydraulic fluid type IV modeling. AMESim uses an embedded formulation based on higher-order polynomial functions. And MATLAB/Simulink formulation was developed based on the graphs of standard SAE AS1241 [10]. The equations presented in the previous subsections are valid for both MATLAB/Simulink and AMESim models [17].

RESULTS

Both models received the same input: five cycles initiating in the central position, reaching the retraction end, the extension end, and returning to the central position. The mean temperature of the chambers and the mean temperature of the external surface of the manifold were evaluated to compare the results.

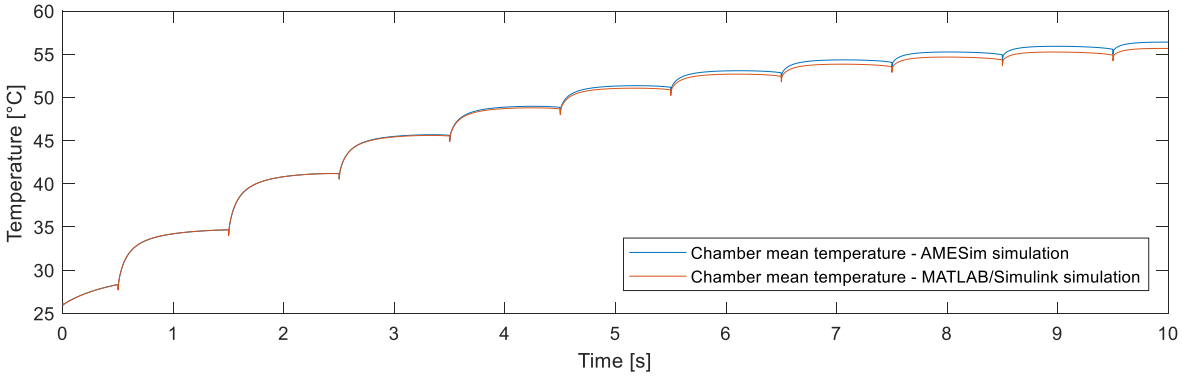

Figure 5 – Comparison of chambers mean temperature.

As shown in Figure 5, the behavior of both models was similar. The final value of the chambers average temperature simulated by MATLAB/Simulink had a percent variance of 1.3% from the AMESim result. And the surface temperature of the manifold obtained a difference of less than 1%, represented in Figure 6.

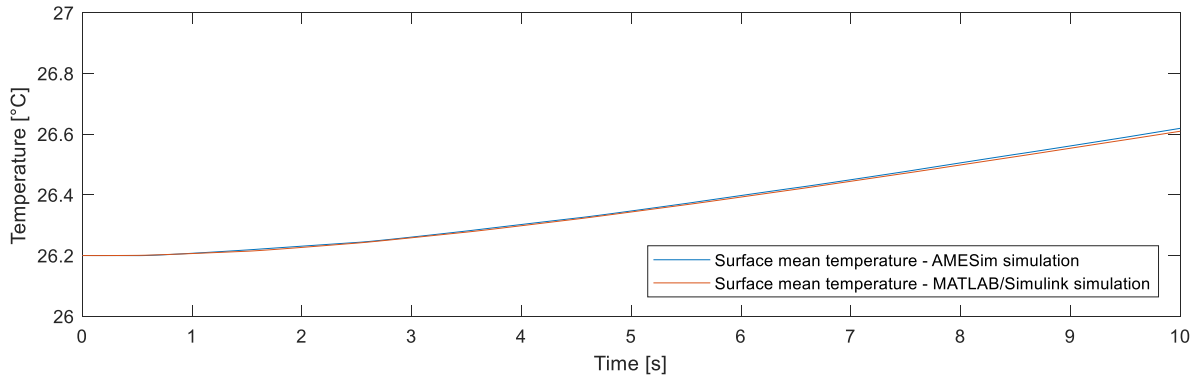

Figure 6 – Comparison of manifold surface temperature.

Software selection needs to be based on the research objective. The MATLAB/Simulink platform guarantees that all variables and implemented equations are known. However, the implementation of the equation is quite costly and subject to errors. AMESim has a more user-friendly interface; however, it has coupled physics. If the model designer does not study the details of modeling each component, some equations can be unintentionally added. Furthermore, for systems with many components, AMESim brings more advantages due to the model's speed of processing and development effort. However, the choice of a modeling platform is also a result of factors such as the number of licenses available in the organization.

Regarding the results, for the simulation performed, Figure 5 suggests that the chamber mean temperature reaches a plateau of around 55°C. Thus, superheating does not occur for the simulated case. The simulation was repeated with different thermal coefficients and higher operating pressure. Also, the cycles were extended to 200 seconds. The results are compiled in Figure 7.

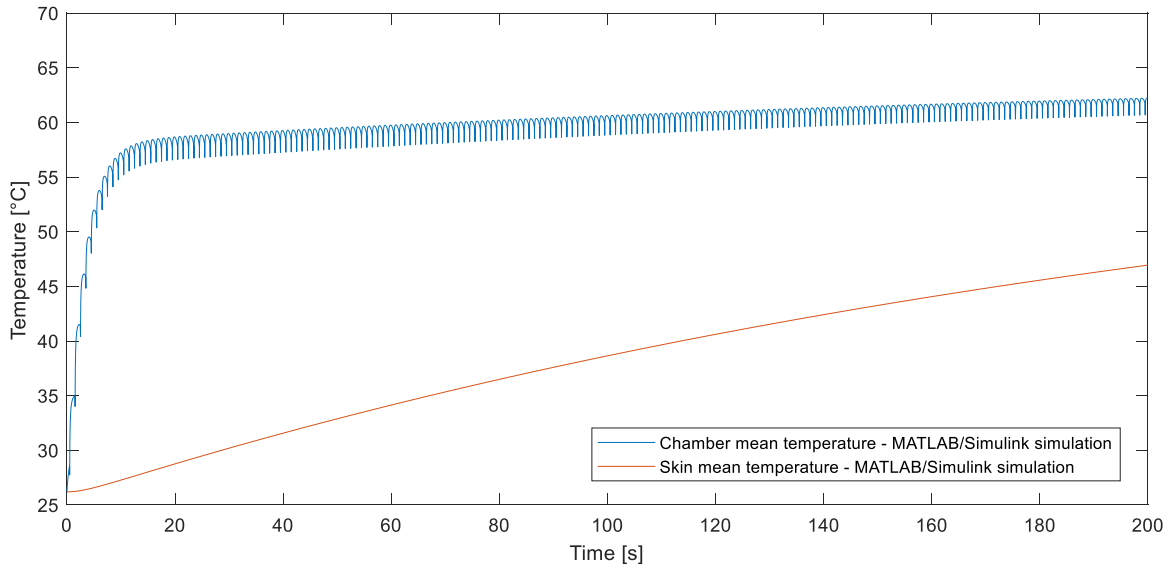

Figure 7 – Temperatures of second system condition simulated with MATLAB/Simulink.

Figure 7 shows that the chamber temperature reaches a higher plateau around 60°C and the manifold skin temperature is above 40°C due to the greater thermal coefficient. Moreover, the whole system elevates its temperature faster than the first case.

Analyzing an aircraft's flight envelope, performing a hundred cycles reaching the retraction end and the extension end of a primary flight control surface is not probable. However, a maintenance procedure or equipment test could require high cycling of the electro-hydraulic servo actuator. This simulation is an example of the capabilities of the model as it can evaluate the system temperature after design changes and for different operating conditions. In this way, it is possible to understand the impacts of the components dimensioning, geometry, and material changes on the system temperature. Also, the model can be applied to identify operation limitations such as the completion of a maintenance procedure that requires cycling with the electro-hydraulic servo actuator on damped mode.

CONCLUSION

Both models achieved satisfactory results, and it was possible to simulate the temperature of the manifold. A more detailed heat transfer assessment could more accurately evaluate the temperature of each component. In addition, it would be interesting to compare the results achieved with data from tests, perform a sensitivity analysis regarding the temperature impacts of each design change or perform a parametric identification to fit the models. However, the objectives of this research were achieved, and the models can be used to evaluate the flight control system operation in damped mode, focusing on predicting overheating.

NOMENCLATURE

A	Area
β	Bulk modulus
α	Coefficient of thermal expansion
ρ	Density
c_q	Discharge coefficient
EHSV	Electro-Hydraulic Servo Valve
E	Energy
h	Enthalpy
C_t	Equivalent capacitance
$\dot{Q}$	Heat transfer rate
U	Internal energy
m	Mass
$\dot{m}$	Mass flow
MSV	Mode Select Valve
U_t	Overall transfer coefficient
p	Pressure
SOV	Solenoid Valve
c_p	Specific heat at constant pressure
T	Temperature
R	Thermal resistance
t	Time
R_{tot}	Total thermal resistance
V	Volume

ACKNOWLEDGMENTS

The authors thank Fundação Casimiro Montenegro Filho (FCMF) and Embraer for funding the research.

REFERENCES

[1] UNITED STATES. Federal Aviation Administration 14 CFR- Part 25 Subpart D: design and construction: 25.671. Washington, DC: FAA, 1970.

[2] SERAFIM, C. F. Modelling and simulation of actuators in damping mode to comply with flutter requirements. 2019. 102 p. Dissertation (Master of Aeronautical and Mechanical Engineering) – Instituto Tecnológico de Aeronáutica, São José dos Campos, 2019.

[3] VALDO, M. F. Servo hydraulic technology in flight control. In: INNOVATIVE ENGINEERING FOR FLUID POWER AND VEHICULAR SYSTEMS, 2012, São Paulo. Workshop [...]. São Paulo: [s. n.], 2012. Available at: https://www.cisb.org.br/images/pdf/MarioValdo.pdf. Accessed on: 14 Jul. 2021.

[4] MIZIOKA, L.S. Modelagem e análise de desempenho do servo atuador do sistema de leme de uma aeronave sob variação de temperatura. 2009. 128f. Dissertação (Mestrado – em Sistemas Aeroespaciais e Mecatrônica) - Instituto Tecnológico da Aeronáutica, São José dos Campos, 2009.

[5] SIDDERS, J. A. Thermal-hydraulic performance prediction in fluid power systems. Journal of Systems and Control Engineering, v.210, n.4, p. 231-242, 1996.

[6] CHENGGONG, L.; ZONGXIA, J. Calculation method for thermal-hydraulic system simulation. ASME Journal of Heat Transfer, v.130, issue 8, article number 084503, 2008.

[7] ADRIANO, G. F. Análise térmica de sistemas hidráulicos de aeronaves. 2010. 85 f. Dissertação (Mestrado Profissional em Engenharia Aeronáutica) – Instituto Tecnológico de Aeronáutica, São José dos Campos, 2010.

[8] ZHANG, X.; LI, J.; YIN, Y. Thermal analysis and simulation of aircraft hydraulic system. Advanced Materials Research. v. 204-210, p 1984-1989, 2011.

[9] LI, K.; LV, Z.; LU, K.; YU, P. Thermal-hydraulic modeling and simulation of the hydraulic system based on the electro-hydrostatic actuator. Procedia Engineering, v. 80, p. 272-281, 2014.

[10] SAE INTERNATIONAL. AS1241: fire resistant phosphate ester hydraulic fluid for aircraft. Warrendale: SAE, 2016. 33p.Revision D.

[11] MERRITT, H. E. Hydraulic control systems. Boston: John Wiley & Sons, 1967. 358p.

[12] VON LINSINGEN, I. Fundamentos de Sistemas Hidráulicos. 5th ed. Florianópolis: Ed. da UFSC, 2016. 398p.

[13] SAE INTERNATIONAL. 1362: aerospace hydraulic fluids physical properties. Warrendale: SAE, 2008. 57p.

[14] SONNTAG, R. E.; BORGNAKKE, C.; VAN WYLEN, G. J. Fundamentals of thermodynamics. 6th ed. Hoboken: John Wiley & Sons, 2002, 816p.

[15] KARNOPP, D. C.; MARGOLIS, D. L.; ROSENBERG, R. C. System dynamics: modeling, simulation, and control of mechatronic systems. 5th ed. Hoboken, NJ: John Wiley & Sons, 2012. 636p.

[16] BERGMAN, T. L. et al. Fundamentals of heat and mass transfer. 7th ed. New Jersey : John Wiley & Sons, 2011. 1048p.

[17] SIEMENS. LMS Imagine.Lab. Thermal hydraulic library help. AMESim Rev. 8A Leuven, BE: Siemens, 2017a.

FRUGAL APPROACH FOR THE DESIGN OF A REHABILITATION PHYSICAL SYSTEM

Ruben Dario Solarte Bolaños
Federal University of Santa Catarina
rubendariosolarte@gmail.com
Florianópolis, Santa Catarina, Brazil

Antonio Carlos Valdiero
Federal University of Santa Catarina
antoniocvaldiero@gmail.com
Florianópolis, Santa Catarina, Brazil

Joao Carlos Espindola Ferreira
Federal University of Santa Catarina
jcarlos.ferreira@gmail.com
Florianópolis, Santa Catarina, Brazil

Vinícius Vigolo
Federal University of Santa Catarina
vinicius.vigolo@laship.ufsc.br
Florianopolis, Santa Catarina, Brazil

Isaac Varela Brito Guimarães de Souza
Federal University of Santa Catarina
Isaacdesouza10.11@gmail.com
Florianópolis , Santa Catarina, Brazil

Tárik El Hayek Rocha Pitta De Araujo
Federal University of Santa Catarina
pittatarik@gmail.comFlorianópolis , Santa Catarina, Brazil

ABSTRACT

In the rehabilitation process, robotic structures can support the different medical-surgical actions. These recovery process activities often involve repetitive movements that must be performed several times at various amplitudes. Robotic structures for rehabilitation can be driven by three types of active drives, namely electric, pneumatic and hydraulic actuators. Pneumatic systems have become increasingly present in various market segments and are widely used in the industry, mainly due to their ease of maintenance, low cost, safety and applicability in various processes. Currently, the concept of Frugal Innovation is being discussed, which emerges as a way to produce effective and affordable products using fewer resources to reach less-served customers. Frugal Innovation is centered on saving resources, is characterized by simplicity and clarity and aims to reach the low-income market. This article proposes the application of Frugal development methods in the design of a lower limb rehabilitation system. With the application of frugal concepts, pneumatic actuators were chosen. The choice of the pneumatic cylinder is presented from the required pneumatic force. The application of the Frugal Innovation approach in the design of this type of products demonstrates the relevance of applying these methods in efforts to mitigate or reduce the growth of the technological gap between underdeveloped and developed countries.
[DOI: https://doi.org/10.3384/ecp196006]

Keywords: *Pneumatics systems, Robotic, Rehabilitation process, Frugal Innovation, product development.*

INTRODUCTION

Frugal innovation is a highly relevant innovation concept today [1], [2] and, more broadly, for the development of new products or even enterprises, as well as learning [3]. Nevertheless, according to [4], the concept of frugal innovation has been cited since 2009. Frugal engineering consists of a set of principles and methods used to design and develop low-cost, high-quality products to satisfy the needs of low-income customers in developing markets [5].

World Health Organization (WHO) estimates that over one billion people, nearly 15% of global population, live with at least one kind of disability or 1 in 7 individuals suffers from disability and 2% to 4% have severe difficulties in locomotion [6], [7]. Disability disproportionately affects women, and older and poor people, in particular indigenous individuals and ethnic minorities [7]. Disability is a global health and human rights issue that leads to poor health outcomes, lower educational achievement, and less economic participation and has a higher incidence in low and middle income countries, which include many in Latin America [7].

Cost constraints are also a key issue when considering applications of physical rehabilitation devices in low-income countries [8]. Robotic rehabilitation devices are currently priced in the $75,000 to $350,000 range before any additional hidden costs related to shipping, taxes, maintenance, and installation/training [8]. This is particularly an ominous limitation as 85% of all stroke deaths occur in low- and middle-income countries.

Helping address this research gap, this paper investigates how a constraint-based approach can be applied to the frugal product development for rehabilitation process. Based on the theory of constraints, this work used a structured and iterative approach of constraint-based thinking to define frugal product design requirements for physical rehabilitation.

 Proceedings of the 6th Workshop on Innovative Engineering for Fluid Power – WIEFP 2022, 22-23 November 2022. ABIMAQ, São Paulo, SP, Brazil.

The approach contains a problem and solution space consisting of the following four iterative steps [9]:

a) the identification of constraints or existing limitations, hindrances behind the status quo that need to be changed;

b) a root-cause analysis to understand the underlying causes for each of the identified constraints;

c) a mapping of each of those causes to specific product characteristics or requirements;

d) development of a minimal viable product or a prototype. To the best of authors' knowledge, this is the first study combining constraints and innovation using an ex-ante approach to develop frugal products.

With the application of frugal concepts, pneumatic actuators were chosen, showing the relevance of applying these methods in efforts to mitigate or reduce the growth of the technological gap between underdeveloped and developed countries.

METODOLOGHY AND USER REQUIREMENTS DEFINITION

Figure 1 provides an overview of the constraints that authors considered critical and influenced the development of frugal product.

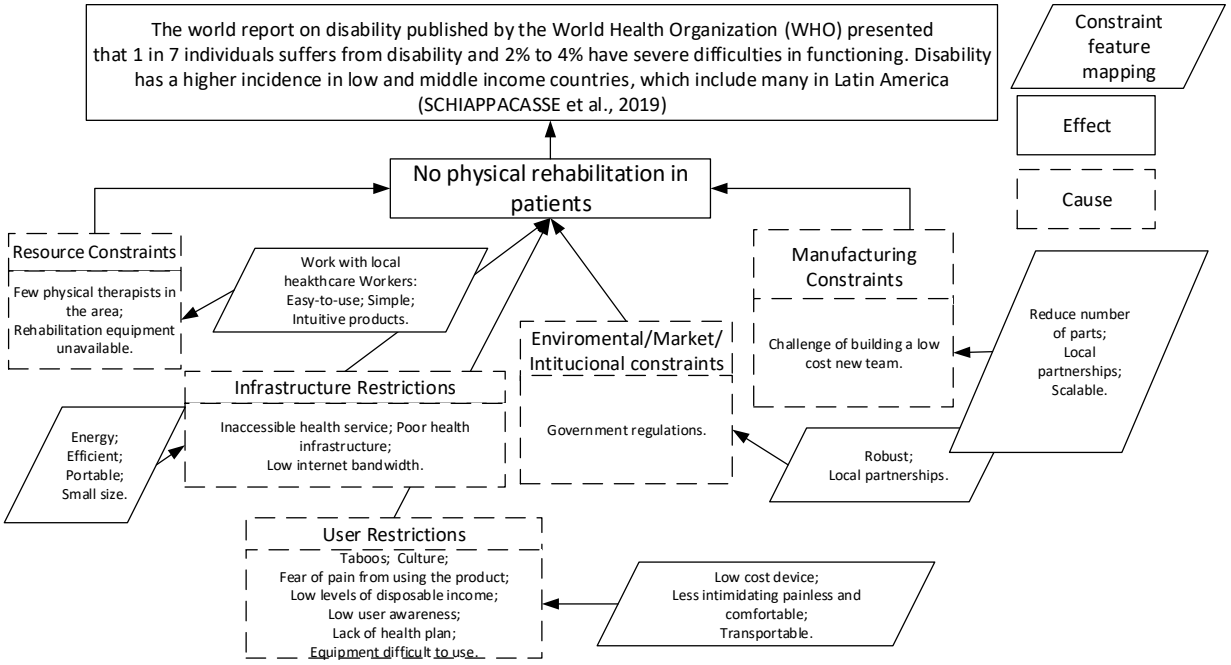

Figure 1 – Mapping of constraints to frugal features for physical rehabilitation products

These constraints are defined based on work that applies constraint-based thinking to frugal developments [9]–[11]. In addition, researches that propose developments of rehabilitation systems in emerging countries are studied for the process of defining the restrictions [8], [12], [13]. In conclusion, the restrictions are defined taking into account the analysis of the restrictions presented in Table 1, in conjunction with the restrictions defined in other similar works and on the analysis of local researches, mainly in Brazil.

According to [9], a number of factors stimulate frugal innovation and can be placed in the categories depicted in Table 1.

Table 1 – Types of constraints

Process Constraints	Product Constraints
Time	Product requirements
Equipment	Customer and market needs
Human resources	Business needs
Money	Intellectual property
Technology	Product legacy
Process legacy	Regulations
Manufacturing capability	Public health
Organizational structure	

RESULTS

A bibliographic review of some physical rehabilitation systems was carried out, then efforts were found such as: [6], [8], [13]–[16]. These efforts are based on proposing mechatronic products to assist the physical rehabilitation process in people; for example, [8] presents a prototype to help recovering mobility in the fingers of the hand; [16] proposed a product for the rehabilitation of upper and lower limbs, that is legs and arms.

These works were evaluated to choose the solution that best represents the listed frugal user requirements (Table 2). The user requirements are listed based on Constraint feature Mapping presents in Figure 1.

Table 2 – Determination of the utility function values of product conceptions

User Requirements	Weight	(JARRETT; MCDAID, 2017)	(GONÇALVES *et al.*, 2020)	(KOÇAK; GEZGIN, 2022)	(GONÇALVES; RODRIGUES, 2019)	(CIOBANU *et al.*, 2018)	(GOERGEN, 2020)
Price	1,6	3	4	4	4	3	4
Transportability	1,5	4	4	4	4	3	4
Complexity	1,4	4	4	4	4	4	4
Supplyability	1,4	3	3	3	3	3	3
Usability	1,3	3	4	4	4	3	5
Robust	1,2	3	3	3	3	3	5
Connectivity	1,2	3	3	3	3	3	3
Aesthetics	1,2	4	4	4	4	4	3
Applicability	1,2	3	3	3	3	3	4
safety of use	1,1	4	4	4	4	4	4
Value of the utility function		44,5	47,4	47,4	47,4	46,1	51,1
Ordering of conceptions		6^{th}	Second	Third	Fourth	5^{th}	First

The weights of each requirement (Table 2) were prioritized through the use of the house of quality (QFD) presented in [17]. The method "Value of the utility function" was used here for conceptions evaluation (Table 2) [17]. As can be seen, the solution that best meets the user requirements according to the triage done in Table 1 is the one presented by [12]. The Figure 2 presents an overview of the concept presented by the authors, where frugal features can be identified, such as:

1. Low price (Manpower costs; component costs; production costs and total cost): [12] is one of the cheapest products in relation to cost/number of rehabilitation functions.
2. Transportability (Weight and modularity or product): [12] is one of the most modularized and transportable products considering its weight and size.
3. Low complexity (number of components, complexity of software and others): Measuring the complexity through to use [18] method, [12] have similar complexity to the other products studied.
4. Supplyability (complexity of finding the components (national suppliers? regional suppliers?, international suppliers?): [12] have national suppliers for its fabrication.

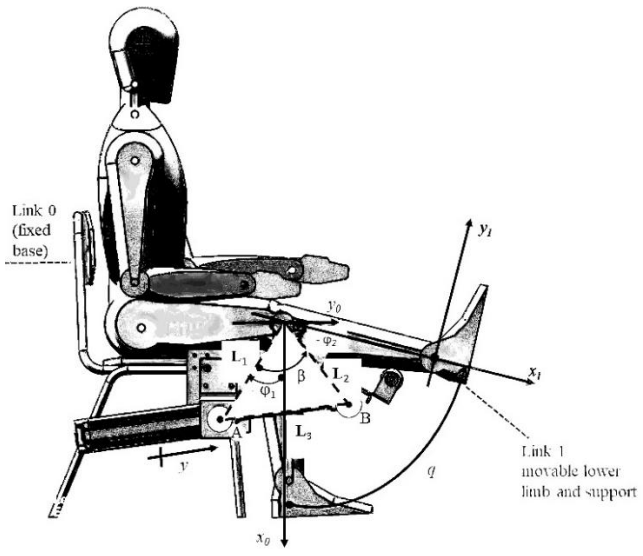

Figure 2. Pneumatically driven robotic bench for upper and lower limb rehabilitation [16]

According to [16], the pneumatic actuators can absorb unwanted forces, because their main energy source is the air, whose characteristic is to be compressive. Moreover, the pneumatic actuators present a high force/weight ratio, implementation with low costs, flexibility for installation and reliability, which characterizes considerable advantages. Consequently, robots that use this technology are getting lighter and show less inertia, resulting in a more secure system.

[16] used the relationship between the actuator length variation ($\boldsymbol{y}$) and the respective joint displacement variation ($\boldsymbol{q}$) given by equation 7; through the use of equation 7, it is possible to arrive at the necessary course parameter in the cylinder y (mm); just enter the necessary angular displacement (q) in the rehabilitation process.

$$y_{(q)} = \sqrt{{L_1}^2 + {L_2}^2 - 2|L_1||L_2|\cos(q - \Delta\varphi) - L_3} \quad (1)$$

Where $L_1, L_2, L_3\ and \Delta\varphi$ are construction parameters.

As a proposal, this work intends to use the mathematical models presented by [16] to provide a new concept that reduces costs in the new product since the original idea is considered expensive due to the price of a pneumatic 5/2 valve (>R$400). The Figure 3 presents: a. the original pneumatic drive system of the robot and b. the system proposed as future work.

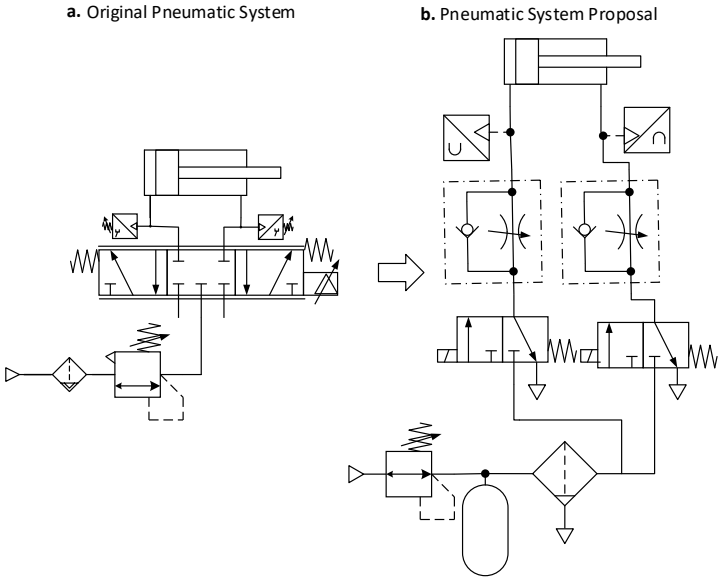

Figure 3. Pneumatic circuit of the robot prototype for limb rehabilitation [19].

The future work has as a goal to build a rehabilitation bench using valves on-off. On-off pneumatic valves are available from R$30. The cylinder sizing methods presented by [20] and [16] will be used.

Other configurations such as the one presented in [33] will be studied to analyze the price of components vs. energy consumption, to conclude which configuration best meets the Frugal and Sustainable approaches.

The assembly of a pneumatic system involves several factors, such as the dimensions of the actuators, the type of cylinder, the precision required in the system and the total cost of the project. When the idea is to carry out a project that can be used on a large scale and that can attract smaller buyers and in emerging countries, it becomes necessary that the main focus is the final cost of the product, and that it can perform the required work without great losses.

This article presents the initial stage of the user requirements definition process for frugal innovations. This work combines the PRODIP reference model and the Constraint-Based thinking method on the way to develop a special methodology for the development of frugal mechatronic products for industry 4.0 and 5.0.

ACKNOWLEDGMENTS

The authors would like to express their gratitude UFSC (Federal University of Santa Catarina) for the support to this project (SIGPEX Numbers: 202002173 and 202002437) with scientific initiation, master and doctoral research. This research was partially supported by the CAPES (Coordination for the Improvement of Higher Education Personnel), “Development of a low-cost robotic agricultural greenhouse” (SigPex no.

202203044, CNPq proc. no. 306229/2021-8) and CNPq (National Council for Scientific and Technological Development).

REFERENCES

[1] L. Corsini, V. Dammicco, and J. Moultrie, “Frugal innovation in a crisis : the digital fabrication maker response to COVID-19,” vol. 19, pp. 1–16, 2020, doi: 10.1111/radm.12446.

[2] R. Tiwari and C. Herstatt, “Editorial : ‘ Pushing the envelope ’ – transcending the conventional wisdom on frugal innovation,” *Int. J. Technol. Manag.*, vol. 83, pp. 1–14, 2020.

[3] F. J. Riar, P. M. Bican, and J. Fischer, “It wasn’t me: Entrepreneurial failure attribution and learning from failure,” *Int. J. Entrep. Ventur.*, vol. 13, no. 2, pp. 113–136, 2021.

[4] P. Pradel and D. Adkins, “Towards a design for frugal : Review of implications for product design .,” pp. 0–13, 2019.

[5] E. Rosca and J. Bendul, “Frugal and Lean Engineering: A Critical Comparison and Implications for Logistics Processes,” *Lect. Notes Logist.*, no. February 2016, pp. 335–345, 2017, doi: 10.1007/978-3-319-45117-6_30.

[6] M. Koçak and E. Gezgin, “PARS , low-cost portable rehabilitation system for upper arm,” vol. 11, 2022, doi: 10.1016/j.ohx.2022.e00299.

[7] C. Schiappacasse *et al.*, “Physical Medicine and Rehabilitation in Latin A meric a : Development and Current Status Physical medicine Rehabilitation Latin America Education Clinical activities,” vol. 30, pp. 749–755, 2019, doi: 10.1016/j.pmr.2019.07.001.

[8] R. S. Gonçalves, L. S. F. Brito, L. P. Moraes, G. Carbone, and M. Ceccarelli, “A fairly simple mechatronic device for training human wrist motion,” *Int. J. Adv. Robot. Syst.*, vol. 17, no. 6, pp. 1–15, 2020, doi: 10.1177/1729881420974286.

[9] N. Agarwal, J. Oehler, and A. Brem, “Constraint-Based Thinking : A Structured Approach for Developing Frugal Innovations,” vol. 68, no. 3, pp. 739–751, 2021.

[10] S. Chakravarty, “Resource constrained innovation in a technology intensive sector: Frugal medical devices from manufacturing firms in South Africa,” *Technovation*, vol. 112, no. August 2020, p. 102397, 2022, doi: 10.1016/j.technovation.2021.102397.

[11] S. Chakravarty, “Technovation Resource constrained innovation in a technology intensive sector : Frugal medical devices from manufacturing firms in South Africa,” *Technovation*, vol. 112, no. October 2021, p. 102397, 2022, doi: 10.1016/j.technovation.2021.102397.

[12] R. GOERGEN, A. C. Valdiero, L. A. Rasia, J. de souza Oberdofer, and R. . Gonçalves, “Development of a parameter adaptation robot for lower limb rehabilitation,” *Proc. IEEE 2019 9th Int. Conf. Cybern. Intell. Syst. Robot. Autom. Mechatronics, CIS RAM 2019*, pp. 7–11, 2019, doi: 10.1109/CIS-RAM47153.2019.9095792.

[13] R. S. Gonçalves and L. A. O. Rodrigues, *Development of a novel parallel structure for gait rehabilitation*, no. January. 2019.

[14] C. Jarrett and A. J. McDaid, “Robust control of a cable-driven soft exoskeleton joint for intrinsic human-robot interaction,” *IEEE Trans. Neural Syst. Rehabil. Eng.*, vol. 25, no. 7, pp. 976–986, 2017, doi: 10.1109/TNSRE.2017.2676765.

[15] I. Ciobanu *et al.*, “The usability pilot study of a mechatronic system for gait rehabilitation,” *Procedia Manuf.*, vol. 22, pp. 864–871, 2018, doi: 10.1016/j.promfg.2018.03.122.

[16] R. GOERGEN, “Modelagem matemática de uma bancada robotizada para reabilitação física com acionamento pneumático e controle de força,” UNIVERSIDADE REGIONAL DO NOROESTE DO ESTADO DO RIO GRANDE DO SUL - UNUJUI, 2020.

[17] N. Back, A. Ogliari, A. Dias, and J. C. Da Silva, *Projeto Integrado de Produtos: Planejamento, Concepção e Modelagem*, 1st ed. Barueri/SP, 2008.

[18] R. D. Solarte Bolaños, S. C. M. Barbalho, A. C. Valdiero, A. G. Mavignier, and J. C. Espindola Ferreira, “Measuring Static Complexity in Mechatronic,” 2022.

[19] G. Naves da Silva, “Open FluidSim: uma ferramenta multiplataforma para sistemas hidráulicos e pneumáticos:,” Universidade de Brasilia, 2018.

[20] V. Vigolo, A. C. Valdiero, R. S. Bolaños, G. de M. Luz, R. S. Gonçãlves, and V. J. de Negri, “Projeto de um servoposionador pneumático com controle de força,” in *CONEM 2022*, 2022, vol. 80, no. 2022.

THE HISTORY AND FUTURE OF FLUID POWER PUMPS AND MOTORS

Samuel Kärnell
Linköping University
samuel.karnell@liu.se
Linköping, Sweden

ABSTRACT

Positive displacement pumps have been around for thousands of years, but it was first in the beginning of the 19th century they started to be used for power transmission purposes. At that time, the fluid was water, and the applications were primarily presses. During the century, the technology developed and towards its end, fluid power systems were used to transmit power to hundreds or even thousands of consumers within several cities. However, in the 20th century, these large-scale fluid power transmission systems were outcompeted by the electric grid. But at the same time, the focus for fluid power was shifted towards self-contained, oil-based systems, which were suitable in many mobile applications powered by combustion engines. Once again, fluid power systems are now undergoing a transition. This especially apply to mobile applications, where combustion engines are being replaced by electric motors. This puts new requirements on the hydraulic systems as well as the pumps and motors that are to be used. Electrification means increased focus on energy efficiency, and speed-control becomes more relevant than before. New system designs are therefore highly relevant. Depending on the architecture that is chosen, different requirements will be set on the pumps and motors. Aspects such as multi-mode operation, high- and low-speed performance, and displacement control will be discussed in this paper.
[DOI: https://doi.org/10.3384/ecp196007]

Keywords: *fluid power, positive displacement, history, electrification, mobile machinery*

THE EVOLUTION OF POSITIVE DISPLACEMENT MACHINES

This paper focuses on positive displacement pumps and motors, which are used in fluid power to convert power between the mechanical and hydraulic domains. The term “machine” will hereafter be used to refer to both pumps and motors.

In the following sections, the evolution of positive displacement machines will be presented. An overview of the main events is also shown in Figure 1.

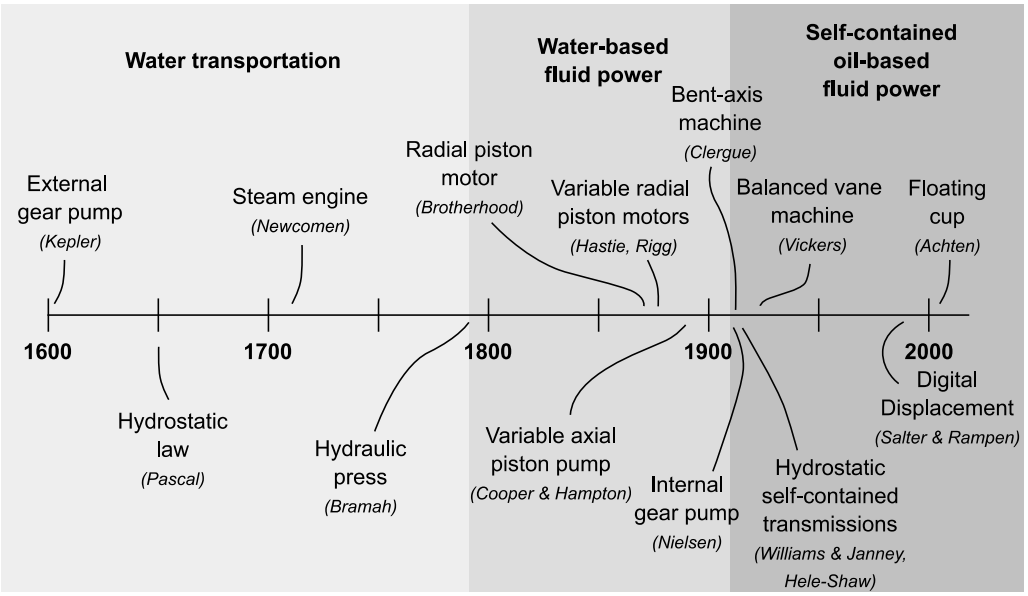

Figure 1 – Timeline

The Pre-Fluid Power Age

Naturally, there are quite some uncertainties when it comes to the history of positive displacement machines. Words such as "first" are therefore used with caution. However, the first man-made positive displacement machine appears to date back to ancient Egypt. The machine in question was a simple screw pump, often referred to as Archimedes' screw. It was used to move water from the river Nile [1]. The next major invention in the field appears to have been the piston pump. The invention is usually credited to the Greek inventor Ctesibius, who was active around 250 BC. His pump was based on a reciprocating piston that used check valves for commutation – one for the inlet and one for the outlet. The pump was powered by a lever, but similar pumps with rotational inputs were soon developed. An example where such a pump can be found is Heron's wind-powered organ. However, piston pumps were not only used for entertainment, but likely also for firefighting purposes [2].

Years passed by without major (documented) happenings regarding positive displacement pumps and motors. However, in 1588, Agostino Ramelli published a book called "Le diverse et artificiose machine del Capitano Agostino Ramelli" [3]. The book is often considered to be the first mechanical engineering handbook. It contains illustrations and descriptions of several pump types, including the first known records of vane pumps, some types of swashplate pumps, and screw pump arrangements. Around year 1600, Johannes Kepler developed what appears to be the first gear pump [4]. This was an external gear pump and several similar gear pump designs came out later in the 17th century, such as the Pappenheim pump. Furthermore, at that time, Blaise Pascal formulated the hydrostatic law, and the first experiments with steam engines were conducted. Then, in the beginning of the 18th century, Thomas Newcomen developed the first commercial steam engine, which later was improved by James Watt. However, the steam engines were mainly used to pump water from mines, and the pumps in question were typically force pumps (i.e. piston pumps similar to the ones Ctesibius invented).

The Age of Fluid Power

So far, almost all applications have been related to some kind of water conveyance. It was not until year 1795, when Joseph Bramah patented the hydraulic press [5], that fluid power really became a power transmission technology. The pump that Bramah used in his invention was principally quite similar to Ctesibius ancient pump. However, now the development in fluid power started to boom. Primarily in Great Britain. Bramah himself came up with several applications for fluid power, such as a simple crane, and a machine that could pull out trees with their roots. He also proposed the idea to have central pumping stations that could be used to provide power to different machines within a city [6]. This idea became reality in several different cities within Great Britain towards the end of the 19th century [7]. The pumps that were used in the early pumping stations were double acting so-called three-throw ram pumps, which is a piston type pump based on crank shafts [8].

In the beginning of the 19th century, typical fluid power applications were presses for packing but also presses for extracting oil from seeds. However, also rotary applications appeared, meaning that the development for rotary actuators got a push forward.

In the second half of the 19th century, many different types of rotary machines started to appear. It was primarily motors, which at that time often was referred to as "water engines". It is not surprising that William George Armstrong – the inventor of the accumulator – also developed rotary machines. In the 1830's, he invented a rotary pump with swiveling paddles, but later he focused more on a solution with oscillating pistons placed in line, connected to a crank shaft. Another somewhat similar design was developed by John Ramsbottom, who also invented the split piston ring, which is commonly found in piston machines even today. His motor was widely used in many different applications. The porting to the inlet and outlet (i.e. the commutation) was achieved with the oscillation of the pistons. Another very popular water engine was the Brotherhood engine, invented by Peter Brotherhood in the beginning of the 1870's. It was a type of radial piston motor with three cylinders placed 120 degrees apart. It could be powered by either, water, steam, or compressed air. A rotary valve (similar to the valve plate used in e.g. axial piston pumps today) was used for commutation. In a paper from 1888 about the hydraulic power network in London, Edward B. Ellington wrote as follows about them: "they are too well known to require detailed description" [8]. It was also stated that the efficiencies were around 60-70 %. The brotherhood engine was a fixed displacement motor. However, variable displacement motors started to appear at this time too. John Hastie took the Brotherhood design and made it variable. For obvious reasons, this is usually referred to as the "Brotherhood-Hastie engine" [9]. Hastie also came up with a variable radial piston motor with oscillating pistons. His motor with automatic control is presented in his paper "On Water-Power Engines with Variable Stroke" from 1879 [10]. At that time, he had had at least one motor in operation for two years. Another radial piston motor with variable displacement was developed by Arthur Rigg during the second half of the 1880s. In the previously mentioned paper from Ellington, it is stated that a Rigg engine is used to drive a dynamo for electric lighting [8].

Until this point, focus has been on radial piston machines and machines based on crank shafts, and most of them have been designed for motor applications. However, in 1893, William Cooper and George Hampton patented a variable axial piston pump of swashplate design [11]. Notice that it was not the first swashplate pump (such pumps were already described by Ramelli in the 16th century), but it appears to be the first variable swashplate pump. In the application, the following sentence can be found: "Our invention relates to a pump adapted for use at either high or low speeds, and especially adapted for use with electric motors or other constant rotary power". The pump suffered from leakage due to non-compensated forces on the valve plate. The problem was, however, solved by Charles Manly, who introduced radial porting [12]. In the beginning of the 20th century, Harvey Williams and Reynold Janney from Waterbury Tool Company came up with several improvements of the swashplate pump, and they incorporated it in a hydraulic transmission, where they had one machine working as a pump and one as a motor [13], [14]. Furthermore, they propagated for the use of oil as the power transmitting fluid, which primarily only had been used in seed presses before [2]. Oil had the advantage of not freezing, offer better lubrication, and prohibit corrosion. Furthermore, at that time, there was a movement towards self-contained hydraulic systems. Fluid power networks were still around (the one in London one closed in 1977), but the electric grid started to outcompete them since the electric grid was more appropriate for longer transmission distances.

Waterbury Tool Company was not alone in developing transmissions based on oil in those days. Henry Selby Hele-Shaw did also work with such development. He came up with the so-called Hele-Shaw pump, which is a radial piston pump with variable displacement that can run as a motor too, and the principal design is still in production today. In an article in the magazine The Commercial Motor from 1912, it is stated that the Hele-Shaw pump could achieve efficiencies above 90 % [15]. Whether this is trustworthy can be argued. Nevertheless, the bent-axis machine also appears to date back to this period. In 1909, Francis Hector Clergue was given a patent on such a machine [16].

Even though oil-based fluid power started to emerge, pumps were naturally still developed for water drainage applications. Around 1910, Jens Nielsen invented the internal gear pump and co-founded the Viking Pump Company [17]. The pump was invented with the application quarry drainage in mind. A main selling point was that the pump was the ability to handle contaminated fluids. The company is still around, producing pumps for harsh applications, but internal gear pumps are nowadays also used in fluid power, where they are known for being quiet.

Another pump that is stated to be quiet is the vane pump. It can be understood that the vane pump has been around for quite some time since it was included already in Ramelli's book from 1588. However, in 1920s, Harry Vickers developed the balanced vane pump [18], in which the forces on the bearings are substantially reduced since it has two strokes per revolution and radial forces are thereby cancelled out.

At this point (i.e. about 100 years ago), most major commercial pump and motor types have been brought up. That includes, external and internal gear machines, balanced and non-balanced vane machines, radial, axial, and inline piston machines. Naturally, there has been quite some improvements of the machines over the years, but the principal ideas are in many aspects still the same. There are, however, some more recent concepts that are getting increased focus. One is the so-called Digital Displacement® technology, which saw light towards the end of the 1980's at the University of Edinburg [19]. Since then, it has been developed under the company Artemis Intelligent Power, which recently was acquired by Danfoss. The technology is based on piston machines, in which the commutation for each piston is electronically controlled. Thereby, individual pistons can be deactivated and hence the displacement controlled. Currently, pumps are available for costumers [20], but machines that can work as both pumps and motors are about to come. Danfoss is focusing much on the excavator market, but their machines have been tested in many other applications, such as transmissions for wind power plants. A main motivator for Digital Displacement is that the technology offers high efficiency even at low displacement fractions, which is not the case for conventional variable machines. It also has very low idling losses and fast response. Another advantage is that it can offer several pump/motors in one unit since pistons can be grouped to serve different actuators.

Another more recent technology is the so-called floating cup technology, invented by the company Innas. It appeared in the early 2000s, both as a pump [21] and a transformer [22]. It has been shown to be very good at low speeds, which is rare among conventional machine types, especially pumps. The floating cup technology has recently been commercialised by Bucher Hydraulics and it is applied in mobile machinery, amongst others in an electrified Mecalac excavator [23].

Additionally, there is a new piston-type pump called floating piston pump [24]. The pump type is, however, not yet commercially available.

ELECTRIFICATION

Since the mid-20th century, combustion engines have typically been used to power hydraulic systems in mobile machinery. In many applications, the combustion engines are now about to be replaced by electric machines, and batteries are often supposed to be used as energy storage, especially for smaller machines. This

will likely affect both the general architecture of the hydraulic system and the requirements on the hydraulic machines. One reason is that energy efficiency becomes prioritized since the battery size should be minimized. Another reason is that the characteristics of electric machines are completely different than for combustion engines. For example, electric machines typically have the following properties:

- They can run in both directions.
- They can be controlled down to zero speed.
- They can transfer power in both directions.

This is very different from combustion engines, which usually run in one direction and have a comparatively limited speed range. They are also totally incapable of creating fuel from mechanical power. Furthermore, an electric machine is in general also much simpler and more compact than a combustion engine of comparative power rating. These aspects create headroom for new system architectures. Note that it in some cases also is likely that electro-mechanical actuators will replace hydraulic, but this will not be discussed here.

System Architecture

Most fluid power applications have several actuators that need to be controlled individually. Traditionally, the power is hydraulically distributed to the different actuators, and throttling valves are used to control the distribution. However, that is inherently inefficient, but it does not have to be that way – power can be controlled and/or distributed in other ways. In an electrified system, the power distribution can either be hydraulic, mechanical, or electric. This is exemplified in Figure 2.

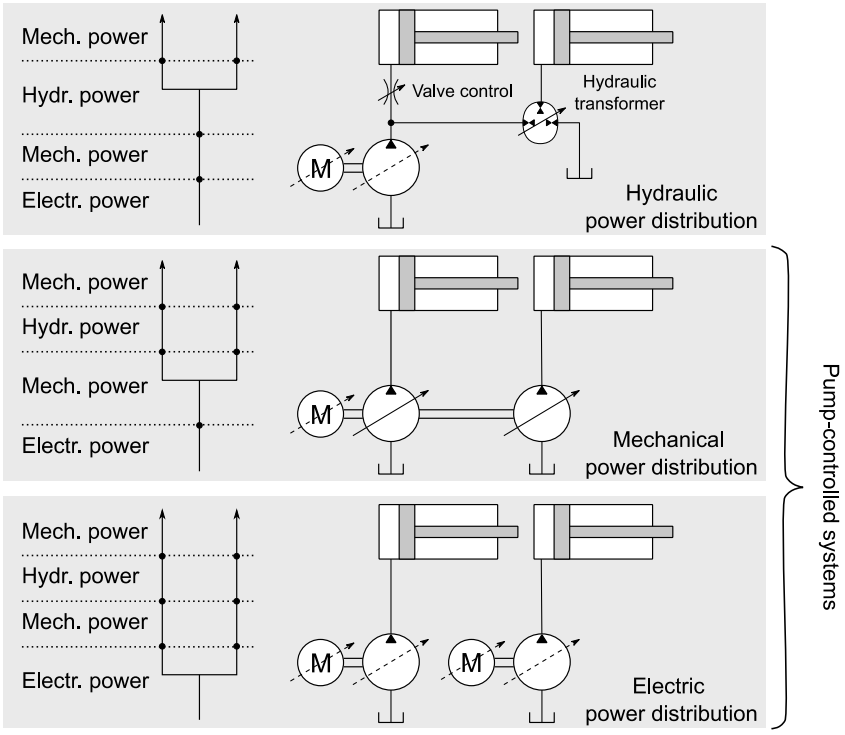

Figure 2 – Power distribution methods

For hydraulic power distribution, transformers can be used instead of valve control. Throttling losses can thereby be avoided, and energy recuperation can also be allowed. Transformers can either be based on rotary machines [22] or on fluid inertial effects [25]. To date, such solutions are, however, not commercially available. Another promising approach within hydraulic power distribution is to make use of multi-chamber cylinders and/or multiple pressure lines [26].

System architectures based on mechanical and electric power distribution are often referred to as pump-controlled systems. At a first glance, it can seem straight forward to design such systems. However, there are many possible solutions. An overview can be found in [27]. The concepts can be displacement controlled and/or speed controlled, they can be based on open or closed circuits, they can use one or more pumps per actuator, and they can be passively or actively controlled. The list of alternatives continues. The question that

is left to answer in this paper is, however, how should the hydraulic pumps and motors be designed to match these future hydraulic systems?

THE FUTURE OF FLUID POWER PUMPS AND MOTORS

When considering systems with hydraulic power distribution, hydraulic motors are of high interest for rotary motions. However, these should preferably be displacement controlled, and have the possibility to go over-center (i.e. negative displacement). This to allow bi-directional motions. It is often also desired to have motors that can work as pumps to allow energy recovery. When it comes to linear motions, development on transformers is required. The primary pump in systems based on hydraulic power distribution does not necessarily have to be able to operate as a motor since accumulators often are used to store energy. Furthermore, it typically only needs to work at one or a few defined pressure levels.

When it comes to pump-controlled systems, there are, as stated above, many different possibilities, and each of them put somewhat different requirements on the hydraulic machines. However, in general it can be stated that the machines should be able to work as both pumps and motors. If the machine is supposed to work in an open circuit, only two quadrants of operation is required. If it is supposed to work in a closed circuit, four quadrants are necessary. The quadrants are defined by flow direction and pressure difference and notice that the flow direction principally can be varied with both the displacement setting and the rotational speed. However, since electric machines generally can run in both directions, it is reasonable to have a hydraulic machine that also works well in both rotational directions. Displacement control over-center can be considered as less relevant, assuming that speed-control is used. It should also be stated that it often is desirable to have a pressurized low-pressure side in pump-controlled systems, amongst others to avoid cavitation in motoring mode. The machines should be built to withstand that.

Furthermore, to avoid the need for too large electric machines, it is desired to increase the speed of the pumps. This to reduce the required displacement and thereby the required torque. However, notice that an increased speed might have negative impact of the noise from the pump. Variable displacement can also be used to downsize the electric machine. This is since a smaller displacement can be used at higher pressure levels. Smaller displacement settings can also be used to improve the efficiency at low flow rates, since the machines then can operate at higher speeds, where they typically are more efficient. However, hydraulic machines must still be better at low-speed operation since variable displacement cannot always be used. In fact, many of the most promising pump-controlled systems require two hydraulic machines for each actuator. For this to be commercially relevant, the design should be kept simple.

Currently, there is much research on integrating hydraulic machines into electric machines. This to offer compact and efficient solutions. Obviously, this is of interest for all architectures, and not at least for systems with electric power distribution, where multiple units are required.

CONCLUSION

Traditionally, hydraulic machines have typically had one specific role and the operating conditions have been quite bounded. This is about to change. To meet the requirements that comes with new system architectures, hydraulic machines must be able to work both as pumps and motors, and often in both directions of movement. They should be better at low speeds and at the same time allow higher speeds. Displacement control will still be of interest. Partly because if allows smooth motor control of systems with hydraulic power distribution, but also because it can be used to improve the efficiency and downsize electric machines in other types of systems, but the displacement control must be more efficient than it is in conventional machines. It is easy to write these sentences, but the future will tell how easy it to achieve the desired performance of the hydraulic machines.

REFERENCES

[1] B. A. Stewart and T. Howell, Encyclopedia of Water Science, CRC press, 2003.

[2] S. Skinner, Hydraulic Fluid Power - A Historical Timeline, Lulu, 2014.

[3] A. Ramelli, Le diverse et artificiose machine del capitano Agostino Ramelli, Paris, France, 1588.

[4] F. Prager, "Kepler as Inventor," Vistas in Astronomy, vol. 18, p. 887–889, 1975.

[5] J. Bramah, "Obtaining and Applying Motive Power". Patent GB179502045A, 1795.

[6] J. Bramah, "Method of Organizing and Constructing Water Mains and Other Pipes". Patent GB-181,203,611, 1812.

[7] B. Pugh, The Hydraulic Age: Public Power Supplies Before Electricity, Mechanical Engineering Publications, 1980.

[8] E. B. Ellington, "The Distribution of Hydraulic Power in London.(Includes Plates and Appendices).," in Minutes of the Proceedings of the Institution of Civil Engineers, 1888.

[9] W. J. Lineham, A Textbook of Mechanical Engineering, Chapman and Hall, 1912.

[10] J. Hastie, "On Water-Power Engines with Variable Stroke," Proceedings of the Institution of Mechanical Engineers, vol. 30, p. 484–493, 1879.

[11] W. Cooper and G. P. Hampton, "Rotary Reciprocating Pump". Patent US patent: US511044A, December 1893.

[12] C. M. Manly, "Rotary Pump or Motor.". Patent US Patent 765,434, July 1904.

[13] H. D. Williams, "Apparatus for Transmitting Power and Regulating Speed.". Patent US Patent 1,044,838, November 1912.

[14] R. Janney, "Variable-Speed-Transmission device.". Patent US Patent 924,787, June 1909.

[15] "The Latest Hele-Shaw Hydraulic System," The Commercial Motor, June 1912.

[16] F. H. Clergue, "Improvements in Pumps and Fluid-Actuated Motors". Patent GB190821654A, September 1909.

[17] "Viking Pump: Market Leading Innovation and Excellence," World Pumps, vol. 1999, p. 14–18, August 1999.

[18] H. F. Vickers, "Vane Pump or Motor". Patent US Patent 1,898,914, February 1933.

[19] S. H. Salter and W. H. S. Rampen, "Improved Fluid-Working Machine". Patent WO Patent App. PCT/GB1990/001,478, April 1991.

[20] "Data Sheet - Digital Displacement Pump Gen 2," Danfoss, 2021.

[21] P. A. J. Achten, "Designing the Impossible Pump," in Hydraulikdagarna, 2003.

[22] P. A. J. Achten, T. van den Brink, J. van den Oever, J. Potma, M. Schellekens, G. Vael and M. van Walwijk, "Dedicated Design of the Hydraulic Transformer," in 3rd International Fluid Power Conference", 2002.

[23] "Mecalac", "Mecalac e12: a 100% Electric Excavator for Urban Building Sites," [Online]. Available: https://www.mecalac.com/en/e12-electric-wheel-excavator.html. [Accessed 23 July 2022].

[24] L. Ericson and J. Forssell, "A Novel Axial Piston Pump/Motor Principle With Floating Pistons: Design and Testing," in Proceedings of the ASME/BATH 2018 Symposium on Fluid Power and Motion Control, FPMC2018, 2018.

[25] R. Scheidl, H. Kogler and B. Winkler, "Hydraulic Switching Control-Objectives, Concepts, Challenges and Potential Applications.," Hidraulica, 2013.

[26] V. H. Donkov, T. O. Andersen, M. Linjama and M. K. Ebbesen, "Digital Hydraulic Technology for Linear Actuation: A State of the Art Review," International Journal of Fluid Power, vol. 21, 4 December 2020.

[27] S. Ketelsen, D. Padovani, T. O. Andersen, M. K. Ebbesen and L. Schmidt, "Classification and Review of Pump-Controlled Differential Cylinder Drives," Energies, vol. 12, p. 1293, 2019.

OPTIMIZATION OF PRESSURE RELIEF GROOVES FOR MULTI-QUADRANT HYDRAULIC MACHINES IN DIFFERENT SYSTEM ARCHITECTURES

Thomas Heeger
Linköping University
thomas.heeger@liu.se
Linköping, Sweden

Liselott Ericson
Linköping University
Liselott.ericson@liu.se
Linköping, Sweden

ABSTRACT

In hydraulic axial piston machines, each chamber switches between the high-pressure and the low-pressure port with every revolution. How this process, the commutation, is done, is an essential part of pump design. The commutation typically targets a smooth pressure transition to minimize compressible flow pulsations. However, an ideal pressure match is not possible over the whole operating range of the machine. Thus, pressure relief grooves are considered a "necessary evil" in the state of the art, which can reduce flow pulsations over a wide operating range on the expense of slightly increased losses. Depending on the drive cycle and especially the number of quadrants a hydraulic machine is used in, the optimal pressure relief groove design differs. The increased losses and pulsations for enabling 4-quadrant operation of hydraulic machines are shown. Pump-controlled systems lead to hydraulic machines running in different drive cycles than in conventional valve-controlled systems, affecting ideal groove design. This paper focuses on how to optimize pressure relief grooves and thus presents the methodology incl. the simulation model, formulation of the objective function, and choice of optimization algorithm. Optimizations are carried out for 1-, 2- and 4-quadrant operation. Pareto fronts for a trade-off between flow pulsations and losses are presented, for both a valve-controlled system and a pump-controlled system carrying out the same task in an excavator boom application.
[DOI: https://doi.org/10.3384/ecp196008]

Keywords: *axial piston pump, multi-quadrant, relief or silencing groove, design optimization*

INTRODUCTION

With the ongoing trend towards electrification of hydraulic systems, efficiency and noise become even more important for hydraulic machines. High efficiency is important to reduce required battery size or increase machine uptime, whereas the absence of a combustion engine makes noise from hydraulic machines more audible.

Valve plates play a crucial role for both the efficiency and noise of hydraulic machinery. In the state of the art, pressure relief grooves (also called silencing grooves) are designed to provide a good compromise of efficiency and noise over the whole operating range. Thus, several works have dealt with ideal pressure relief groove design for hydraulic machines.

[1] describes the effect of pressure relief groove design on pump flow ripple and provides analytical equations for relief groove design based on a single operating point. [2] shows possible objectives to quantify noise in hydraulic machines and investigates the formulation of different objective functions. [3] describes a multi-objective optimization of pressure relief grooves in axial piston pumps described by their start and end angles as well as the slope of the opening area over the groove angle. [4] additionally allows non-linear groove area functions. [5] introduces a multi-objective optimization of the opening areas during commutation for a gear pump, followed by a second optimization in which the optimal opening area is approximated by simple geometric features such as circles and triangles.

This work uses multiple operating points to approximate drive cycles for pressure relief groove design. It applies multi-objective optimization on hydraulic machinery which works in 1-, 2- and 4-quadrants. The penalty for 4-quadrant operation is shown. Furthermore, optimizations for the hydraulic machines in two different systems are carried out and compared: a valve-controlled system and a pump-controlled system. The potential for energy recuperation on a system level and the losses and pulsations on a pump-level are quantified based on an exemplary excavator boom application.

 Proceedings of the 6th Workshop on Innovative Engineering for Fluid Power – WIEFP 2022, 22-23 November 2022. ABIMAQ, São Paulo, SP, Brazil.

VALVE PLATE DESIGN AND PRESSURE RELIEF GROOVES

Hydraulic positive displacement machines can principally work both as a pump and a motor. For the pumping case, displacement chambers are connected to the low pressure (LP) kidney to suck in fluid and the high pressure (HP) kidney to deliver the fluid. In axial piston machines, the kidneys are located in the valve plate. In-between the kidneys, so-called bridges close the displacement chambers and prevent cross-porting (i.e., flow from the HP kidney to the LP kidney through a direct connection provided by the displacement volume) at commutation. Besides separating the inlet channel from the outlet channel, the valve plate needs to provide a smooth pressure transition for each piston chamber. This reduces compressible flow pulsations [6].

For a smooth pressure transition, pre-compression takes place before the displacement volume connects to the HP kidney and de-compression takes place before the displacement volume connects to the LP kidney. Figure 1 shows the principal design for a valve plate for each operating quadrant. As the displacement volume at bottom dead center (BDC) is larger than at top dead center (TDC), the corresponding angle in the valve plate is also larger [7]. The quasi-static pressure change during pre- and de-compression can be calculated as

$$p_{II} - p_I = \beta_e \ln \frac{V_{disp,I}}{V_{disp,II}} \tag{1}$$

with the index I representing the state when entering the bridge and index II representing the state when leaving the bridge. [8]

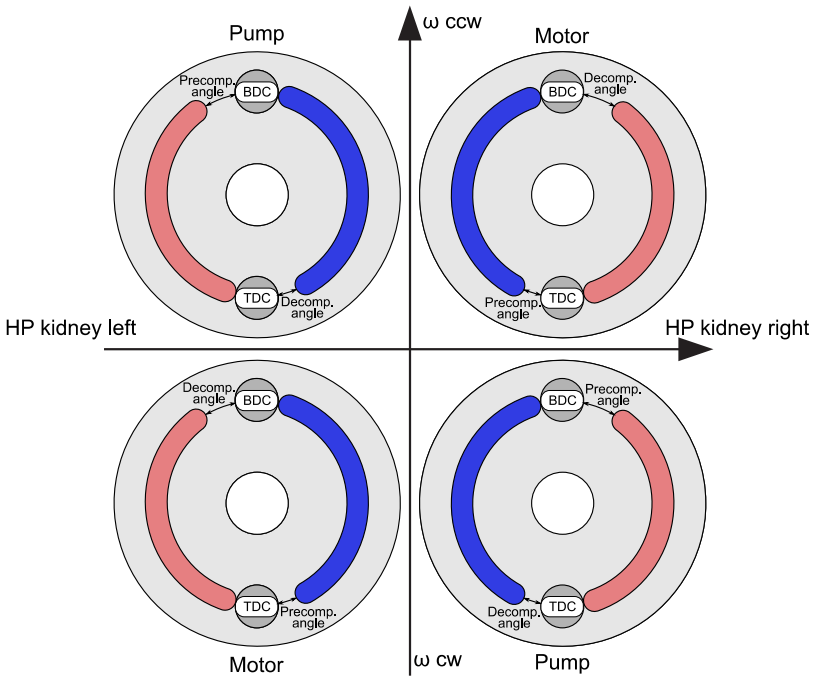

Figure 1 – Principal design of optimized valve plate design for different operating quadrants for a fluid power pump/motor [7].

Equation (1) shows that pre- and decompression angles as shown in Figure 1 can only be customized to one pressure level. For this reason, pressure relief grooves are typically used. Pressure relief grooves are small cuts in the valve plate that provide a small opening between the displacement chamber and the kidneys [9]. The pressure transition is smoothened for a wider range of pressure levels by providing a small channel. However, the flows through the pressure relief grooves lead to undesired losses, so that pressure relief grooves are seen as a "necessary evil" [6].

Palmberg states that pressure relief grooves with quadratically increasing area can provide better results than pressure relief grooves with linearly increasing area and thus the pressure relief grooves in this work are chosen to have a quadratically increasing area. The relative charge time has a dominant effect on the flow pulsations, and therefore the groove area during charging is important. Instead of as a function of time, the groove area can also be expressed as a function of geometry, with A being the orifice area, x being the groove

angle, ω being the shaft frequency, R_b being the cylinder barrel radius and t being the time. For quadratically increasing groove areash. [1]

$$A = k_x \cdot x^n \tag{2}$$

$$x = \omega \cdot R_b \cdot t \tag{3}$$

MODEL-BASED OPTIMIZATION OF PRESSURE RELIEF GROOVES

The following chapter will present a methodology for model-based optimization of pressure relief grooves by discussing the architecture, design variables, objectives and constraints, the simulation model, the choice of operating points and the optimization algorithm used. The process flow is shown in Figure 2.

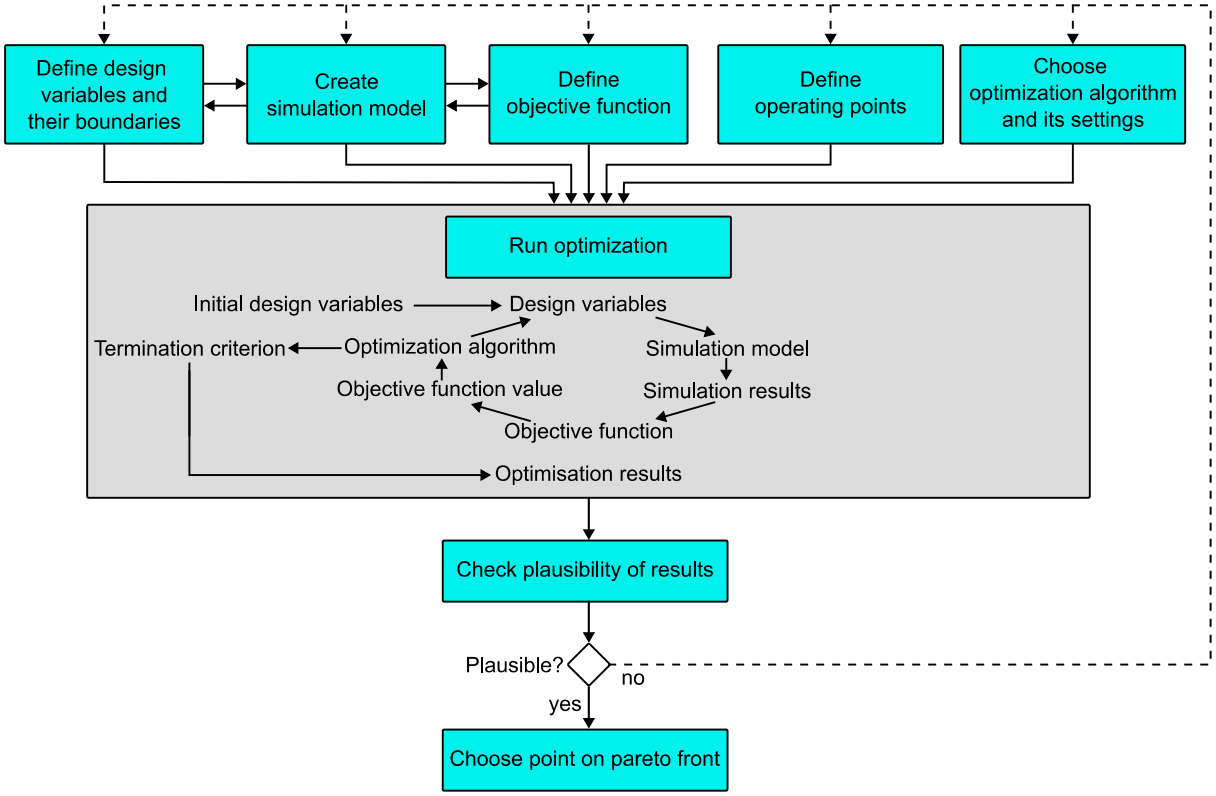

Figure 2 – Process flow of optimization procedure.

Architecture

The optimization algorithm is implemented in MATLAB. The hydraulic machine is simulated in Hopsan. The design variables and simulation time are sent to Hopsan via API, and after the simulation the simulation results are sent to MATLAB as raw data, so that post-processing takes place in MATLAB. The simulation time is always chosen as one period (i.e., the time it takes between two successive pistons pass the same point).

Design Variables

The valve land between the HP kidney and the LP kidney is fixed and covers exactly the angle of one cylinder port opening. At the start and end of each kidney, a pressure relief groove is added. From a manufacturing point of view, each pressure relief groove can be described by the groove angle, the groove shape, and the final area of the groove. As Palmberg [1] stated that grooves with quadratically increasing area can provide better results than pressure relief grooves with linearly increasing area, the groove shape is fixed to a triangular shape with an area that increases quadratically with the groove angle. Cross-porting [9] is not considered in this work to reduce the amount of design variables and thus the computational effort. However, cross-porting could further reduce flow pulsations on the expense of increased losses.
The groove angle and the final groove area for each groove are to be optimized. However, there are a lot of

combinations of groove angles and areas that provide poor results due to the interaction of these two parameters. Therefore, k_x (see Equation (2)) replaces the grooves area as design variable, see Figure 3. That means that k_x scales the groove area with the groove angle, and therefore it facilitates the search for an optimal result.
If the machine only operates in 1 or 2 quadrants, only 2 grooves are needed (1 for pre-compression, 1 for de-compression, see Figure 1). In that case, the design variables for the grooves that are not needed might be removed to simplify the problem.

Objectives and Constraints

The objectives and constraints can be defined in a similar way as done in [8]. The objectives are low losses and low noise. In comparison to machines with zero-lapped valve plates, designs that reduce losses typically also reduce noise and vice versa, i.e., the biggest share of loss reduction and noise reduction goes hand in hand. However, for fine-tuning the characteristics, a trade-off between the two objective needs to be made. Pareto fronts are created so that this trade-off between losses and noise can take place a posteriori. As a simplification, the proxy for noise can be peak-to-peak flow pulsations. The LP flow pulsations and the HP flow pulsations are combined to one overall value by weighting them according to their energy content (i.e., their pressure level). To not fully neglect LP flow pulsations for elevated HP levels, a minimum weight for LP flow pulsations can be implemented. However, using peak-to-peak flow pulsations as proxy for noise is a simplification, and more criterions can be used to evaluate noise [2] [4] and the human perception of different frequencies could be taken into account.
The constraints are that a minimum pressure level is to be guaranteed to avoid cavitation and a maximum pressure level is not to be exceeded to avoid excessive mechanical loads. The constraints are implemented as soft constraints.

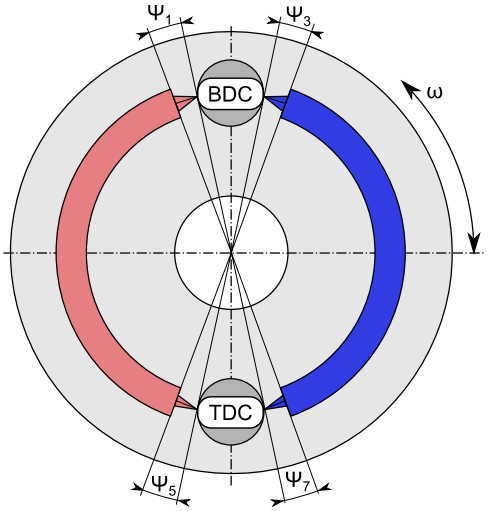

Figure 3 – Sketch of design variables. Each groove is described by its angle (Ψ_1, Ψ_3, Ψ_5 and Ψ_7) and its k_x (Ψ_2, Ψ_4, Ψ_6 and Ψ_8).

Simulation model

A Hopsan model is used to simulate the steady-state behavior of the pump for pressure relief grooves. Hopsan is a one-dimensional multi-domain simulation tool using the transmission line theory. The structure of the simulation model is illustrated in Figure 4. For each displacement chamber, the model consists of a volume, which is connected to the HP source resp. the LP source through orifices. Each displacement volume is connected to the valve plate, which has two kidneys. At each kidney end, a triangular pressure relief groove is implemented. The valve land between two grooves is the same as for a zero-lapped valve plate. The size of each

displacement volume depends on the shaft angle, and the area and circumference of each orifice depend on the shaft rotation angle.

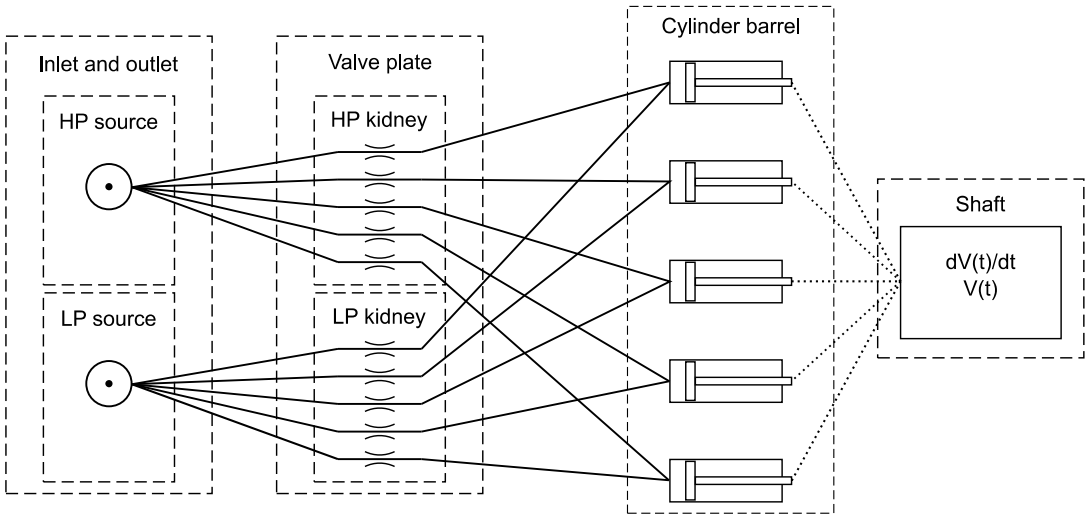

Figure 4 – Illustration of pump model structure. Of course, any number of cylinders can be implemented. [8]

Choice of operating points and trade-off between operating points

Pressure relief grooves are meant to improve the behavior of the hydraulic machine for a wide range of operating points. But the simulation time increases for an increasing number of simulated operating points. Thus, specific operating points need to be selected.

Figure 5 visualizes two different methods of choosing operating points to be considered for optimization. When no drive cycle is available, different pressure and speed levels can be covered with a minimal number of simulations using the Latin Hypercube method [10]. To obtain a 2-quadrant machine, these operating points are additionally "mirrored" with reversed rotational direction of the hydraulic machine as illustrated on the left-hand side of Figure 5. This means that a 2-quadrant machine in this work covers pump and motoring mode by reversing rotational direction, and the pressure sides are not switched. To obtain a 4-quadrant machine, the operating points are additionally appointed with reversed pressure sides of the hydraulic machine.

For a given drive cycle of the hydraulic machine, operating points are clustered into pressure ranges and speed ranges, as exemplary visualized on the right-hand side of Figure 5. The points in the cluster where the machine spends a large amount of time are used as inputs to the optimization. The trade-off between operating points is based on the time spent in each operating point. Thus, the objectives are condensed into average flow pulsations and total losses over the cycle. It is important to consider that losses over a cycle are a more useful objective than efficiencies for specific operating points (e.g., a low efficiency at an operating point with low power might be accepted due to the low absolute losses).

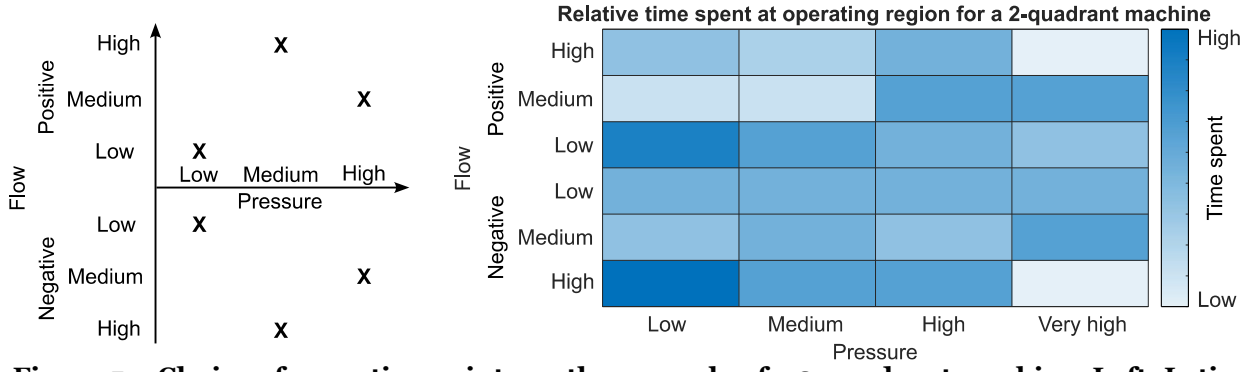

Figure 5 – Choice of operating points on the example of a 2-quadrant machine. Left: Latin Hypercube Method. Right: Clustering of drive cycle data. The data shown here is randomly generated and does not represent a real drive cycle.

Furthermore, operating points which are considered most critical for cavitation are included (i.e., maximum speed, full displacement, and minimum pressure [4]). These operating points are given a low weight, as their performance is not important; however, the constraints are not to be violated for these operating points to guarantee safe operation of the hydraulic machine across its whole operating range.

Choice of optimization algorithm

The Non-dominated Sorting Genetic Algorithm II (NSGA-II) algorithm is used [11]. This algorithm combines the characteristics of individuals and uses mutations to explore the design space. In each generation, new individuals with better objective values can replace individuals with the lower objective values. The Pareto front results from the Pareto-optimal individuals in the last generation.

Exemplary results for 1-, 2- and 4-quadrant machines

The presented methodology has been applied for 1-, 2- and 4-quadrant machines. 3 operating points were chosen for the 1-quadrant machine in pump mode using the Latin Hypercube method. The Pareto fronts are shown in Figure 6 and the corresponding typical valve plate designs are shown in Figure 7. The benefit of an a-posteriori evaluation of the results becomes clear. As the Pareto fronts show, small improvements on one objective can come at a high expense for another objective. The Pareto fronts reveal that the losses and the flow pulsations for the 1- and 2-quadrant machines are on a similar level, i.e., there is no significant penalty for 2-quadrant operation. The 2-quadrant machine even achieves slightly better results, as it uses an additional groove (at Ψ_5) to minimize pulsations due to insufficient pre-compression in motor mode. Due to the decreased pulsations in motor mode, the average pulsations of the 2-quadrant machine can be lower than those of the 1-quadrant machine. Despite this, the typical ideal designs of the 1- and 2-quadrant machine are very similar. However, the Pareto fronts show significantly increased losses and flow pulsations for the 4-quadrant machine. The reason for that can be found in its principal design: to allow for quadrant operation, pressure relief grooves in all 4 possible locations are required (compare Figure 1). However, they need to be significantly shorter than for the 2-quadrant machine, to avoid cavitation. Thus, the 4-quadrant machine has “incomplete” pre-compression and therefore higher losses and pulsations.

It is to be noted that there are some differences between the valve plate designs shown in Figure 7 and typical designs in the state of the art. For the 1- and 2-quadrant machines, there typically also is a groove at Ψ_7 instead of a pure pre-/de-compression. However, as LP flow pulsations receive a very low priority in the objective function, the optimization removes the groove and reduces losses at the expense of increased LP flow pulsations. Furthermore, the groove at Ψ_5 for the 2-quadrant machine is not typical.

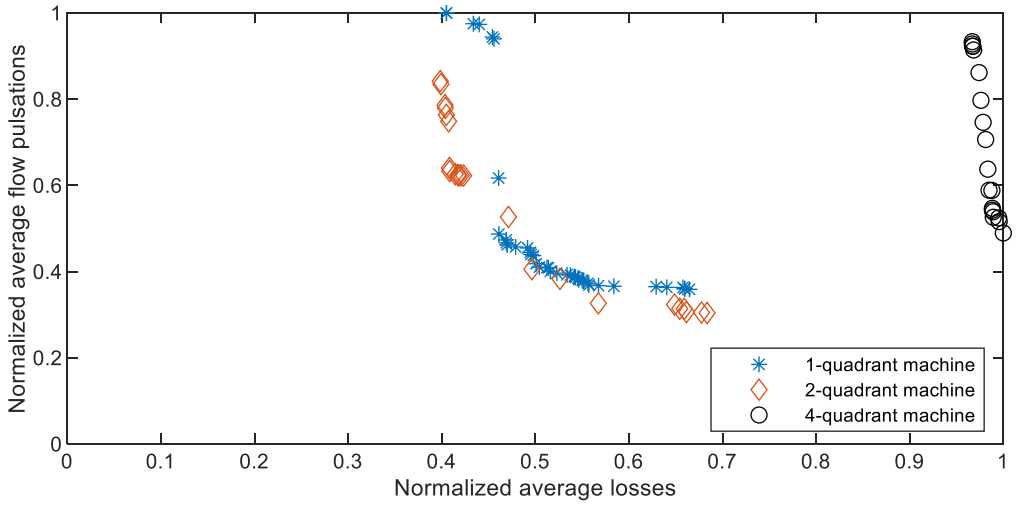

Figure 6 – Pareto fronts for optimized 1-, 2- and 4-quadrant machines

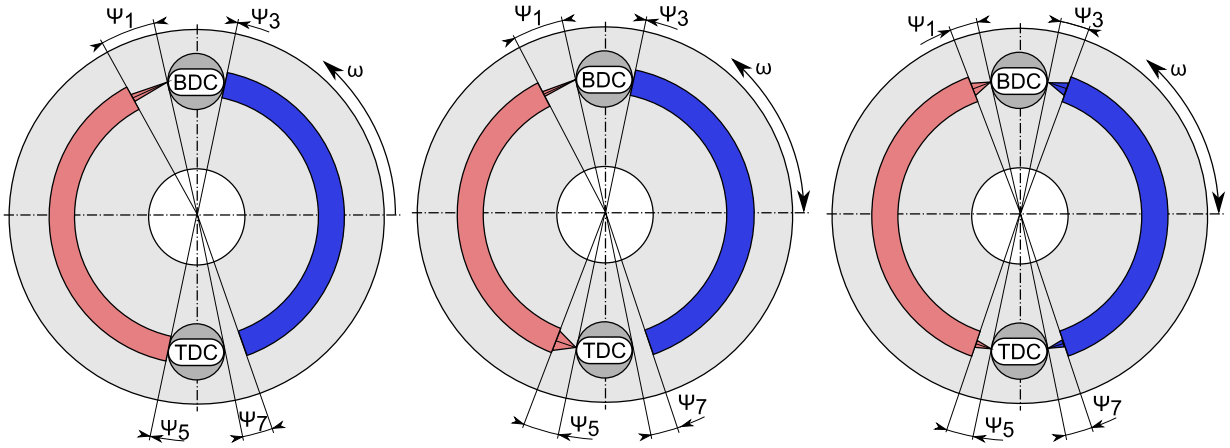

Figure 7 – Qualitative valve plate designs for optimized 1-, 2- and 4-quadrant machines (from left to right)

TRANSLATING REQUIREMENTS FROM 1-QUADRANT MACHINE FOR VALVE-CONTROLLED SYSTEM TO 2- AND 4-QUADRANT MACHINES FOR PUMP-CONTROLLED SYSTEM

Pump-controlled actuators have the potential to contribute to reducing greenhouse gas emissions by reducing throttling losses. Used in electro-hydraulic actuators, they enable energy recuperation [12]. A simple valve-controlled hydraulic actuator system and a pump-controlled system which could replace it are shown in Figure 8. The shown multi-pump system provides more freedom for system control compared to single-pump systems.

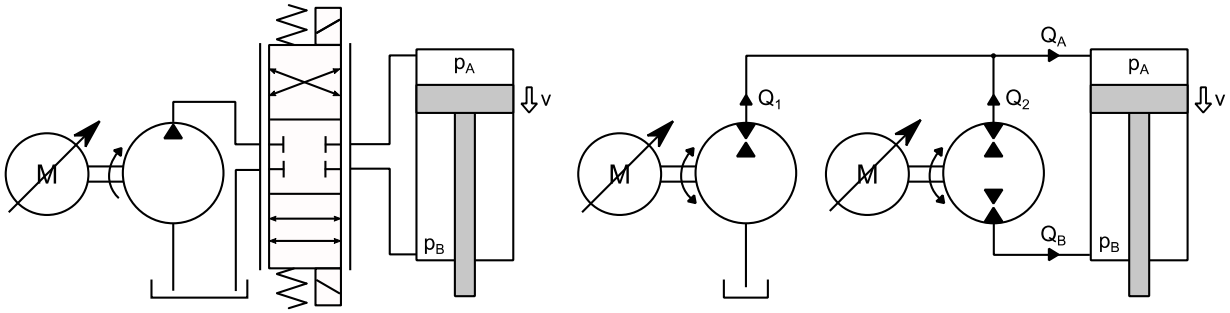

Figure 8 – A valve-controlled system (left) and a possible pump-controlled system (right)

Assuming that the pump-controlled system carries out the same task as the valve-controlled system (i.e., actuator force and speed are identical), the requirements for the hydraulic machines in the pump-controlled system can be deducted from the conventional valve-controlled system. The knowledge on chamber pressures and velocity of the actuator can be a baseline for this.

The actuator shall provide the same force for both systems, see Equation (4). The pump-controlled system's low-pressure is significantly above atmospheric pressure, providing increased stiffness. When both actuator chambers are at this pressure level, the actuator provides a force as calculated in Equation (5). At this force the high-pressure side and the low-pressure side of the actuators switch, providing a smooth transition. Neglecting losses, the pressures for the pump-controlled system are calculated in Equations (6) to (9), and the flows are calculated in Equations (10) to (12). The operating speeds of the hydraulic machines are calculated in Equation (13). With these equations the inputs for the optimization in 2 quadrant and 4 quadrant machines in the pump-controlled system shown in Figure 8 can be calculated and add more detail to a comparison of the pump-controlled system to the valve-controlled system.

$$F_{pc} = F_{vc} = p_{A,vc} \cdot A_A - p_{B,vc} \cdot A_B \tag{4}$$

$$F_{switch} = p_{Low} \cdot (A_A - A_B) \tag{5}$$

$$\begin{aligned} p_A &= p_{Low} \text{ , for } F_{pc} \leq F_{switch} \\ p_A &= \left(F_{pc} + p_B \cdot A_B\right)/A_A \text{ , for } F_{pc} > F_{switch} \end{aligned} \tag{6}$$

$$p_B = \left(p_A \cdot A_A - F_{pc}\right)/A_B \text{ , for } F_{pc} \leq F_{switch} \tag{7}$$

$$p_B = p_{Low} \text{ , for } F_{pc} > F_{switch}$$

$$\Delta p_1 = p_A - p_{Tank} \tag{8}$$

$$\Delta p_2 = p_A - p_B \tag{9}$$

$$Q_A = v \cdot A_A \text{ , } Q_B = -v \cdot A_B \tag{10}$$

$$Q_1 = Q_A - Q_2 = v \cdot (A_A - A_B) \tag{11}$$

$$Q_2 = -Q_B \tag{12}$$

$$n_{1,2} = Q_{1,2}/V_{1,2} \tag{13}$$

EXEMPLARY RESULT FOR EXCAVATOR BOOM APPLICATION

Equations (4) to (13) were applied on a drive cycle for an excavator boom application. For the sizing of the hydraulic machines, it was assumed that they all possess the same maximum speed, and then their displacements were chosen according to the maximum flow that passes the machine. For the given drive cycle, the 1-quadrant machine runs at maximum speed when filling the A-side of the cylinder, whilst the 2-quadrant and 4-quadrant machine run at maximum speed when the A-side is vented.

Table 1 shows the displacements and powers of the hydraulic machines. The pump-controlled system requires an increase of the total installed displacement and power. The advantage of the pump-controlled system becomes obvious: whilst the average input power (in pump mode) is only slightly elevated, a large amount of power is available for recuperation, thus offering great potential for increased system efficiency.

Table 1 – Displacement and average power of the hydraulic machines

	1-quadrant machine	2-quadrant machine	4-quadrant machine
Displacement [cm³/rev]	42.0	29.9	35.3
Total average power [kW]	18.6	15.3	16.1
thereof pump mode [kW]	18.6	9.9	10.5
thereof motor mode [kW]	0	5.4	5.5

Figure 9 shows exemplary Pareto fronts when optimizing the hydraulic machines for equivalent cycles for the system shown in Figure 8. Despite the increased average power running through the hydraulic machines for the pump-controlled system, the combined total losses are on a similar level. Concerning flow pulsations, note that each machine was optimized individually, i.e., the flow pulsations of one machine were not used as input to another machine. When assuming that the peak-to-peak flow pulsations of the machines for the pump-controlled systems are summated, they are still at a similar level to the valve-controlled system's machine. However, in practice both machines will run at different speeds. Thus, the flow pulsation will occur at different frequencies and the worst case of peaks of both machines being aligned with one another will rarely happen.

Furthermore, it is to be noted that the drive cycle was taken from an excavator boom application, which rarely switches the direction of force on the cylinder. Thus, the optimization of the 4-quadrant machine yielded in a design which is a mixture of the typical design for 2- and 4-quadrant machines: while there are no grooves (or extremely short grooves) at Ψ_3 and Ψ_5 (typical for 2-quadrant machines), the grooves at Ψ_1 and Ψ_7 have a smaller angle to avoid cavitation (typical for 2-quadrant machines). For a different application which switches pressure sides more often, e.g., an excavator arm, a design more typical to the classical 4-quadrant design as shown in Figure 7 is to be expected, and thus the 4-quadrant machine will have higher levels of flow pulsations and losses.

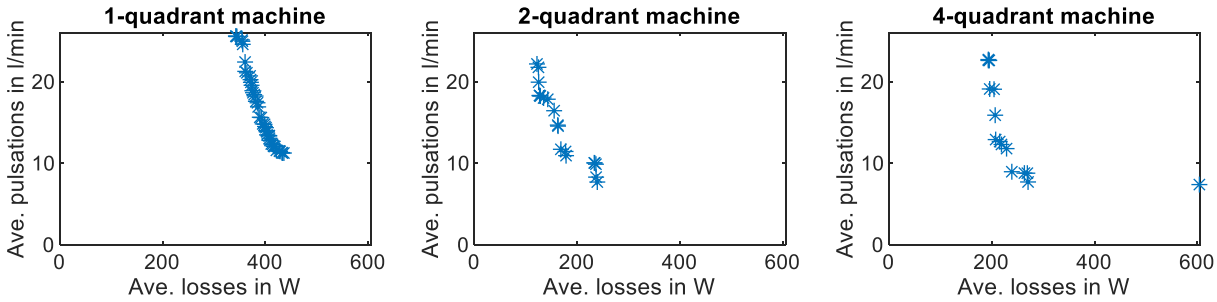

Figure 9 – Pareto fronts for optimized machines for excavator boom drive cycle

CONCLUSION

A methodology for pressure relief groove optimization has been presented and applied on machines for 1-, 2- and 4-quadrant operation and their general designs have been shown. The penalty for enabling 4-quadrant operation has been shown. Furthermore, the methodology has been applied on hydraulic machines for a valve-controlled system and a pump-controlled system on the example of an excavator boom drive cycle. The optimization results show that despite the large potential for energy savings on a system level and the higher average power passing through the hydraulic machines, there is no significant penalty in terms of losses or flow pulsations when using a pump-controlled system.

ABBREVIATIONS

HP	High-pressure
LP	Low-pressure

NOMENCLATURE

k_x	Groove area constant [m²/rad^n]
n	Exponent in groove area function [-]
n_i	Speed of hydraulic machine i [rev/s]
$p_{I,II}$	Pressure in displacement chamber before / after bridge [Pa]
Δp_1	Pressure difference over pump 1 [Pa]
Δp_2	Pressure difference over pump 2 [Pa]
p_A	Pressure in cap side of cylinder [Pa]
p_B	Pressure in rod side of cylinder [Pa]
p_{Low}	Pressure in cylinder's low-pressure side [Pa]
p_{Tank}	Pressure in tank line [Pa]
t	Time [s]
v	Cylinder velocity [m/s]
x	Groove angle [rad]
A_A	Cylinder cap end area [m²]
A_B	Cylinder rod end area [m²]
F_{pc}	Force in pump-controlled system [N]
F_{switch}	Force at which high-pressure side of cylinder is switched [N]
F_{vc}	Force in valve-controlled system [N]
Q_1	Flow through hydraulic machine 1 [m³/s]
Q_2	Flow through hydraulic machine 2 [m³/s]
Q_A	Flow into cap side of cylinder [m³/s]
Q_B	Flow into rod side of cylinder [m³/s]
R_b	Cylinder barrel radius [m]
$V_{disp,I,II}$	Displacement volume before / after bridge [m³]
V_i	Displacement of hydraulic machine i [m³/rev]

β_e	Fluid's bulk modulus [1/Pa]
ω	Shaft speed [rad/s]
$\Psi_{1,3,5,7}$	Design variables for groove angles [rad]
$\Psi_{2,4,6,8}$	Design variables for groove area constants [m^2/rad^n]

ACKNOWLEDGMENTS

This research was funded by the Swedish Energy Agency (Energimyndigheten, Grant Number 50181-1).

REFERENCES

[1] J. O. Palmberg, "Modelling of flow ripple from fluid power piston pumps," in 2nd Bath International Power Workshop, University of Bath, UK, 1989.

[2] L. Ericson, J. Ölvander and J.-O. Palmberg, "On optimal design of hydrostatic machines," in Proceedings of the 6th International Fluid Power Conference, IFK, Vol WS, 2008.

[3] G. K. Seeniraj and M. P. Ivantysynova, "A Multi-Parameter Multi-Objective Approach to Reduce Pump Noise Generation," International Journal of Fluid Power, vol. 12, pp. 17-7, 2011.

[4] P. K. Kalbfleisch and M. Ivantysynova, "Computational Valve Plate Design in Axial Piston Pumps/Motors," International Journal of Fluid Power, September 2019.

[5] S. Gulati and A. Vacca, "A General Method to Determine the Optimal Profile of Porting Grooves in Positive Displacement Machines: the Case of External Gear Machines," in 10th International Fluid Power Conference (10. IFK), Dresden, Germany, 2016.

[6] N. D. Manring, Fluid Power Pumps and Motors: Analysis, Design and Control, McGraw Hill Book CO, 2013.

[7] L. Ericson, S. Kärnell and M. Hochwallner, "Experimental Investigation of a Displacement-controlled Hydrostatic Pump/Motor by Means of Rotating Valve Plate," in Proceedings of 15:th Scandinavian International Conference on Fluid Power, (SICFP'17), Linköping, Sweden, 2017.

[8] T. Heeger and L. Ericson, "A New Degree of Freedom for Variable Axial Piston Pumps with Valve Plate Rotation," in Proceedings of the 17:th Scandinavian International Conference on Fluid Power, SICFP21, June 1-2, 2021, Linköping, Sweden, 2021.

[9] T. Kim, P. Kalbfleisch and M. Ivantysynova, "The effect of cross porting on derived displacement volume," International Journal of Fluid Power, vol. 15, p. 77–85, May 2014.

[10] M. D. McKay, R. J. Beckman and W. J. Conover, "A Comparison of Three Methods for Selecting Values of Input Variables in the Analysis of Output from a Computer Code," Technometrics, vol. 21, p. 239, May 1979.

[11] K. Deb, S. Agrawal, A. Pratap and T. Meyarivan, "A fast and elitist multiobjective genetic algorithm: NSGA-II," IEEE Trans. Evol. Comput., vol. 6, pp. 182-197, 2002.

[12] S. Ketelsen, D. Padovani, T. O. Andersen, M. K. Ebbesen and L. Schmidt, "Classification and Review of Pump-Controlled Differential Cylinder Drives," Energies, vol. 12, 2019.

DEVELOPMENT OF PNEUMATIC TECHNOLOGY FOR AUTOMATION AND CONTROL OF SMALL HYDROPOWER PLANTS

Vinícius Vigolo
Federal University of Santa Catarina
vinicius.vigolo@laship.ufsc.br
Florianópolis, Santa Catarina, Brazil

Gregori Picolotto Conterato
Reivax Automation and Control
gregori.conterato@reivax.com
Florianópolis, Santa Catarina, Brazil

Victor Juliano De Negri
Federal University of Santa Catarina
victor.de.negri@ufsc.br
Florianópolis, Santa Catarina, Brazil

ABSTRACT

Small hydropower plants have been seen as a more sustainable source of energy in comparison with large hydropower plants due to the smaller required flooding area. However, every source of energy production has, inevitably, an impact on the environment. Aiming to reduce the usage of fossil-based products, such as hydraulic oil, a joint effort has been made between the Laboratory of Hydraulic and Pneumatic systems and the companies Reivax Automation and Control and China Three Gorges, in order to introduce the pneumatic technology to the hydrogeneration sector. Characteristics such as easy installation and maintenance, low acquisition costs, and mainly, low environmental impact, make the pneumatic technology an excellent candidate to replace the hydraulic servo actuators that have been traditionally used for automation and control in hydropower plants, which use large quantities of hydraulic oil and provide a high risk of a river bed contamination due to possible leakages or incorrect disposal of hydraulic oil. This paper presents two cycles of development of a pneumatic solution to automate and control the generating unit of small hydropower plants. It includes the first proposed solutions, proof of concepts and drawbacks that were faced, as well as the new challenges and achievements that rose during the design process. The paper also presents the most up-to-date results from a pilot project where a fully pneumatic solution was applied for a generating unit with 438 kVA of generating capacity and a model of development that was identified based on common activities performed during the first two cycles of development.
[DOI: https://doi.org/10.3384/ecp196009]

Keywords: *Small hydropower plants, sustainability, pneumatic technology, pneumatic servo-actuators*

INTRODUCTION

Electricity generation by hydropower plants has been known as one of the major contributors to renewable energy sources around the globe. In Brazil, for instance, hydro generation corresponds to about 59% of the total energy production [1] and considering the total installed capacity, Brazil is in the third position in the ranking for renewable energy generation [2]. However, every source of energy inevitably results in an environmental impact, either if it is renewable or not renewable. In the case of hydroelectricity generation, the main impacts are related to the flooding caused by the water reservoir, which produces carbon dioxide and methane that results from biomass decomposition in the flooded area and also the destruction of animal life [3].

Therefore, the development of power plants with small capacities has been discussed as an alternative to reduce the environmental impacts of hydro generation [3, 4], since they require a small or even no reservoir, such as the run-of-river power plants [3, 5]. Based on this, many environmental activists and ecologists do not consider large-scale hydro generation as renewable and clean energy [6], such as the International Rivers Network, which released a declaration to exclude hydropower bigger than 10 MVA from the list of renewable energy options [7]. Therefore, small hydropower plants (SHPs) have become a possible substitute for large hydropower, and it has been encouraging the development of SHP in many countries around the world [8]. The classification of generating capacity of hydropower plants varies according to each country, in Brazil, there are three major groups of hydropower plants, the Hydropower Generating Plants (HGPs), with capacities up to 5 MW, Small Hydropower Plants (SHPs), with capacities between 5 MW and 30 MW and Hydroelectric Power Plant with capacities greater than 30 MW [9].

In this context, the Laboratory of Hydraulic and Pneumatic Systems (LASHIP) from the Federal University of Santa Catarina and the company Reivax Automation and Control have been working together to develop a solution to automate and control the generating unit of SHPs by using pneumatic technology, which

 Proceedings of the 6th Workshop on Innovative Engineering for Fluid Power – WIEFP 2022, 22-23 November 2022. ABIMAQ, São Paulo, SP, Brazil.

is known for its low environmental impact, excellent cost-benefit ratio and easy maintenance. The application of pneumatic technology in hydropower plants reduces the usage of fossil-based fluids in addition to the reduction of the acquisition and installation costs, being a viable alternative for the standard hydraulic servosystems traditionally applied for these applications.

Therefore, this paper presents an overview of the development process of pneumatic technology for SHPs, including the milestones and drawbacks faced during two cycles of development, making it possible to identify a development model that was successfully applied in order to introduce a new technology on the market.

FIRST CYCLE – IS IT A MARKET OPPORTUNITY?

The first step in the development process was the identification of the requirements of the application. In this sense, several tasks need to be performed to control and automate the hydraulic generating unit. The main task consists of speed regulation of the generator unit to set the desired frequency of the produced energy, which is performed by the speed governor of the hydraulic turbine (Figure 1-a), controlling the inflow of water according to the demanded power. The speed governor must follow a reference velocity and the main operations performed are as follows:

- Turbine start-up: Opening of the distributor vanes, starting the rotation of the generating unit until it reaches nominal rotational speed;
- Synchronism: Adjust the frequency of the generated energy to match the grid's frequency;
- Load taking: Connection of the generator with the grid;
- Load rejection: Disconnections of the generator with the grid;
- Emergency shutdown: The system must be able to close in case of emergency at a pre-determined rate and independent of external power or control sources.

Beyond the speed regulation, the automation of the generating unit consists of a braking system (Figure 1-a), the opening and closing of the admission valve (Figure 1-b), and, in some cases, the actuation of a bypass valve (Figure 1-b) to equalize the upstream and downstream pressure of the admission valve prior its opening. Black-start capability is also desired, that means, being able to start-up the generating unit without electrical energy from the grid.

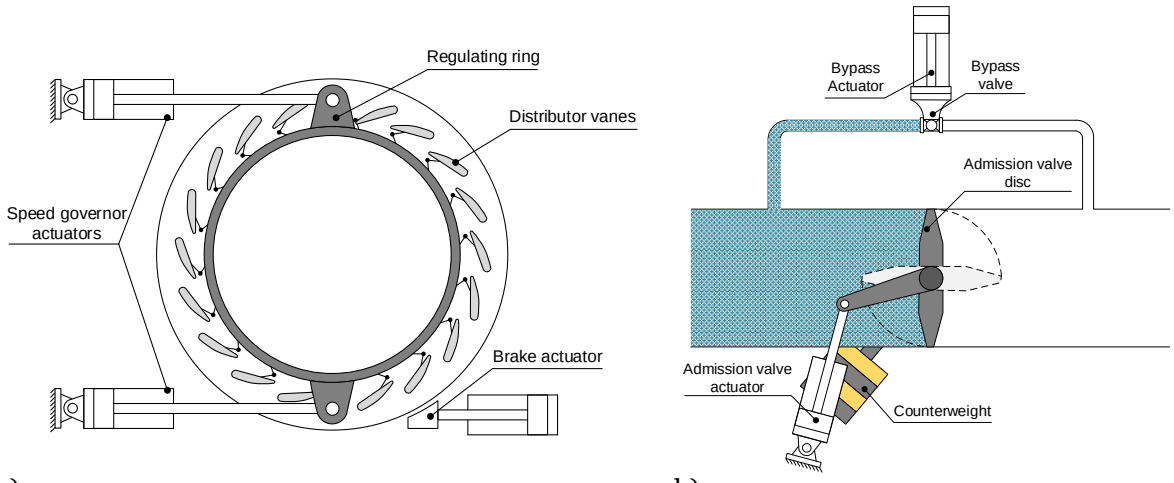

a) b)

Figure 1 - Actuation systems of a hydraulic generating unit; a) Speed governor, b) Admission valve.

The automation and control of hydropower plants have been done traditionally by servo-hydraulic actuators. Robust and reliable, the hydraulic technology is a consolidated solution for applications that demand closed loop control with strict positioning requirements, such as control surfaces of aircraft, pitch angle control of wind turbines, and speed governor of hydro turbines. However, with the advances in pneumatic positioning systems, [10] identified the possibility to apply the pneumatic technology to control the speed governor of hydropower plants, offering an opportunity to reduce the usage of mineral oil, an easier installation and maintenance, and a lower acquisition cost.

Tasks such as load rejection, synchronism, turbine startup, load taking and emergency shutdown, defined the main requirements in terms of dynamic response and steady-state error [11, 12]. Requirements for

the load force were defined by the required maximum mechanical work, which revealed an operating range for the pneumatic technology for machines up to 1 MVA of generating capacity [4].

A classical concept of a servopneumatic system (Figure 2-a), composed of a proportional servovalve (1V3), linear actuators (1A1 and 1A2), and flow control valves (1V1 and 1V2) was considered by [10]. A dynamic simulation model was developed in order to assess the capability of the servopneumatic system to withstand the operating conditions and meet the design requirements. The model included non-linearities inherent in servopneumatic systems, such as the dead zone of proportional valves and friction of the cylinder. The closed loop control was made by a PID controller and a dead-zone compensator was used to minimize the effects of the proportional valve's dead zone.

The preliminary results obtained by simulation evidenced that the pneumatic solution was able to meet the design requirements. On the sequence, a test rig was developed (Figure 2-b) in order to validate de developed model and perform further investigation of the proposed solution. The expected most critical conditions were applied on the test rig through a hydraulic actuator, which generated the load for the servopneumatic system. The results showed the validity of the dynamic model, moreover, it indicated settling times of about 0.56 seconds and 0.24 mm of steady-state errors (Figure 2-c). Tasks equivalent to turbine start-up, emergency shut down, synchronization, and steady-state control could be successfully achieved by the proposed solution.

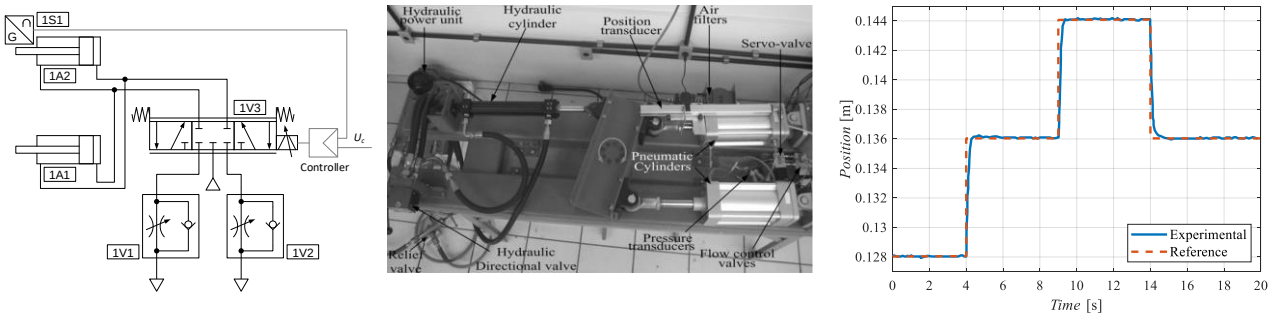

a) b) c)

Figure 2 – First proposed solution (adapted from [10]); a) Pneumatic diagram, b) Test rig, c) Experimental step response

The next step consisted of a small-scale prototype running in a speed governor of a Francis-type turbine with 35 kVA of installed capacity. A servopneumatic system was installed to control the distributor of the turbine (Figure 3-a) and the controller consisted of a PID with a dead zone compensator. Tests were carried out to evaluate the settling time, automatic start-up, and load rejection.

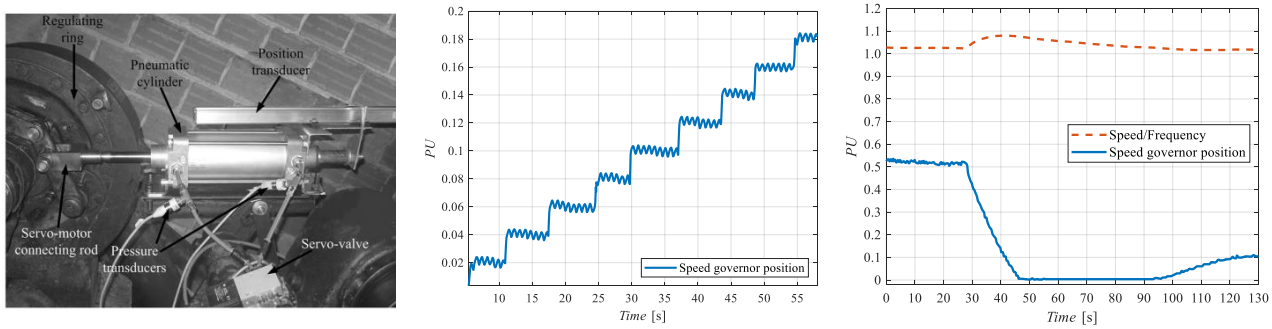

a) b) c)

Figure 3 - Small-scale prototype (adapted from [4]); a) On site installation, b) In load step response, c) Load rejection test

The on-site results showed a settling time of less than 0.25 seconds (Figure 3-b). At steady-state, an oscillation of less than 1 mm was observed, which was caused by the vibration of the machine (The unit PU stands for a relative value compared to the maximum nominal value of the variable). An overshoot of 8% occurred for load rejection tasks (Figure 3-c), which is acceptable since a reference value for overspeed in load rejection is up to 30%. Even with adverse operating conditions of the generating unit, due to clearances in the turbine mechanisms, the servopneumatic system was able to work within the recommended values of settling time and speed overshoot, which were 1.25 seconds and +30%, respectively, for this application [12, 13].

One limitation of the standard servopneumatic system was the high cost associated with the servovalve, which reduced the economic appeal of the proposed solution. Therefore, in [14] it was designed a servopneumatic system actuated by fast switching on/off valves (1V1 and 1V2 of Figure 4). The control strategy was composed of a PID, a compensator for the saturation zone of the valve, and a Pulse Width Modulation (PWM) technique, with frequencies between 10 and 75 Hz.

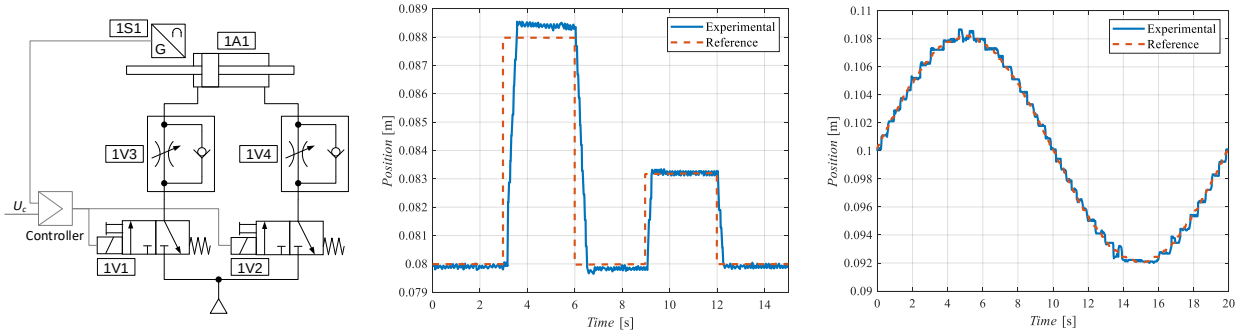

a) b) c)

Figure 4 - Solution based on fast-switching on-off valves (adapted from [14]); a) Pneumatic diagram, b) Experimental step response, c) Experimental trajectory following.

Results for unloaded tests showed an accuracy of +/- 0.5 mm, either for step response (Figure 4-b) and trajectory following (Figure 4-c). The promising results would make it possible to significantly reduce the acquisition costs of the actuation system for speed governors. However, the switching frequency applied on the directional valves reduced its life span, making it difficult to be used for applications that run continuously, such as speed governors.

Aiming the increase the energy efficiency of servopneumatic systems, [15] proposed a solution to reuse the expansion energy of the compressed air when the cylinder is moving in the same direction of the load. The solution is presented in Figure 5-a), which is composed of a standard servopneumatic system with a proportional servovalve (1V1) and a fast-switching 3/2 crossflow valve (1V2) connecting chambers A and B of the actuators (1A1 and 1A2). The control strategy consisted of a PI controller and dead zone compensator for the servovalve and a PI controller with a set of rules and PWM technique for the crossflow valve.

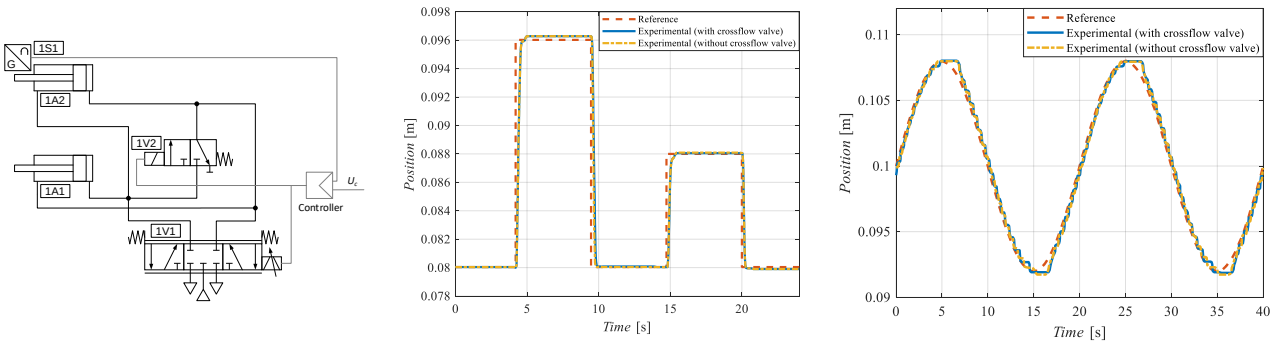

a) b) c)

Figure 5 - Solution focused on energy efficiency (adapted from [15]); a) Pneumatic diagram, b) Experimental step response, c) Experimental trajectory following

Tests performed with 5 kN of load, with and without the crossflow valve, showed no significant difference between both solutions in terms of dynamic response and positioning accuracy, with errors no bigger than +/- 1 mm (Figure 5-b, c). However, the crossflow valve resulted in an average saving of 54% of compressed air, resulting in a payback of about 2 years for a hypothetical application in a speed governor, compensating for the extra costs related to the acquisition of the fast-switching valve and a differential pressure sensor. Moreover, the limitations of the life span of the cross-flow valve are mitigated, since this valve will be used just for displacements that occur in the same direction of the load, such as the closing movements of the distributor, which occurs less frequently.

The first cycle of development of the pneumatic technology was capable to demonstrate the technical viability of the proposed solution, with robust data gathered through dynamic simulation models, experimental test rigs, and a small-scale application with a Francis turbine. At the end of the first cycle, the main challenges that needed to be overcome were the acquisition cost of the servopneumatic valves and the actuation of the

admission valve of the generating unit, where high actuation forces are commonly needed and a standard linear actuator would not be capable to attend the design conditions.

SECOND CYCLE – ADDING NEW REQUIREMENTS

After the first cycle of development to test the technical viability of using pneumatic technology for automation and control of SHPs, a new cycle of development started with The Brazilian National Electric Energy Agency (Aneel) R&D project number PD-00387-0117/2017. The new goals included the reduction of acquisition costs, the development of a solution to actuate the admission valve based on pneumatic power, and the implementation of a pilot project in a 438 kVA Francis turbine, being the first system to permanently operate the turbine with pneumatic technology.

Again, the design process started by understanding the requirements of the application. Beyond the dynamic response and steady-state error of the speed governor, emergency closing and black-start were added to the list of requirements. For the turbine admission valve, a high actuation force is necessary due to the counterweight and water column over the valve's disc. It also required an automatic closing, without the need for electric energy. Several conceptions and technologies were evaluated as possible solutions to actuate the speed governor and the admission valve, the main basis for the decision-making was the meeting of the design requirements as well as the economic viability of the solution. Discussions about possible solutions are given in [16, 17].

Figure 6-a) presents the proposed architecture for position control, where two proportional pressure regulator valves with discrete actuation (1V1 and 1V2) have proved to be more suitable since this model of valves is capable to align characteristics of proportional operation with high flow capacity, moderate acquisition costs, and a large number of manufacturers. Emergency valves (1V3 and 1V4) were installed between the proportional valves and the pneumatic actuators, in such a way that in an eventual emergency condition or loss of power, the distributor will be automatically set to its closed position. Moreover, flow-control valves (1V5 and 1V6) are used to adjust the maximum opening and closing velocities. Black-start operations can be performed with the pneumatic energy stored in the compressed air reservoir. The control strategy consisted in a PID controller that converts the position error into a pressure reference for the pressure regulator valves. An anti-windup technique is applied to the integrator controller to avoid the unbounded growing of the integral error. Also, a pressure offset is used to set the average working pressure of both chambers, and in this case, this value is equal to half of the supply pressure.

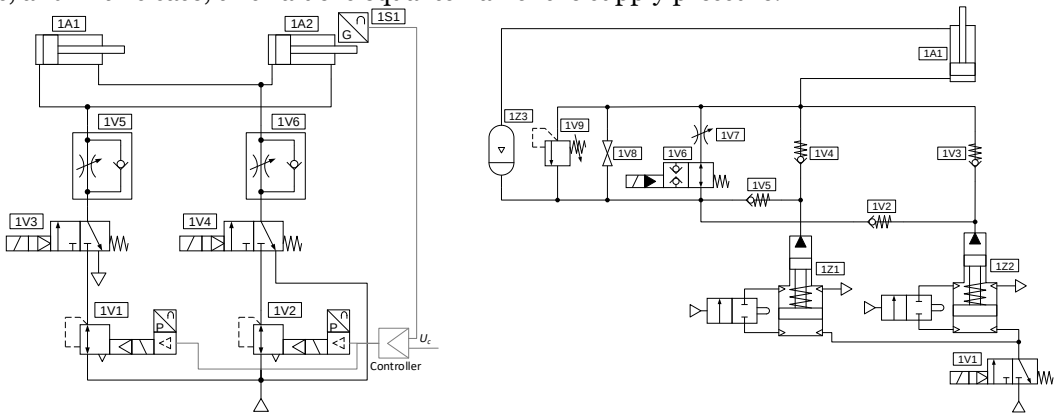

a) b)

Figure 6 - Proposed solution to automate and control the generating unit; a) Actuation system for the speed governor; b) Actuation system for the admission valve

For the actuation of the admission valve, a hydropneumatic jack was designed in partnership with the company Bovenau, where new functionalities were implemented in order to attend to the design requirements. Figure 6-b) presents the hydro-pneumatic diagram of the developed solution. A set of two pneumatic pumps (1Z1 and 1Z2) is being used to increase the opening velocity of the valve. The jack's actuator is 1A1. A 2/2-way normally open hydraulic valve (1V6) grants an automatically closing of the admission valve in the case of loss of power. The closing velocity is regulated by a flow-control valve (1V7) and, the manual valve (1V8) can be used as a redundancy for the retracting movement of the hydropneumatic jack. The equipment is remotely operated by switching the feeding valve (1V1) and the hydraulic return valve (1V6).

The proposed solutions were evaluated through dynamic simulations, which results corroborate with the capacity to attend the design requirements of the application [16, 18]. A test rig named Platform of Dynamic Loading (Figure 7) was developed aiming to perform experimental tests and further investigate the proposed

solutions. The main characteristic of the test rig is its capacity to generate forces up to 260 kN, providing means for the actuation systems of the distributor and the admission valve to be tested in full-scale conditions.

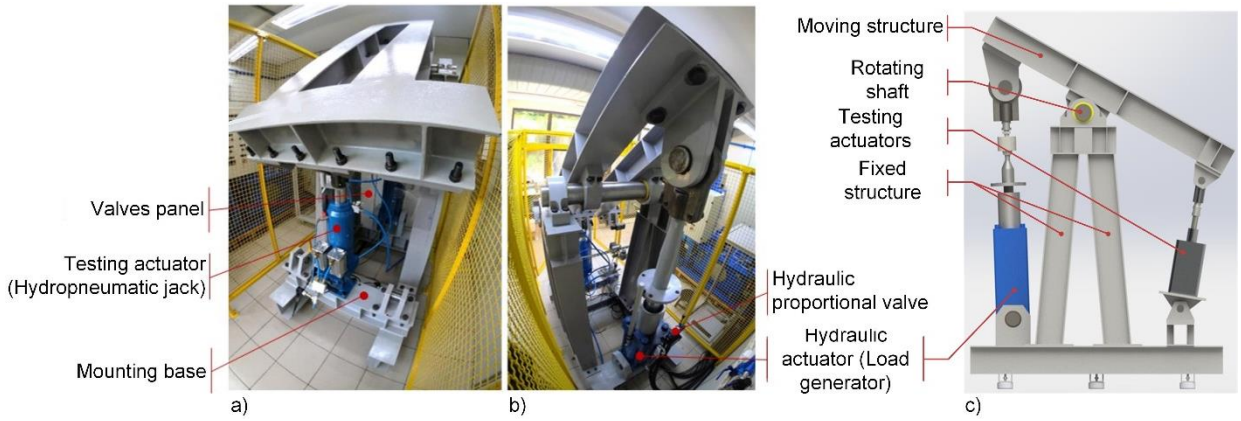

Figure 7 - Platform of Dynamic Loading (adapted from [19]); a) Front View, b) Rear view, c) Side view

In order to simulate the real and most adverse conditions of the distributor, the applied force over the pneumatic actuators was set to 26 kN, corresponding to the maximum force expected on the pilot project application [16]. Equivalent tests for the opening of the distributor, synchronism of the generator with the electrical grid, and load rejections were carried out and presented in Figure 8.

As can be seen in Figure 8, the position control system was able to follow the reference values with excellent dynamic response and low positioning error. At steady state, the biggest error observed during the testing was 0.64 mm. Moreover, the response time for the load rejection (closing of the distributor) was 7.2 seconds, which is within the specification for this application according to the turbine manufacturer.

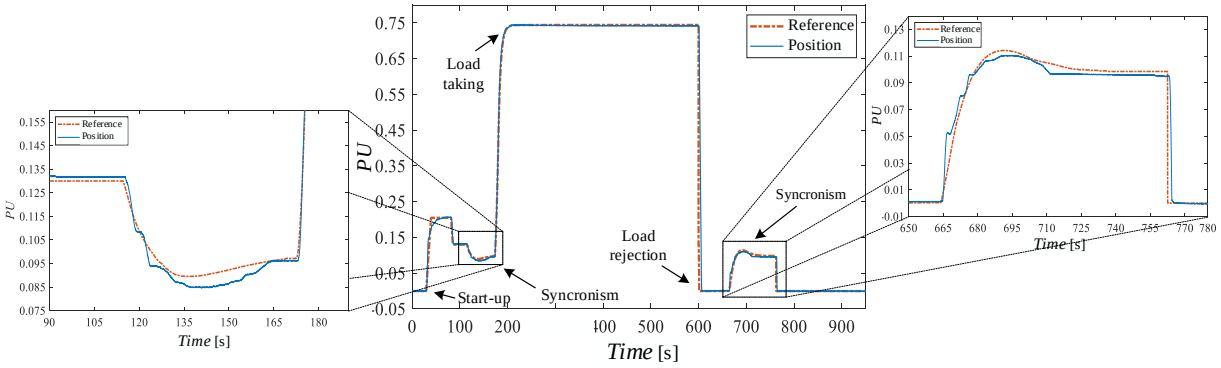

Figure 8 - Test rig results for position control using pressure regulator valves (adapted from [19])

The hydropneumatic jack was also tested at the test rig with a load force of 153 kN, which is the maximum force expected for the pilot project application according to the admission valve manufacturer. It presented a constant and regular behavior during the opening, in such a way that the opening time was completed in 150 seconds. The capacity of the hydropneumatic jack to maintain the extended position for a long period of time was also tested and the nominal load (153 kN) was kept for a period of 8 hours with the pneumatic supply pressure completely ceased during this period. At the end of the experiment, the retracting was just 0.35 mm, showing excellent stability.

Based on the results obtained through simulation and test rig experiments, the development of the pilot project began. The goal was to install a pneumatic system for the complete automation and control of the auxiliary generating unit from the hydropower plant located in Salto Grande-SP, Brazil, which is under the concession of the company China Three Gorges Brasil. The generating unit is composed of a horizontal Francis turbine and a synchronous generator. With an average water head of 18.5 m, the generating unit has a total of 438 kVA of installed capacity.

The selection of the actuators and valves for the distributor was made based on the operating point method [20, 21]. A hydropneumatic jack with a maximum capacity of 294 kN was designed in partnership with the company BOVENAU. The spatial distribution of the pneumatic components at the operation site is presented in Figure 9–a), as well as a few images of the generating unit after the installation of the components (Figure 9–b, c, d).

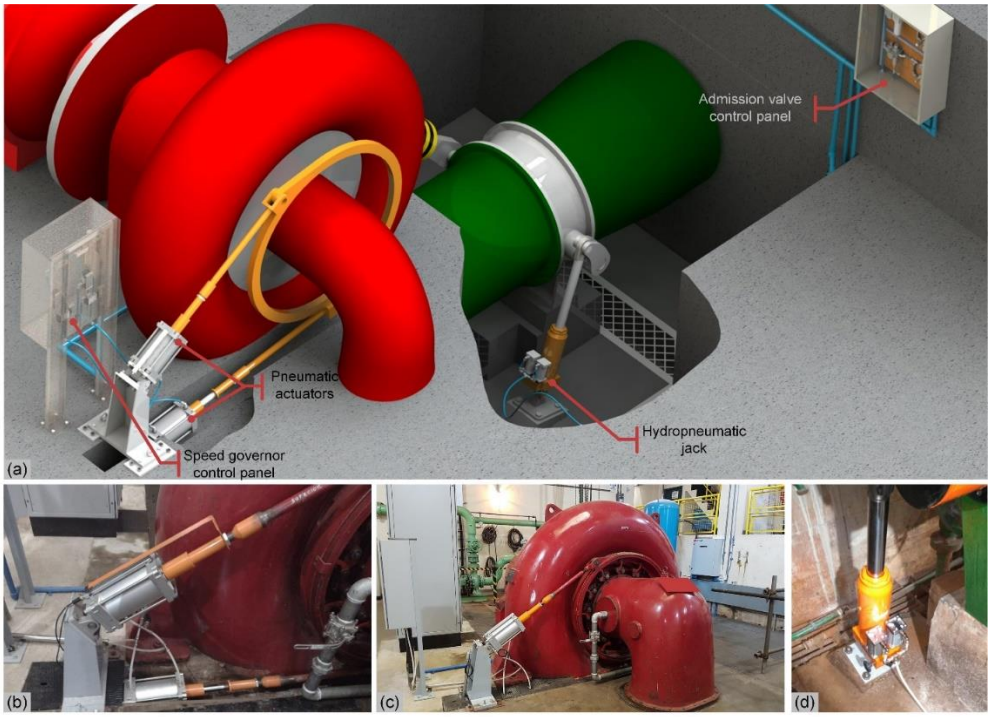

Figure 9 - Pilot project installation site (adapted from [22]); a) General view of the pneumatic solution, b) Pneumatic actuators of the distributor, c) Front view of the Francis turbine, d) Hydropneumatic jack.

Figure 10-a it is presented the data for the generating unit operating in load and isolated from the grid. The electrical load was created by a resistor bench, where different nominal loads were adjusted, starting with 22 kW (0.05 PU) and following with 70 kW (0.16 PU). The servopneumatic system was capable to follow the reference trajectory with an excellent dynamic response. This behavior is reflected in the generator frequency, which presented an oscillation between 0.9953 to 1.005 PU (59.72 to 60.3 Hz) at steady-state, which is within the limit of +/- 0.5 Hz established by the Electric System National Operator. During the transition from 22 kW to 70 kW, a frequency oscillation of 0.0347 PU (2.082 Hz) occurred and the time to reach nominal frequency was approximately 18 seconds. For these cases, the Electric System National Operator recommends a maximum time of 45 seconds for operation at frequencies between 57.5 and 58.5 Hz, demonstrating that the dynamic response of the servopneumatic system meets the requirements.

It is also important to note that the fluctuations in the rotational speed are also caused by the operational mode of the generator unit, which is isolated operation (The most difficult operational mode to control). Due to the low inertia of the turbine-generator set, the speed tends to fluctuate more when compared with bigger turbines or even when compared with the same machine operating synchronized with the national grid.

The dynamics of the system were also evaluated by a load rejection task (Figure 10-b), which was performed from a power of 72 kW (0.1662 PU). As it can be seen, the servopneumatic system was capable of properly respond to this perturbation, reducing the opening of the distributor from 0.33 PU to 0.12 PU, which is the opening to keep the nominal frequency without load. Moreover, the overspeed was 5.8%, which is within the recommendation of the turbine manufacturer, where an overspeed limit of 30% is used to trip the generating unit.

Figure 10-c) presents the data for the opening and closing of the turbine admission valve, which is made by the hydropneumatic jack. The task was performed with the generating unit in operation. The closing and opening times were 23.35 and 101.67 seconds, respectively. According to the manufacturer of the admission valve, the opening time must be between 80 and 160 seconds. The desired closing time was not specified, but the main rule is that the water hammer effect must be avoided. Since this phenomenon was not observed during the testing, it was assumed that the obtained closing time was acceptable.

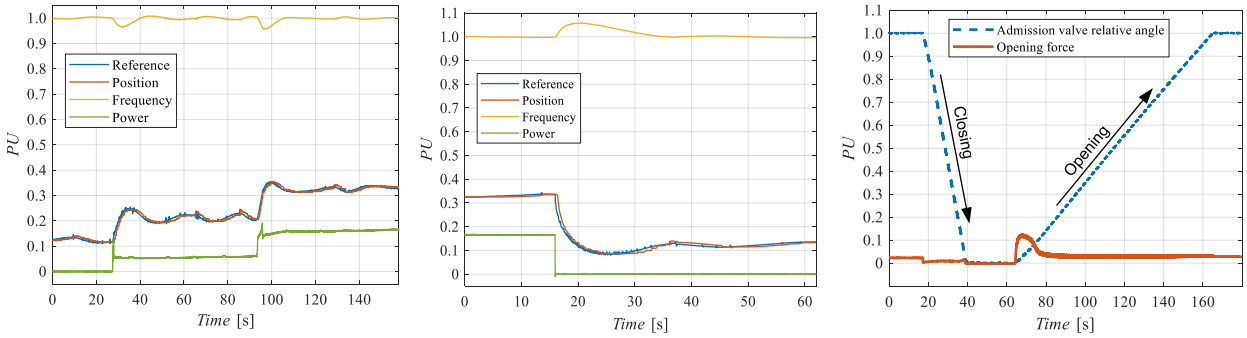

a) b) c)

Figure 10 - Pilot project results (adapted from [22]); a) In load speed regulation, b) load rejection test, c) Closing and opening of the admission valve

The tests performed with the pilot project proved the capacity of the pneumatic technology to automate and control the generating unit of small hydropower plants, being capable of successfully performing tasks of opening, closing, load taking, and load rejection of the speed governor, as well as opening and closing of the admission valve. Moreover, the pneumatic solution has been found to be economically viable, with acquisition costs 45% lower than an equivalent hydraulic solution [22].

IDENTIFICATION OF A DEVELOPING MODEL

After two complete cycles of development of the pneumatic technology for SHPs, it is possible to identify a set of 5 common activities performed in both cycles, which can be organized into a development model, providing a path to be followed during the development of new technologies related to hydropower generation. This model is depicted in Figure 11, in which the blue spiral line indicates the first cycle and the green spiral line indicates the second cycle.

The set of activities that compose the development cycle results in a progressive understanding of the application's needs and the feasibility of a proposed solution to meet the requirements. It also reduces the risks inherent in every development process, because the solutions are progressively tested in different environments and conditions, and just when one activity is successfully completed, the next one will start. As the spiral grows, the maturity of the technology increases. Nonetheless, the costs and risks involved also increase, justifying the necessity to start the development process with a good understanding of the problem, testing possible solutions through simulations and test rigs, and applying it to small-scale prototypes.

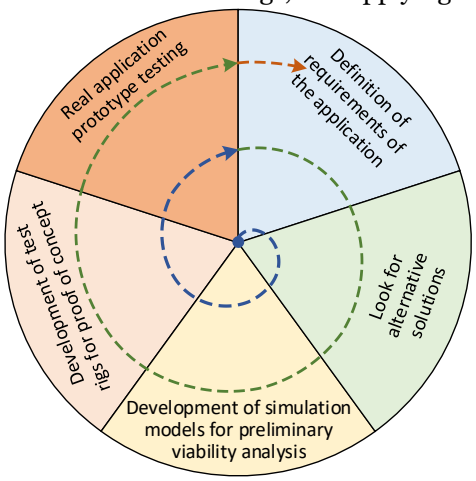

Figure 12 – Spiral development model

The red spiral line in Figure 12 indicates the beginning of the third cycle of development, which has already started for the development of the pneumatic technology for SHPs. Right now, new perspectives and challenges are being discussed. Among them, is the application of pneumatic systems to control the pitch angle of Kaplan turbines, where challenges are raised due to the transmission of pneumatic power into the turbine's rotor as well as the delay caused by the long transmission line.

CONCLUSION

This paper presented the development process of a fully pneumatic solution for the automation and control of small hydropower plants. The development occurred through two cycles of development, where the proposed solutions were progressively tested and evaluated and the rise of new requirements were addressed.

The actual solution consists of linear actuators and two proportional pressure regulators to control the speed governor. The admission valve is actuated by a hydropneumatic jack, developed specifically for this application. Both solutions have built-in capacities for emergency closing (fail safe) to operate in case of electrical power loss. They also make it possible to perform black-start tasks, allowing a full startup of the hydropower plant without energy from the grid.

After two complete cycles of development, it was demonstrated the capacity of the pneumatic technology to automate and control the generating unit of small hydropower plants. The pneumatic solution offers the advantage of having an easier installation and maintenance process, with an acquisition cost roughly 45% lower than an equivalent hydraulic solution, which has been traditionally applied for these applications. Recent analysis made by Reivax pneumatics team has shown that with commercial components it is possible to reach turbines with power up to 30 MW.

Beyond the economic viability, the presented technology promotes the reduction of fossil-based fluids and reduces the risks of river bed contamination, contributing to the constant demand from society for cleaner energy production in accordance with the current development trend of small hydropower plants as an alternative to reduce environmental impacts.

ACKNOWLEDGMENTS

The authors are thankful to the Program of University Scholarship of Santa Catarina (UNIEDU) and The Brazilian National Electric Energy Agency (Aneel) for the funding and support for this project, which is part of the research and development project code PD-00387-0117/2017, and the company China Three Gorges Brazil for the support during the project.

REFERENCES

[1] ANEEL "Sistema de Informações de Geração da ANEEL - SIGA", accessed 08/09/2022, 2022, https://bit.ly/2IGf4Q0

[2] International Renewable Energy Agency (Irena) "Data and Statistics", accessed 08/09/2022, 2022, www.irena.org/statistics

[3] Nautiyal, H., Goel, V. "Sustainability assessment of hydropower projects," Journal of Cleaner Production. Vol. 265, 2020. pp 121661.

[4] Mendonza, Y. E. A., De Negri, V. J., Soares, J. M. C. "Pneutronic Speed Governor for Small Hydropower Plants – A New Application for Pneumatics," Journal of the Brazilian Society of Mechanical Sciences and Engineering. Vol. 38, n. 8, 2014. pp 2621-2633.

[5] Bhat, V. I., Prakash, R. "Life cycle analysis of run-of river small hydro power plants in India," The Open Renewable Energy Journal. Vol. 1, n. 1, 2008.

[6] Pang, M., Zhang, L., Ulgiati, S., Wang, C. "Ecological impacts of small hydropower in China: Insights from an energy analysis of a case plant," Energy policy. Vol. 76, 2015. pp 112-122.

[7] Network for Alternative Technology and Technology Assessment "NATTA's journal Renew", n. 153, accessed 08/09/2022, jan-fev 2005, http://eeru.open.ac.uk/

[8] Premalatha, M., Abbasi, T., Abbasi, S. "A critical view on the eco-friendliness of small hydroelectric installations," Science of the Total Environment. Vol. 481, 2014. pp 638-643.

[9] ANEEL, "Resolução Normativa N° 875, de 10 de Março De 2020 " Agência Nacional de Energia Elétrica, 2020

[10] Mendonza, Y. E. A. "Desenvolvimento de um sistema servopneumático para regulação de velocidade de turbinas em pequenas centrais hidroelétricas," Universidade Federal de Santa Catarina, Florianópolis, 2006.

[11] IEEE, "Recommended Practice for Preparation of Equipment Specifications for Speed-Governing of Hydraulic Turbines Intended to Drive Electric Generators," ANSI/IEEE Std. 125, Institute of Electrical and Electronics Engineers, USA, 2007

[12] IEC, "Guide to specification of hydraulic turbine governing systems," IEC 61362:2012, International Electrotechnical Commission, Switzerland, 2012

[13] IEEE, "Guide for the Application of Turbine Governing Systems for Hydroelectric Generating Units," IEEE Std. 1207-2004, Institute of Electrical and Electronics Engineers, New York, 2004

[14] Locateli, C. C. "Modelagem e Desenvolvimento de um Sistema de Controle de Posição Pneumático com Acionamento por Válvulas ON/OFF," Universidade Federal de Santa Catarina, Florianópolis, 2011.

[15] Endler, L., De Negri, V. J., Castelan, E. B. "Compressed air saving in symmetrical and asymmetrical pneumatic positioning systems," Proceedings of the Institution of Mechanical Engineers, Part I: Journal of Systems and Control Engineering. Vol. 229, n. 10, 2015. pp 957-969.

[16] Conterato, G. P., Spada, T. A. B., Vigolo, V., Weiss, L. A., Klita, R. H., Leoncini, L. L., Araujo, P. d., Negri, V. J. d., "Modeling a Pneumatic Speed Governor Using Electronic pressure valves and directional valves," In: 25th ABCM International Congress of Mechanical Engineering, Uberlândia, 2019.

[17] Spada, T. A. B. "Desenvolvimento teórico-experimental de um sistema para o acionamento de válvulas de adução em PCHs baseado em tecnologia pneumática," Universidade Federal de Santa Catarina, Florianópolis, 2020.

[18] Spada, T. A. B., Conterato, G. P., Vigolo, V., Weiss, L. A., Klita, R. H., Leoncini, L. L., Araujo, P. d., Negri, V. J. d., "Modeling a Hydro-Pneumatic System to Actuate a Turbine Inlet Butterfly Valve," In: 25th ABCM International Congress of Mechanical Engineering, Uberlândia, 2019.

[19] Vigolo, V., Conterato, G. P., Spada, T. A. B., Weiss, L. A., Leoncini, L. L., Araujo, P. G. D., Zanutto, M. A., Negri, V. J. D., "Using pneumatic technology for automation and control of small hydropower plants: A cost reduction and environmentally friendly approach," In: Hydro 2022, Strasbourg, France, 2022.

[20] Vigolo, V., De Negri, V. J. "Sizing Optimization of Pneumatic Actuation Systems Through Operating Point Analysis," Journal of Dynamic Systems, Measurement, and Control. Vol. 143, n. 5, 2021.

[21] Vigolo, V., Conterato, G., Spada, T., Weiss, L. A., De Negri, V. J., "Energy efficiency and performance of servopneumatic drives for speed governors based on operating points," In: International Fluid Power Conference (12 IFK), Dresden, 2020.

[22] Vigolo, V., Conterato, G. P., Spada, T. A. B., Weiss, L. A., Leoncini, L. L., Araujo, P. G. D., Negri, V. J. D., "Development of an Innovative Pneumatic System for Automation and Control of Small Hydroelectric Plants (In portuguese)," In: XXVI Seminário Nacional de Produção e Transmissão de Energia Elétrica (XXVI SNPTEE), Rio de Janeiro, 2022.